METAL FLUORIDE SUPPORTED PALLADIUM: SYNTHESIS, CHARACTERIZATION AND INDUSTRIALLY IMPORTANT CATALYTIC APPLICATIONS

A THESIS SUBMITTED TO
SAVITRIBAI PHULE PUNE UNIVERSITY

FOR THE AWARD OF
DOCTOR OF PHILOSOPHY IN CHEMISTRY

BY

VAIBHAV R. ACHAM

RESEARCH GUIDE

Dr. S. B. UMBARKAR

CATALYSIS DIVISION
CSIR-NATIONAL CHEMICAL LABORATORY
PUNE-411008, INDIA

OCTOBER 2014

Certificate of the Guide

Certified that the work incorporated in the thesis, **"Metal Fluoride Supported Palladium: Synthesis, Characterization and Industrially Important Catalytic Applications"** submitted by ***Vaibhav R. Acham,*** for the degree of ***Doctor of Philosophy,*** was carried out by the candidate under my supervision in the Catalysis Division, CSIR-National Chemical Laboratory, Pune - 411008, India. Such material as has been obtained from other sources has been duly acknowledged in the thesis. To the best of my knowledge, the present work or any part thereof has not been submitted to any other university for the award of any other degree or diploma.

Date:

Dr. Shubhangi B. Umbarkar
(Research Supervisor)

CSIR-NATIONAL CHEMICAL LABORATORY, PUNE

Declaration by the Candidate

I, hereby declare that the thesis entitled **"Metal Fluoride Supported Palladium: Synthesis, Characterization and Industrially Important Catalytic Applications"** submitted by me for the degree of ***Doctor of Philosophy*** to the Savitribai Phule Pune University, is the record of work carried out by me at ***Catalysis Division, CSIR-National Chemical Laboratory, Pune - 411008*** under the guidance of ***Dr. Shubhangi B. Umbarkar.*** Such material as has been obtained by other sources has been duly acknowledged in this thesis. I declare that the present work or any part thereof has not been submitted to any other University for the award of any other degree or diploma.

Date: Vaibhav R. Acham

Signature of the Candidate

Dedicated to…

My Family,

& My Teachers

Acknowledgements

It is my great pleasure to express my heartfelt gratitude to my research supervisor, ***Dr. S. B. Umbarkar****, for her unending support, encouragement and invaluable guidance throughout the period of Ph.D work. I sincerely thank for the care, support and affection that I received from her in the entire period.*

I take this opportunity to express my deepest sense of gratefulness and reverence towards ***Dr. M. K. Dongare****, for his constant inspiration and guidance throughout the course of this work. My deep personal regards are due for him forever.*

I am grateful to ***Prof. Erhard Kemnitz, Humboldt University, Germany,*** *for providing me the facilities to carry out a part of my Ph.D work under CSIR-BMBF collaborative project and for his help during my Ph.D tenure. I am thankful* ***Dr. Anton Dimitrov, Humboldt University, Germany,*** *for the help during my stay in Berlin. I am also thankful to CSIR, India and BMBF, Germany for financial support during my stay in Berlin.*

I express my thanks to ***Dr. Ankush Biradar*** *for his help and efforts during difficult time in the course of Ph.D.*

I would like to thank the head of the division, ***Dr. A. P. Singh*** *for providing me all the divisional facilities required for my research work. I am grateful to* ***Dr. S. Sivaram*** *and* ***Dr. S. Pal****, erstwhile and current Directors, CSIR-NCL, for allowing me to carry out the research work in a prestigious and well-equipped laboratory. UGC, New Delhi is gratefully acknowledged for the research fellowship.*

It gives me a great pleasure to express my deep sense of gratitude and indebtedness to Dr. Deshpande, Dr. Gopinath, Dr. Vinod, Dr. Ingle, Dr. Awate, Dr. Tejas, Ms. Violet, Mr. Jha, Mr. Purushothaman, Mr. Dipak Jori, Mr. Madhu, Mr. Punekar and all the other scientific and nonscientific staff of NCL for their help, guidance and suggestions in carrying out the research work.

I sincerely thank my Labmates ***Dr. Trupti, Dr. Neelam, Dr. Ankur, Dr. Suman, Swati, Prakash, Rajesh, Samadhan, Vidhya, Macchindra, Ashvini, Sumeet, Atul, Pavan, Lina, Reshma, Dhananjay, Savita and Tanushree*** *for their friendly help and kind cooperation during the period. I also thank all my friends in the division and in NCL especially* ***Dr. Anand****,* ***Dr. Revannath****,* ***Mangesh****,* ***Nagesh****,*

Bhausaheb, Ketan *and many others for their cooperation, encouragement, invaluable help and moral support in one way or other, which made my work much easier.*

I take this occasion to thank all my teachers, well-wishers classmates & friends in various stages for their love, encouragement and kind cooperation that I received from them whose names are not mentioned here.

The words are not enough to express all my love and thankfulness towards ***Aai-Pappa*** *and* ***Mummi-Dada*** *and all my beloved family members for their blessings that I could reach here.*

Finally I would like to thank my beloved wife ***Agraja*** *for her love, trust and care.*

Vaibhav R. Acham

Never regards your study as a duty but as an enviable opportunity to learn and to know more your personal joy and for the profit of community to which your later work belonging.

– Sir Albert Einstein

Table of Contents

List of abbreviation

AAS	Atomic Absorption Spectroscopy
BE	Binding Energy
BET	Brunauer-Emmett-Teller
BJH	Barret−Joyner−Halenda
EDAX	Energy Dispersive X-ray Spectroscopy
FID	Flame Ionization Detector
FTIR	Fourier-Transformed Infrared
GC	Gas Chromatography
GCMS	Gas Chromatography-Mass Spectroscopy
HS	High Surface
ICP-AES	Induced coupled plasma – Atomic emission spectroscopy
MAS	Magic Angle Spinning
MCM	Mobil Composition of Mater
MS	Molecular sieves
NMR	Nuclear Magnetic Resonance
PAS	Photoacaustic Spectroscopy
TEM	Transmission Electron Microscopy
TG-DTA	Thermogravimetry-Differential Thermal Analysis
TLC	Thin Layer Chromatography
TOF	Turn Over Frequency
TON	Turn Over Number
TPD	Temperature Programmed Desorption
TPR	Temperature Programmed Reduction
TPO	Temperature Programmed Oxidation
UV-DRS	Ultra-Violet Diffused Reflectance Spectroscopy
XPS	X-ray Photoelectron Spectroscopy
PXRD	Powder X-Ray Diffraction

List of symbols & units

Å	Anstrong Unit
a.u.	Arbitary Unit
cps	Counts per seconds
° C	Celsius (unit of measurement for temperature)
cm^{-1}	Wavenumber
E_a	Energy of activation
h	Hour (s)
s	Second (s)
Mol	Mole (s)
nm	Nanometer
ppm	Parts per million
%	Percentage
δ	Chemical shift
ν	Frequency

List of figures

List of schemes

List of tables

Abstract of the thesis

Metal Fluoride Supported Palladium: Synthesis, Characterization and Industrially Important Catalytic Applications

Research Student: **Vaibhav R. Acham**

Registration Date: 04/03/2010 (**R. No. SAO/Ph.D./ID-10867/A-65/2010)**,
Savitribai Phule Pune University.

Research Guide: **Dr. S. B. Umbarkar**

Catalysis is a science of accelerating chemical transformations mainly to convert simple raw materials to complex molecules with versatile applications. Catalysis is one of the very important area in chemical research which is contributing for sustainable development. Heterogeneous catalysts are preferred to homogeneous catalysts due to obvious advantages like easy separation and recycle. Along with activity and selectivity, an efficient industrial heterogeneous catalyst should be regenerable, thermally and mechanically stable, reproducible and economical.

Metal nanoparticles supported on various heterogeneous supports like, metal oxides, zeolites, polymers, asbestos and carbonaceous material play important role in industrial catalysis. Palladium is one of the very widely used metals in catalysis for academic as well as for industrial purposes. Supported palladium catalysts have been used in variety of reactions such as hydrogenation, oxidation, coupling reaction etc. Although the catalytic science has achieved many successes, due to high demand of clean and green technology in chemical processes, there is broad scope in utilizing novel materials as catalysts for further developments.

Metal fluorides are widely known for its applications in the area of ceramics, thin optical films, energy storage devices, hosts for laser devices and anti-reflective coatings. However these materials are relatively less explored as catalytic materials or supports for catalysts. Generally metal fluorides are obtained either as synthetic compounds or from natural minerals and ores. Although the metal fluorides having used as catalyst for certain organic transformations in academics, there is broad area of industrial catalysis unacquainted with metal fluorides based catalytic materials. It will be interesting to study the metal fluoride as nonconventional support for

palladium (Pd) and study this activity for typically for Pd catalyzed reaction like hydrogenation, aerobic oxidation etc.

The primary objective of this thesis is to generalize the one pot sol-gel synthesis method of Pd supported on alkaline earths metal fluoride and to study their catalytic potential for various organic reactions of academic and industrial interest. To accomplish above revealed objectives, Pd supported on alkaline earth metal fluorides were synthesized and their Lewis acidic/ basic properties have been investigated in the present work. The detailed objectives of the thesis are as follows:

- To synthesize Pd supported on metal fluoride catalysts using sol-gel method.
- The detailed characterization of the synthesized catalysts using various physico-chemical characterization techniques.
- Evaluation of catalytic activity for following reactions
    - Hydrogenation of olefins
    - Hydrogenation of triglycerides
    - Aerobic oxidation of alcohols
    - Alcoholysis of epoxides

This thesis work has been arranged in five chapters as below:

The **first chapter** represents a literature review on the use of various heterogeneous catalysts having transition metal as active sites of the catalyst, their advantages and disadvantages. The comprehensive literature reports on metal fluorides for the methods of synthesis and various catalytic activities studied previously by various researchers. This chapter gives in brief literature survey with respect to synthesis and catalytic applications of heterogenized Pd in catalysis.

The **second chapter** deals with synthesis of Pd-$MgF_{2-X}(OH)_X$ and its catalytic applications for hydrogenation of various olefins and oils. Palladium supported on magnesium hydroxyl fluorides were synthesized by one pot fluorolytic sol-gel route using magnesium methoxide as precursor (scheme 1). During fluorolysis, *in-situ* prepared magnesium methoxide was reacted with different concentrations of HF, 100% (alcoholic), 71 and 40% (aqueous) and palladium acetate followed by calcination to get Pd-$MgF_{2-X}(OH)_X$.

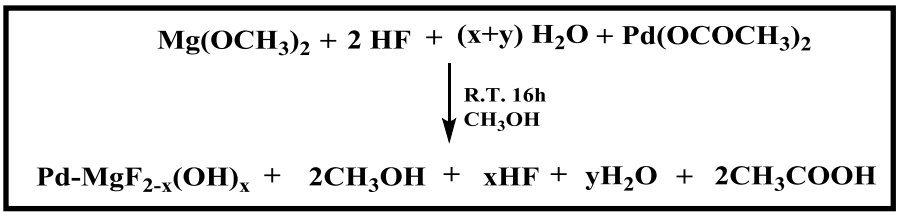

Scheme 1: Synthesis of different Pd-$MgF_{2-x}(OH)_x$ catalysts using sol-gel method.

During the fluorolysis, two competitive reactions namely hydrolysis and fluorolysis (fluorination) of metal alkoxide take place. The extent of fluorination/hydrolysis depends on the concentration of HF used for the synthesis of Pd-$MgF_{2-X}(OH)_X$ catalysts.

All the synthesized catalysts were characterized using several physico-chemical techniques. The PXRD patterns of catalysts showed broad peaks which confirm the nanoscopic nature of the catalysts and with presence of mixed phases of MgF_2 and $Mg(OH)_2$. The nitrogem adsorption–desorption isotherms revealed that the surface area of the catalysts decrease with increase in degree of fluorination from Pd-MgO to Pd-MgF_2-100. The pore size increases with increase in degree of fluorination. The pore volume was in range of 0.19 - 0.23 cm^3g^{-1} for all the catalytic systems. The types of nature of acidity as determined using FTIR- PAS studies of adsorbed pyridine showed the presence of high intense peaks at 1445, 1490 and 1576 cm^{-1} which indicate presence of strong Lewis acid sites. The strength of Lewis acidity was found to be decresed in order Pd-MgF_2-100 > Pd-MgF_2-71 > Pd-MgF_2-40. The hydrogen chemisorption studies used to determine the active metal percentage, metal dispersion and metal particle size, This showed very high Pd dispersion (~ 47%) in Pd-MgF_2-100 catalyst which was decreased to ~ 33% in case of Pd-MgF_2-40. This Pd dispersion was very high as compared to 1 wt% Pd supported on carbon (SA = ~1400 m^2/g) which showed only 30 % Pd dispersion. This high percentage of Pd dispersion in case of Pd-MgF_2-100 may be due to uniform distribution of Pd over the sol-gel synthesized magnesium hydroxyl fluorides and role of support in Pd dispersion.

The UV-Vis spectroscopy results also clearly indicated strong metal support interactions. The XPS indicated the partial positive charge on Pd which may be due to strong Pd-support interactions. SEM-EDAX studies show availability of almost 1 wt% Pd on the surface of all the catalyst. HRTEM studies indicated sheet like structures with Pd with size in range of 5-20 nm. The sheet structured Pd lead to high metal dispersion on fluorinated support. In case of fluorinated supports, Pd showed

nanosheets structures while in case of magnesium oxides spherical nanoparticle formation was observed (fig. 1).

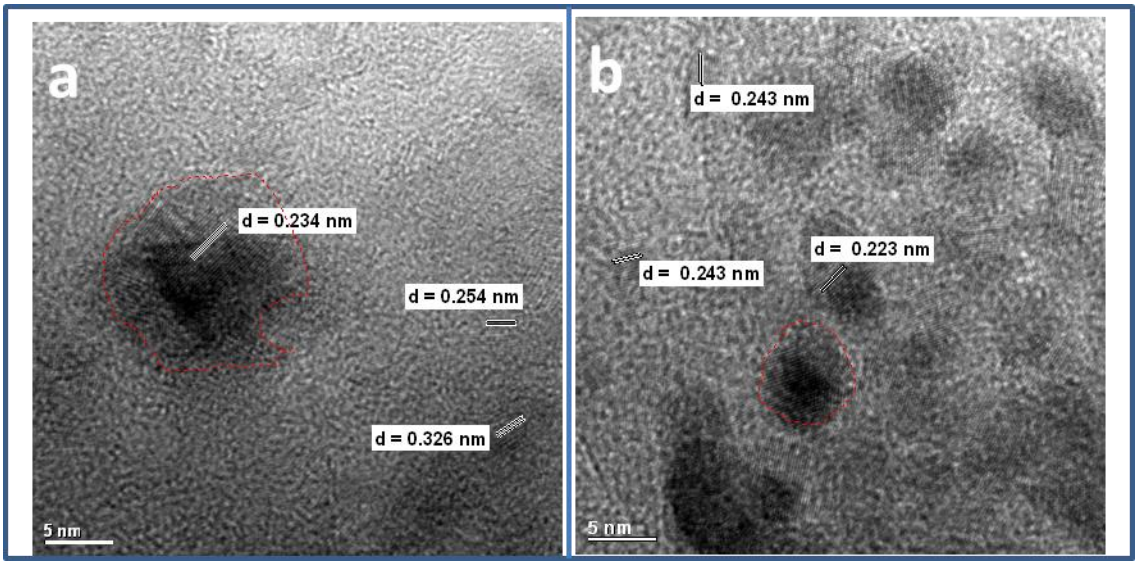

Figure 1: HRTEM images of catalysts a) Pd-MgF_2-100 b) Pd-MgO.

The catalytic activity of the Pd supported magnesium hydroxyl fluorides was evaluated for catalytic hydrogenation of olefins initially with styrene as model substrate as shown in scheme 2. The hydrogenation was carried out at room temperature and atmospheric pressure by bubbling hydrogen gas through the reaction mixture. Pd-MgF_2-100 showed best catalytic activity as compared to other catalysts as well as commercial 5 wt% Pd-C catalysts. The catalyst showed selectivity towards hydrogenation of C=C in presence of other reducible functionalities such as carbonyl, nitro and aromatic rings. Pd-MgF_2-100 showed very high TOF as 634 h^{-1} and rate constant as 11.93 x 10^{-3} S^{-1}. Pd-MgF_2-100 was successfully used for hydrogenation of α-methyl styrene (AMS) to cumene at room temperature and atmospheric pressure. During industrial production of phenol from cumene via cumene hydrogen peroxides AMS is produced as undesired byproduct and either need to separate or hydrogenated into cumene. The high activity of Pd-MgF_2-100 catalyst for hydrogenation AMS to cumene reaction proves its commercial importance.

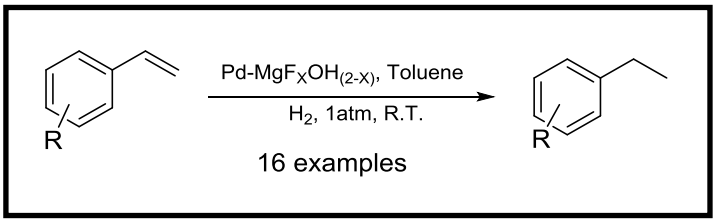

Scheme 2: Hydrogenation of olefins using Pd-$MgF_{2-X}(OH)_X$ catalysts.

To further study the commercial applicability of the catalyst, hydrogenation of triglycerides was carried out using Pd supported on fluorinated catalysts. The Pd-$MgF_X(OH)_{2-X}$ were used for hydrogenation of edible oils (viz. Soyabean, Sunflower, Mustard, Palm), non-edible oils (viz. castor) and fatty acids (viz. oleic, linoleic). The catalyst showed very high activity for such hydrogenation at room temperature and atmospheric pressure with methanol as solvent. For solvent free conditions, the reactions were carried out at slightly higher temperature (upto 90 °C) to keep the hydrogenated product in molten state. The catalyst showed excellent activity in case of all oils including castor which indicated the iodine value (~ 4), hydroxyl value (~ 131), acid value (~ 2) and melting point of castor wax (82 °C) under 10 bar pressure and 90 °C. The extent of hydrogenation can also be controlled by this possible. The catalyst also showed recyclability without any appreciable loss in activity upto three cycles. Palladium analysis by AAS and ICP-AES showed no palladium leaching.

The ***third chapter*** deals with synthesis, characterizations of Pd-BaF_2 for aerobic oxidation of alcohols.

The catalyst was synthesized by typical sol-gel method using *in situ* genetated barium methoxide, aq. HF (71 %), palladium acetate and dry methanol as solvent. The typical synthesis procedure includes dissolution of Ba in methanol under inert atmosphere to form sol of barium methoxide which on fluorolysis with aq. HF produces barium hydroxyl fluoride followed by addition with palladium acetate and drying. This catalyst was characterized by several physico-chemical techniques such as PXRD, UV-Vis spectroscopy, XPS, EDAX-SEM, HRTEM etc. The PXRD characterization of the catalyst showed that presenceof mixed phases of barium fluoride and barium hydroxides. XPS revealed supported Pd exists in Pd^0 and Pd^{II} states. The UV-DRS showed to charge transfer from fluoride of the support to the d-orbital of Pd. EDAX showed about 1 wt% of the Pd loading. In SEM images, Pd-BaF_2-71 appeared in typical rod shaped structure (fig. 2-a). The HRTEM studies showed Pd and PdO particles spread over the surface of BaF_2-71 rods. The Pd particles were varied from 90 -120 nm while PdO of size was 5-10 nm in diameter (fig. 2-b).

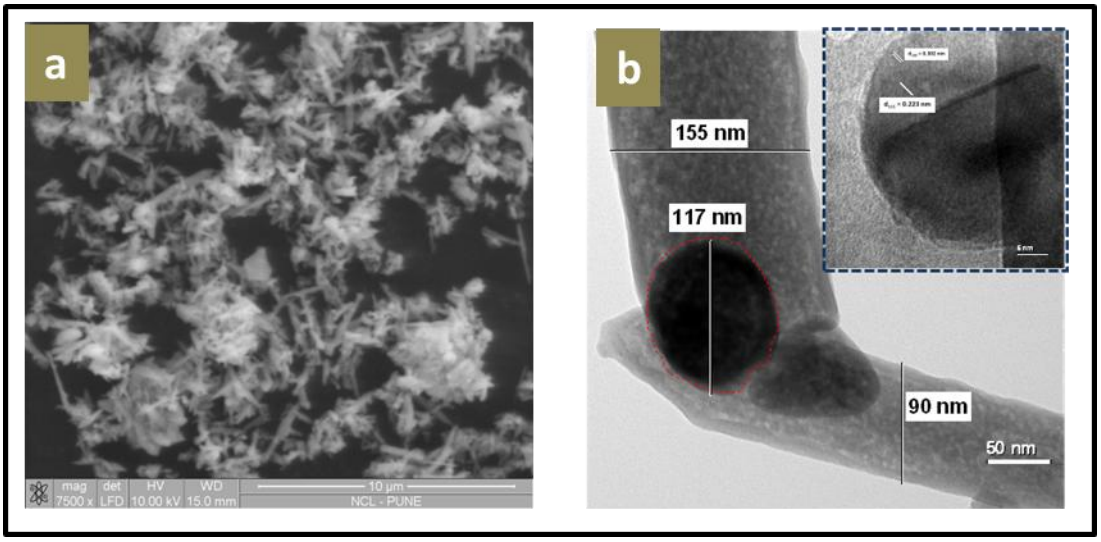

Figure 2: a) SEM and b) TEM image of Pd-BaF_2-71 catalyst

The heterogeneous Pd nanoparticles are well known for selective catalytic aerobic oxidation of alcohols, although several reactions demands for high reaction temperature, use of co-catalysts, use of extra bases like K_2CO_3, use of fluorinated solvents, high catalyst loading, use of non-green oxidants like N-methylmorpholine-N-oxide (NMO), 3-chloroperbenzoic acid (*m*-CPBA) etc. Therefore there is scope for the improvement of novel catalytic systems to resolve the mentioned problems. Pd-BaF_2-71 was used as catalyst under base free conditions for selective oxidation of alcohols using air as oxidants as shown in in scheme 3). Benzyl alcohol was used a substrate and the reactions were carried out at 110 °C in toluene under the flow of air (10 mL min^{-1}) with 10 wt% of the catalyst loading. For aerobic oxidation of alcohols, Pd-BaF_2-71 showed highest catalytic activity among used fluorinated catalysts viz. Pd-SrF_2-71 and Pd-MgF_2-71. The catalyzed showed 100% conversion upto 95% selectivity for aldehydes in 8 h and TOF upto 123 h^{-1}. The catalyst showed selectivity towards carbonyl compounds for aerobic oxidation in presence of other functionalities such as phenols and olefins. The catalyst was successfully recycled upto five cycles without appreciable loss in catalytic activity. No metal leaching confirmed by ICP-AES. *In situ* FTIR spectroscopy was used to determine the mechanism of aerobic oxidation of alcohols which showed activation of oxygen on supported Pd surface which captures the hydrogen from alcohol substrate to give aldehyde via oxidative dehydrogenation mechanism.

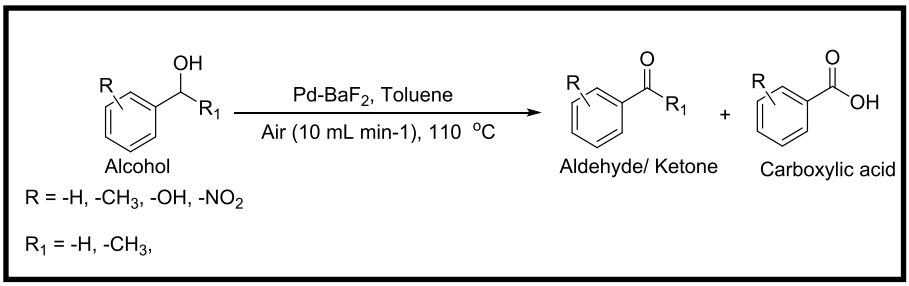

Scheme 3: Aerobic oxidation of alcohols using Pd-BaF_2-71 catalysts.

The ***fourth chapter*** deals with synthesis, characterizations of Pd-SrF_2-71 and its catalytic applications for alcoholysis of epoxides.

The catalyst was synthesized by typical sol-gel method using *in-situ* generated strontium methoxide from strontium metal, aq. HF (71%), palladium acetate and dry methanol as solvent. This catalyst was characterized by several physico-chemical techniques such as PXRD, UV-Vis spectroscopy, NH_3-TPD, XPS, EDAX-SEM, HRTEM etc. The PXRD characterization of the catalyst showed for formation of the mixed phases corresponding to strontium hydroxyl fluoride. The specific surface area of catalyst was 40 m^2gm^{-1} measured using nitrogen adsorption-desorption studies. NH_3-TPD showed intermediate acidity of Pd-SrF_2-71 catalyst and FTIR of adsorbed pyridine indicated presence of typical Lewis acidity. The metal support interactions were explained using UV-DRS and XPS studies. SEM-EDAX studies show availability of almost 1 wt% Pd on the surface of all the catalyst. SEM studies showed globular and crystalline nature of Pd-SrF_2-71 catalyst. The HRTEM studies showed Pd nanoparticles to be evenly distributed. The diameter of Pd nanoparticles were in range of 5 -10 nm.

Epoxides are very important organic intermediates in pharmaceuticals and fine chemicals. Epoxides undergo ring-opening reactions to give β-substituted alcohols with a variety of nucleophilic species with high regio and stereoselectivity. However, the approaches used in literature are often far away from ideal and suffer from drawbacks such as the highly toxic and corrosive nature of the promoter, high acidity and need to use stoichiometric quantities of the promoter, inconvenient handling procedures and long reaction times. To overcome these drawbacks fluorinated solid acid catalysts such as Pd-SrF_2-71 was evaluated for catalytic alcoholysis using cyclohexane epoxide as model substrate as shown in scheme 4. The reactions were carried out in alcohols as solvent at room temperature with 5 wt % catalyst loading.

The catalyst Pd-SrF_2-71 has shown 100% conversion and 96% selectivity for 2-alkoxyalcohols with very high TON up to 2127 in ethanol. The reaction parameters such as catalyst loading effect, temperature effect and time effect were studied to define the optimum reaction conditions for catalytic reactions.

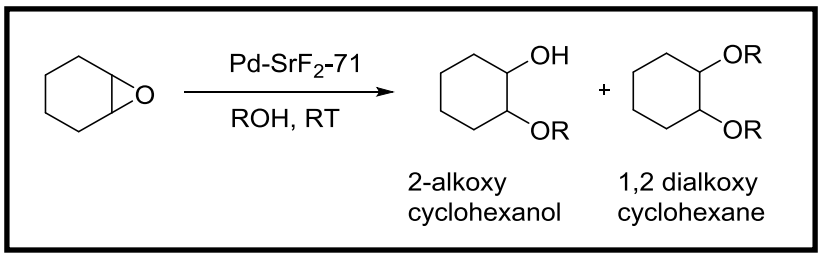

Scheme 4: Alcoholysis of epoxide using Pd-SrF_2-71 catalyst

Under the optimized reaction conditions, various alcohols were screened for alcoholysis. The results showed the selectivity of 2-alkoxy alcohols decreases from primary to benzylic alcohols. The catalyst was subjected to ring opening of various substrates to study the substrate scope of the catalyst. The catalyst showed recyclability without appreciable loss in catalytic activity up to three recycles. No Pd leaching was observed under reaction conditions which as conformed by filtration test and ICP-AES analysis.

The ***fifth chapter*** presents the major outcome of thesis and it will consist of overall summary and conclusions**.** The present studies have proved palladium nanoparticles supported on various alkaline earths metal fluorides as versatile catalyst for various catalytic reactions. These catalysts have potential for sustainable development.

Chapter 1

INTRODUCTION

Abstract

A general introduction to catalysis with a special attention to heterogeneous catalyst is given as motivation for the presented work in the thesis. A special emphasis is given to the metal fluorides, their synthesis and their present position in area of catalysis with few examples. Further an outline of palladium catalyzed heterogeneous organic reaction is discussed in brief in this chapter. An importance of development of new and improved catalysts is illustrated with examples of industrial catalytic reactions which having a vital role in development of green and clean technology. Towards the end, the roadmap of the thesis is described.

1.1. Introduction

Berzelius defined catalysis as "a power of substances that enables to awaken the affinities, which are asleep at reaction temperature by their mere presence and not by their own affinity" in 1835 [1]. The term catalysis persisted heavily argued until around 1900 until Wilhelm Ostwald proposed its definition using concepts of chemical kinetics which has been rewarded Nobel prize in 1909 [2]. Catalysis is the word used to describe the action of a catalyst, which alters the rate at which a chemical reaction attains equilibrium. Catalyst can increase the rate of only thermodynamically feasible processes.

Catalysts have a key role in maintaining life on earth. Catalysis has a dramatic impact in our daily life as well as in industrial processes. The chemical industry is the largest in the world and the annual value of the products manufactured by catalytic processes well exceeds one trillion USD [3]. At present, more than 90% of the industrial chemical processes are catalyst aided and the research interest on catalyst and/or catalysis is increasing continuously [4].

One of the well-known applications of catalysis in everyday life is the catalytic production of ammonia fertilizer which is essential to sustain the current world population [5]. The another example is use of the automotive three-way catalyst for cleaning exhaust gases from gasoline driven combustion engines in automobiles. The catalyst has a remarkable role in petrochemicals, environmental pollution control, fuels, lubricants, dyes, polymers, fine chemicals, pharmaceuticals and also in the area of energy materials etc [6].

A chemical reaction involves breaking of bonds between atoms and the formation of new ones. This process is associated with transformation of energy as shown in energy profile diagram (fig 1.1) illustrating the progress. The catalyst involved in the reaction provides an alternate reaction path as shown by lower curve, which is associated with lower activation barrier than the non-catalytic reactions. Therefore higher overall reaction rate could be achieved.

The numerous catalysts known today can be categorized in various classes. Based on phase of the reactant and the catalysts in the catalytic reactions, catalysis has been classified broadly into two groups as mentioned in fig. 1.2 [7].

1) Homogeneous catalysis

2) Heterogeneous catalysis

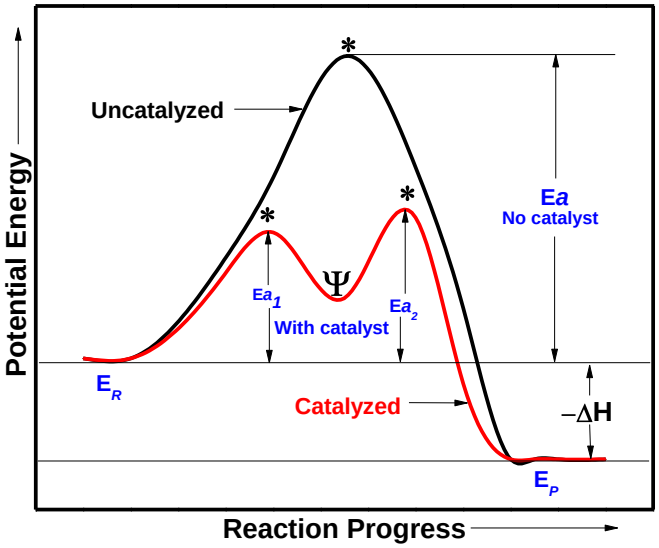

E_R: Energy of reactants; E_P: Energy of products; E_a: Energy of activation;
∗: Transition state; ψ: Reaction intermidiates

Figure 1.1. Energy profile diagram of catalytic reaction.

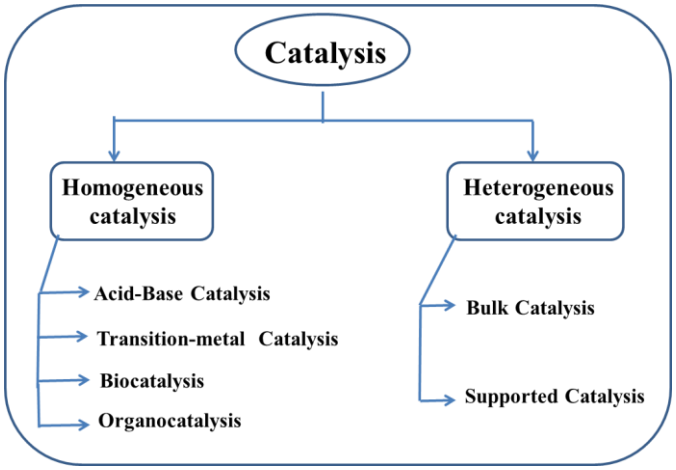

Figure 1.2. Types of catalysis.

Homogeneous catalysis is a sequence of reactions that involve a catalyst in the same phase as the reactants. Generally, a homogeneous catalyst is co-dissolved in a solvent with the reactants. Homogeneous catalysts are generally well-defined chemical compounds or metal (transition) complexes, which consist of a metal center surrounded by a set of organic ligands. The ligands impart solubility and stability to the metal complex and can be used to tune the selectivity of a particular catalyst towards the synthesis of a desirable product. By varying the size, shape and electronic properties of the ligands, the activity of these catalysts can be tuned. Particularly

homogeneous catalytic reactions are highly selective and exhibit high order of rate constant. The reactions catalyzed by transition metal complexes such as hydrogenation, oxidation, carbonylation, hydroformylation and C-C bond formation reactions are example of homogeneous catalysts [8,9].

1.2. Heterogeneous catalysts

Heterogeneous catalysis refers to the form of catalysis where the phase of the catalyst differs from that of the reactants. Normally, these catalysts are solids and dispersed in gaseous or liquid reaction mixture.

Heterogeneous catalysis is surface phenomenon because the active sites present on the surface of catalysts are only accessible for the catalytic reactions. Heterogeneous catalysis have fascinated Nobel prizes for Fritz Haber in 1918 (development for synthesizing ammonia), Carl Bosch in 1931 (process for ammonia production), Irving Langmuir in 1932 (surface chemistry), and Gerhard Ertl in 2007 (chemical processes on solid surfaces) [4]. Heterogeneous catalysts cover almost 90% of the industrial catalytic processes due to advantages like (i) regenerable, (ii) thermally and mechanically stable, (iii) economical and (iv) possess suitable morphological characteristics like high surface area and crystalline nature over homogeneous catalysis [4]. Due to all above characteristic features of heterogeneous catalysts and increasing demands of green catalytic routes for chemical transformations in industries and academia, there is a need of further developments in heterogeneous catalytic research.

1.2.1. Types of heterogeneous catalyst

Heterogeneous catalyst can either be metal (noble/non-noble/transition), semiconductor or metal oxides which in term may be crystalline or amorphous. Each type has its own merits and demerits based on their applications. Depending on the nature and form of an active component, the catalysts can be classified as follows.

A. Bulk metal catalysts

Pure metal and metal alloys are the most significant and extensively used industrial catalysts as they are used to catalyze wide variety of reactions [10]. Relatively, the high densities of skeletal catalysts offer outstanding settling features compared to supported catalysts when used in slurry phase reactors [11]. For example,

iron is used as catalyst for production of ammonia from nitrogen and hydrogen in Haber process [5].

B. Supported metal catalysts

These catalysts comprise of an active phase dispersed on a carrier support. The metals used in industrial catalysis are often costly and hence they are mainly used as a highly dispersed phase on high surface area porous supports (e.g. metal oxides, zeolites, carbon or polymers). For example Re-Pt supported on γ-Al_2O_3 is used in petroleum industries for naphtha reforming [12].

C. Bulk metal oxides

The bulk metal oxide catalysts exists as either amorphous or polycrystalline materials. These show presence of non-zero valent metal and absence of metal-metal bonds. These exhibit both basic and acidic characters, based on their composition, which is important for reactions in catalysis. For example, vanadium pentoxide (V_2O_5) is used as catalyst in contact process for manufacturing sulfuric acid (H_2SO_4) from sulfur dioxide (SO_2) [12].

D. Zeolites

Zeolites are basically aluminosilicates containing aluminum oxide and silicon oxide in tetrahedral form. These are formed, when Al^{3+} replaces some of the Si^{4+} cations in silicates. For each Si^{4+} ion replaced by Al^{3+}, the charge must be balanced by other positive ions such as Na^+, K^+, and Ca^{2+} ions. The zeolites are unique for their molecular sieving characteristics, which are a consequence of their narrow uniform pores [13]. Zeolites are microporous in nature which are exclusively used in catalytic cracking of petroleum. For example zeolites are exclusively used in catalytic cracking to produce petrol and fuel oils [14].

E. Molecular catalysts on supports

Modified inorganic solids or polymer supports with catalytically active groups or molecules are used as industrial catalysts in some reactions. Inorganic solid surface can be functionalized with active catalyst groups as organic polymers. E.g., ion exchange resin is used for methyl-*tertiary* butyl ether (MTBE) synthesis from isobutylene and methanol [15].

1.2.2. Properties of heterogeneous catalysts

The catalytic activities of the heterogeneous catalysts can be explained on the basis of following characteristic properties [4].

1. Physical Properties

A. Surface area and porosity of catalyst

Surface area and porosity is one of the very important factors which affect the catalytic activity of the catalyst. Higher surface area provides easier accessibility of active sites to reactors as well as provides higher dispersion to active components in case of supported catalysts. In general, the activity of the catalyst is proportional to surface area and porosity of the catalyst.

B. Particle size and dispersion

In supported catalyst, the active component size affect inversely to the activity of the catalyst. The dispersion of the active component increases with decrease in size of the active component.

C. Structure and morphology

The crystal structure of the catalyst is related the activity and selectivity of the reaction due to orientation of the reactant molecules across the catalyst.

D. Local environment of elements

The different nuclear isotope of elements in the catalyst structure decides the activity of the catalyst for the reactions. These are mainly important in determination of catalytic reaction mechanism.

2. Chemical Properties

A. Surface chemical composition

The atomic composition of a catalyst surface plays a decisive role for the catalytic properties which is composed of anion and cations. The behaviors of ionic pairs determines the surface electric field gradient, the surface electrostatic potential and the mode of surface relaxation

B. Valence states and redox properties

In catalytic cycle, the active component undergoes redox cycle. In general the oxidation state and reduction potential of the catalyst decides the activity for redox-type of catalyst for redox type of reactions.

C. Acidity and basicity

The cations and anions on catalysts surfaces have been termed as acid-base pairs [9]. In heterogeneous catalytic system, metal ion behaves as Lewis or Brønsted acid while counter ion exhibit basic properties. The hydroxyl groups on the surface may exhibit considerable Brønsted acidity. The exposed coordinative unsaturated cations may accept the free electron pairs of adsorbed species and exhibit Lewis acidity.

1.2.3. General mechanism of heterogeneously catalyzed reaction

Typical steps in heterogeneous catalytic reaction are shown in fig. 1.3. In heterogeneous catalysis, reactant diffuses through a boundary layer surrounding the surface of catalyst in the first step. This is followed by the adsorption of the reactant molecules on the active sites of the catalyst surface. These atoms may form new bonds (chemisorption) with appropriate molecules imposing from the neighboring gas or liquid phase. The formed surface species may migrate from one site to adjacent site to react with others to form new adsorption complex. Then the new complexes decompose and the reaction products leave the catalyst surface (desorption). The activity of a heterogeneous catalyst is defined by the number of the catalytic cycle per unit time per active site on the catalyst surface.

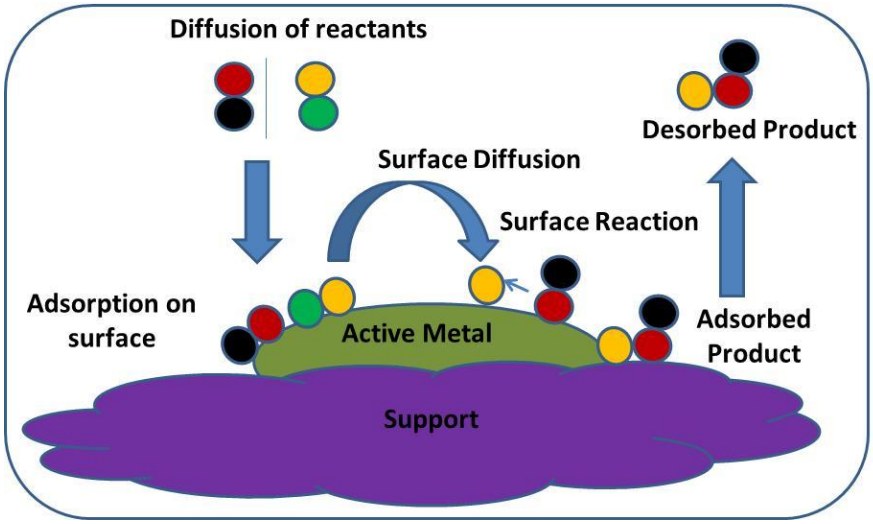

Figure 1.3. A general pictorial representation of heterogeneously catalyzed process.

With catalyst supports, the reaction often occurs on the surface of either the catalyst or the support. On the basis of the surface reactions the catalytic reaction shows there are three type mechanisms.

A. Langmuir-Hinshelwood mechanism: In this type of mechanism, the two molecules A and B, both adsorb to the catalyst surface. If A and B react with each other on the catalyst surface and the new molecule A-B formed and then desorbs.

B. Rideal-Eley mechanism: In this type of mechanism, if one of the two reacting molecules, consider A, adsorbs to the catalyst surface. The second molecule, B, meets A on the surface, without adsorbing on catalyst surface, and they react with each other to form new A-B molecule and then desorbs from catalyst surface.

C. Precursor mechanism: In this type of mechanism, if one of the two molecules, consider A, is adsorbed on the catalyst surface and the second molecule, B, collides with the catalyst surface which forms an active mobile precursor state. This active mobile molecule B when collides with A on the catalyst surface to form molecule A-B which desorbs further.

1.2.4. Metal support interactions

It is well acknowledged that in metal-catalyzed reactions, the support affects the catalytic properties of the metal particles. The electronic properties of the supported metal particles depend on the acid-base and redox properties of the catalyst support. Also the size and shape of heterogeneous catalysts could be significant to judge the performance of catalyst, which is subjected by interactions with the support [16, 17]. Different factors affecting the catalytic activity of metal based catalysts are summarized in fig. 1.4.

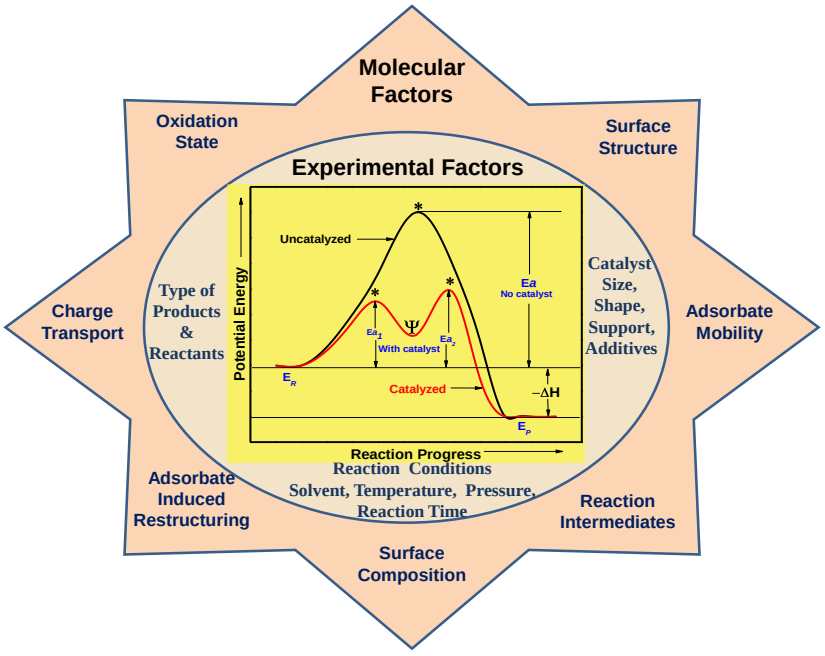

Figure 1.4. Factors affecting reaction kinetics of catalytic reactions.

Mainly the reaction kinetics is affected by two kinds of factors viz., experimental factors and molecular factors. Among these factors, the former are controlled by tuning reaction conditions and the later one is mainly controlled by the metal-support interactions. The metal-support interaction in heterogeneous catalysis depends on the following factors

(i) Nature of metal

(ii) Nature of support

(iii) Method of preparation of catalyst

(iv) Precursors of metal and support in synthesis

The best example of effect of metal support interaction on catalytic activity is palladium catalyzed methane oxidation. When 1 wt% Pd supported on various oxide support is used for methane oxidation it showed different activity due to effects of support on Pd. (table 1.1) [18]. Depending on the support, the temperature for maximum methane conversion has varied from as low as 490 to as high as 885 °C which clearly demonstrates the influence of support on the catalytic activity of Pd catalyst for methane oxidation.

Table 1.1. Effects of various support on Pd catalyzed methane oxidation

Entry	Catalyst	Catalytic Activity			
		T_{10}	T_{30}	T_{70}	T_{90}
1	Pd/Al_2O_3	365	400	445	495
2	Pd/Ga_2O_3	365	420	765	815
3	Pd/In_2O_3	390	440	520	590
4	Pd/Nb_2O_5	565	665	840	875
5	Pd/TiO_2	400	720	840	885
6	Pd/ZrO_2	325	355	400	490
7	Pd/SiO_2	420	585	680	860

Reaction Conditions: CH_4: Air (1:99 volume%), VHSV: 48000 h^{-1}; Pd loading : 1 wt% of support. Temperature at which methane conversions are 10, 30, 70 and 90%.

Despite of several advantages and exclusive properties of reported heterogeneous catalysts, there is broad scope in utilizing novel advanced materials as catalysts. All these facts are constantly motivating the industry towards the application of novel "clean technology". The improvements of "green" and "sustainable" methodologies have the emphasis mainly on points given below [19].

1. To achieve the high activity and selectivity
2. To develop sustainable process by reducing the waste e.g. salt formation, corrosion, isolation of products etc.
3. To use the cheaper renewable feed stocks
4. To evolve the novel multifunctional catalysts
5. To develop the better catalyst systems.

Solid metal fluorides are novel materials which own unique properties such as high physical constants, high ionicity and high stability. Hence these materials can be used as new materials for the advancement of new heterogeneous catalytic system.

1.3. Metal Fluorides

1.3.1. Introduction

Metal fluorides are achieved either from naturally occurring minerals and ores or using synthetic methods. They are used in various forms such as simple binary, oxy/ hydroxyl and complex or doped fluorides, etc. depending on the requirement [20]. These fluorides can be prepared with a wide range of preferred properties by combining different metal cations in the fluoride matrices. Metal fluorides possess strongest electronegative element (fluorine), which produces a higher Lewis acidity on the metal center compared to their corresponding oxides and other metal halides.

They are well-known and extensively used as materials for coating [21], ceramics [22], laser devices [23] and energy storing devices [24] because of its intrinsic characteristics. The recent development of methods of synthesis has opened new possibilities for preparation of efficient catalysts based on metal fluorides. The leading uses of metal fluorides is as reference catalysts in the manufacture of fluorocarbons, e.g. the transformation of ozone depleting chlorofluorocarbons (CFCs) into non-chlorinated, hydrochlorofluorocarbons (HCFCs) and/or hydrofluorocarbons (HFCs) [25], the synthesis of various monomers for fluorinated polymers [26] etc.

The statistical data obtained from *Scifinder* shows that a survey on study of metal fluorides increased enormously from 1950 to 2014 (Fig 1.5. A-B).

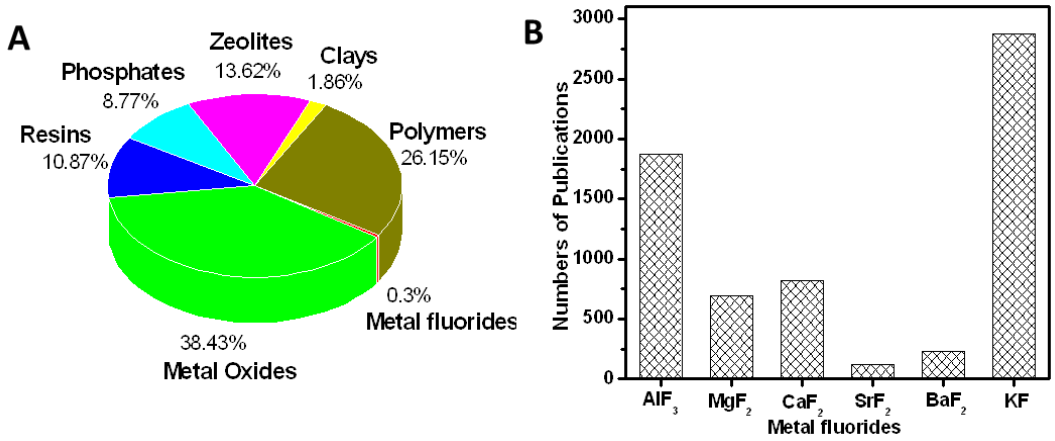

Figure 1.5. A) Contributions of metal fluorides in catalysis as compared to other catalysts and B) Total number of publications on various metal fluorides since 1950.

1.3.2. Synthesis of metal fluorides

The method of synthesis is known to affect the structural features of the catalyst. Typically, metal fluorides are synthesized by several methods as shown in pictorial representation in fig. 1.6.

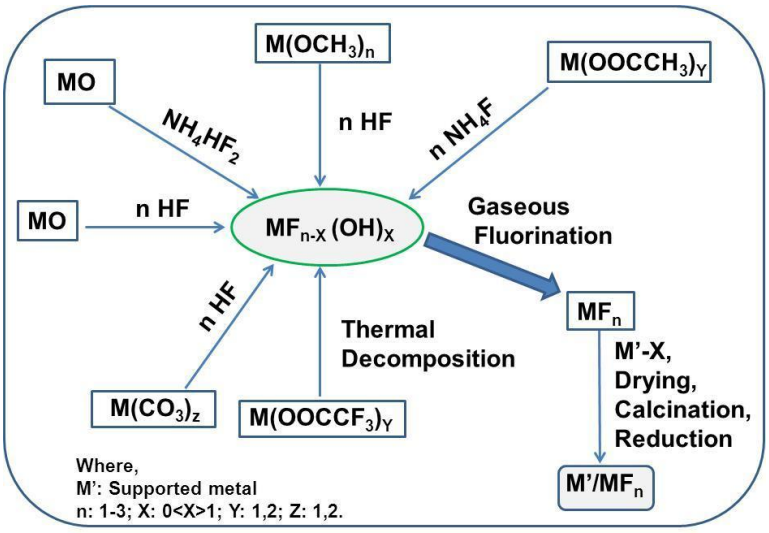

Figure 1.6. Various methods of synthesis of metal fluoride catalysts.

Some of the common catalyst preparation methods used for synthesis of metal fluorides is discussed below.

A. Crystallization / precipitation from aqueous solutions (Classical methods)

Generally metal fluorides are synthesized from metal salts using precipitation method. Metal precursors like metal oxides [27], hydroxides [27], nitrates [28],

carbonates [29], chlorides [30] and alkylates [31] on treatment with 40% aqueous hydrofluoric acid solution resulted in precipitate of metal fluoride. Using this method, hydrates of metal fluoride can be synthesized which possesses low surface areas. Kleist et al. have used this method for the synthesis of aluminium fluoride by fluorination of alumina in aqueous system [32].

B. Gaseous fluorination of metal oxides (solid-gas reaction)

The gaseous fluorination of metal oxides is commonly carried out by passing fluorine vapors on the metal oxides using organic compounds (e.g. CF_4, CHF_3, CH_2F_2, CF_3COOH, CF_3SO_3H, CF_3OCF_3, CF_3CH_2OH etc) [33], fluoro-sulfur compounds (e.g. SF_6, SO_2F_2 and SOF_2) [34] or inorganic compounds (e.g. HF, BF_3, NH_4F) [35] at temperature ranging between 100-500 °C. The degree of fluorination is however functioning of various factors such as temperature, fluorination time and nature of fluorinating agent. This method develops both pure phases of only metal fluorides MF_X as well as mixed phases of hydroxyl fluorides $[M(OH)_xF_y]$ and/or oxyfluorides $[MO_xF_y]$. The mechanism of fluorination depends strongly on the fluorinating agent used [36]. The synthesis of fluorinated alumina ($F\text{-}Al_2O_3$) [37] and chromia ($F\text{-}Cr_2O_3$) [38] were carried using this method.

C. Sol-gel method

The sol-gel method has shown wide range of applications in coating, glass industries and ceramic [39]. It is reported in the synthesis of metal oxides based heterogeneous catalysts [40]. The sol-gel method has been recognized for its versatility, which permits control of the texture, composition, homogeneity and structural characteristics of the solids. The synthesis and the applications of the sol-gel synthesized catalysts have been extensively reviewed in many reports [41,42]. The sol-gel technique offers several advantages for the synthesis of catalytic nanoscopic materials:

a) It is simpler, low temperature process and offers high surface area materials.
b) A control over porosity and microstructural properties can be achieved.
c) It can be easily modified to improve thermal stability and the catalytic activity
d) The method is potentially easier to scale up
e) This method is also suitable for the production of thin-films, coatings and ceramic materials.

The method is based on the hydrolysis and gelation of metal alkoxide or other reactive compounds in alcoholic solutions [43,44]. The schematic representation for sol-gel method is given in scheme.1.1. The chemistry of the processes can be control by altering of various parameters during preparation, such as pH, solvent and amount of water added for reaction.

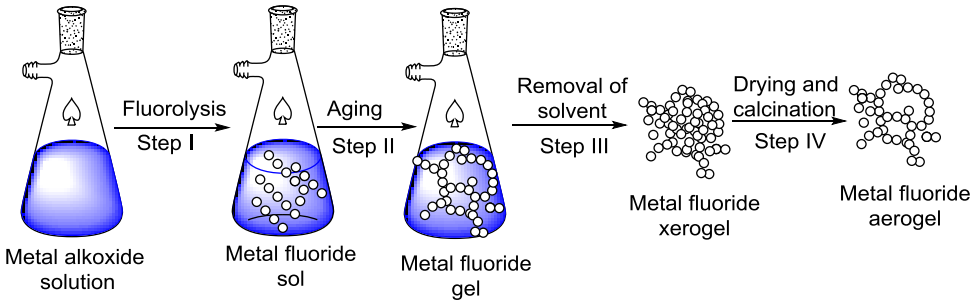

Scheme 1.1. Sol-gel synthesis method of metal hydroxyl fluoride.

The mechanism of sol-gel synthesis is discussed below.

Path I: Hydrolysis (hydroxylation) of the metal alkoxide

$$M\text{-}OR + HF/H_2O \longrightarrow M\text{-}F_x(OH)y + R\text{-}OH \quad (M = \text{metal; } R = \text{alkyl})$$

Path II: Olation (condensation with formation of fluoride/hydroxyl bridges)

$$M\text{-}F + M\text{-}OHF \longrightarrow M\text{-}F\text{-}M\text{-}OH\text{-}M + X\text{-}OH \quad (X = H \text{ or } R)$$

Path III: Oxolation (condensation with formation of fluoride/oxide bridges)

$$M\text{-}F\text{-}M\text{-}OH\text{-}M \longrightarrow M\text{-}F\text{-}M\text{-}O\text{-}M + X\text{-}OH \quad (X = H \text{ or } R)$$

Additionally, other two indirect methods are also known for sol-gel synthesis of metal fluorides as follows

i) Post-fluorination of a metal oxide [45].

ii) Sol-gel formation of metal trifluoroacetate and thermal decomposition [46].

Owing to possession of very high lattice energies of metal fluorides, they are known to undergo crystallization which led to decrease in their surface areas. For example aluminium fluoride synthesized using conventional method has BET surface areas ~20 m^2/g [47]. Kemnitz and coworkers have reported a non-aqueous sol-gel process for the synthesis of high surface area (*HS*) aluminium fluorides with extraordinary surface and catalytic properties [48]. AlF_3 prepared using sol-gel method showed nanoscopic, mesoporous and highly distorted structure with high

surface areas (~450 m^2g) [49]. The Lewis acidity was as high as antimony fluoride (SbF_5) and aluminium chlorofluoride ($AlClF_2$) [50]. Thus aluminium fluoride was used as an acidic catalyst or catalytic support for heterogeneous reaction [51]. The metal fluoride used in ceramics can be prepared using sol-gel method and cold-pressing method [52]. Patil et al. have further explored the synthesis of wide range of fluorides with different functionalities. The sol-gel method also offers the probability of incorporating one or more additional active components of interest into the metal fluorides matrices which enable the high dispersion of "dopant" at nanoscopic scale.

D. Advance special methods for metal fluorides synthesis

The special advanced methods for the synthesis of highly dispersed metal fluorides are listed below [53-57].

1. Plasma fluorination
2. Chemical vapor deposition (CVD)
3. Powder vapor deposition (PVD)
4. Mechanical milling
5. Laser dispersion
6. Pyrolysis of fluorine containing compounds
7. Hydrothermal synthesis
8. Microwave-assisted methods
9. Thermal decomposition of fluorine promoted materials

1.3.3. General introduction to few metal fluorides

A. Magnesium fluoride (MgF_2) [27]

Generally MgF_2 is prepared by following methods

1. Using precipitation method from MgO/$Mg(OOCCH_3)$/ $MgCO_3$/ $Mg(NO_3)_2$.
2. Using sol-gel method from magnesium metal via magnesium methoxide
3. Using advance methods like CVD and PVD

It crystallizes in the rutile form, in which Mg^{2+} ions are bounded with six fluoride ion and each F^- ion by three Mg^{2+} ions [58]. It is an inert solid fluoride without acidic properties [59], however MgF_2 synthesized using sol-gel method possesses moderate Lewis type of acidity [60]. It is used as catalyst for various reactions like hydrodesulfurization, hydrodechlorination and reduction of NOx [61, 62]. MgF_2 plays an important role as support for various oxides (V_2O_5, MoO_3, WO_3, CuO, and Cr_2O_3), fluorides (FeF_3, CrF_3 etc) [63] and metals (Pd, Pt and Ru) [64] also.

B. Strontium fluoride (SrF_2) [27]

Generally SrF_2 can be prepared using three methods as below

1. The reactions of strontium chloride with fluorine gas,
2. The reaction of hydrofluoric acid with strontium carbonate.
3. Thermal decomposition of strontium trifluoroacetate

It is a stable brittle white crystalline solid with melting point of 1477 °C and having boiling point 2460 °C. SrF_2 shows supersonic conductivity at elevated temperatures. It is transparent to light in the wavelengths ranges between 0.15-11 µm. Typically its optical properties are intermediate to CaF_2 and BaF_2. It is proposed that polarization of the electron core of the Sr atom which creates an approximately tetrahedral distribution of charge that interacts with the Sr-F bonds.

C. Barium fluoride (BaF_2) [27]

It occurs in nature as the mineral *frankdicksonite.* It is synthesized using similar to MgF_2. It is used in windows for FTIR spectroscopy in the field of fuel oil analysis. It is used as a common and fastest scintillator for the detection of X-rays, gamma rays and other high energy particles. BaF_2 is also used as a preopacifying agent and in enamel and glazing frits production and in the production of welding agents. It is also used in metallurgy, as a molten bath for aluminium refining.

1.3.4. Applications in organofluorine chemistry

Organofluorine compounds are used widely from oil- and water-repellents to pharmaceuticals, reagents in catalysis and refrigerants. Additionally few organofluorine compounds are pollutants due to their influence in depletion of ozone, global warming, bioaccumulation, and toxicity. Mainly the metals like Pd, Pt, Ni, and Ru supported on typical supports like activated carbon, metal oxides were used in production of organofluorine compounds. The metal fluoride successfully replaced typical supports because of high stability towards fluorine reagent like HF, MF (M = Na, K, Cs) in organofluorine chemistry. Among the noble metal supported catalysts, palladium supported on metal fluorides (MgF_2/AlF_3) possesses high activity and selectivity and stability against hydrochloric acid and/or hydrofluoric acid released during the reaction [65]. They have been comprehensively used for converting the ozone depleting chlorofluorocarbons (CFCs) to hydrofluorocarbons (HFCs) via hydrochlorofluorocarbons (HCFCs) [66]. Similarly, they have also been used for Dismutation [67], isomerization [68], hydehalogenation [69], dehydrohalogenation

[70], fluorination [71] and hydrofluorination [72]. The literature related to applications of metal fluorides in catalytic transformation of organofluorine compounds have summarized in table 1.2.

Table 1.2. Catalytic applications of metal fluorides in organo-fluorine chemistry.

Entry	Reaction with example	Ref.
1	**Dismutation** $5\ CHClF_2 \longrightarrow 3\ CHF_3 + CHCl_2F + CHCl_3$ $5\ CCl_2F_2 \longrightarrow 3\ CClF_3 + CCl_3F + CCl_4$	67
2	**Isomerization** $CF_3CH_2F \longrightarrow CHF_2CHF_2$ $CClF_2CFCl_2 \longrightarrow CF_3CCl_3$ $CF_2BrCFBrCF_3 \longrightarrow CF_3CBr_2CF_3$	68
3	**Hydrodehalogenation** $CCl_2F_2 + 2H_2 \longrightarrow CH_2F_2 + 2HCl$ $CHClF_2 + H_2 \longrightarrow CH_2F_2 + HCl$ $CF_3CCl_2F + H_2 \longrightarrow CF_3CH_2F + 2HCl$	69
4	**Dehydrohalogenation** $CH_3CCl_3 \longrightarrow CH_2{=}CCl_2 + HCl$ $CF_3CH_2F \longrightarrow CF_2{=}CHF + HF$	70
5	**Cl/F exchange or Fluorination** $CH_2Cl_2 + 2HF \longrightarrow CH_2F_2 + 2HCl$ $CF_2CH_2Cl + HF \longrightarrow CF_3CH_2F + HCl$ $ArCl + HF \longrightarrow ArF + HCl$	71
6	**Hydrofluorination** $CCl_2{=}CCl_2 + x\ HF \longrightarrow CF_3CHCl_{(2-X)}F_X + x\ HCl$	72

1.3.5. Applications in fine chemical synthesis

The uses of metal fluorides as catalysts is not only restricted to organofluorine chemistry but also for the synthesis of fine chemicals (table 1.3). Typically metal fluorides shows presence of both Lewis and Brønsted acidic sites on the surface due to unsaturation in coordination and surface hydroxyl groups respectively. Therefore in recent years, metal fluorides have been successfully used as acidic catalyst or catalytic support for variety of acid catalyzed reactions which includes Friedal-Crafts alkylation and acylation [73], *o*-xylene isomerization [74], synthesis of menthol [75], xylose valorization [76], saccharification of cellulose [77], synthesis of vitamin E [78], electrophilic substitution of benzyl alcohols [79], and base catalyzed reactions like Michael additions [80], Suzuki cross coupling [81]. Along the metal fluorides have also used as oxidation catalyst in oxidative dehydrogenation (ODH) of propane [82], oxidation of ethyl benzene [83], ammoxidation of picoline [84], and hydrogenation catalyst reduction of nitrobenzene [85].

Table 1.3. Catalytic applications of metal fluorides in heterogeneous catalysis.

Entry	Reaction with example	Ref.
1	**Friedal-Crafts reactions** 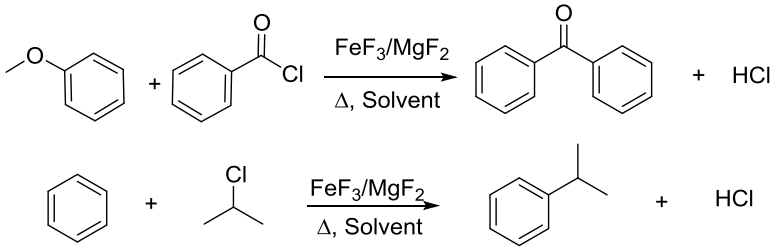	73
2	**Isomerization of *o*-xylene** 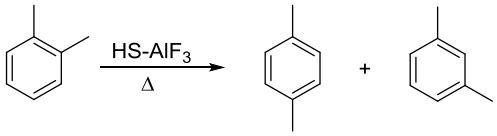	74
3	**Synthesis of menthol** 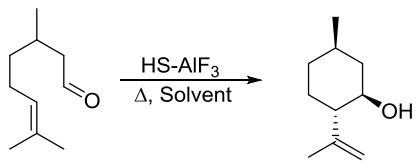	75

4	**Valorization of xylose** 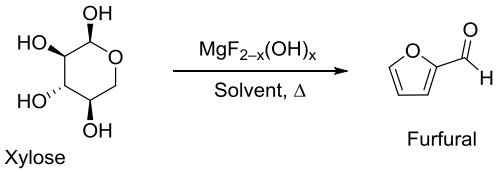 	76
5	**Saccharification of cellulose** 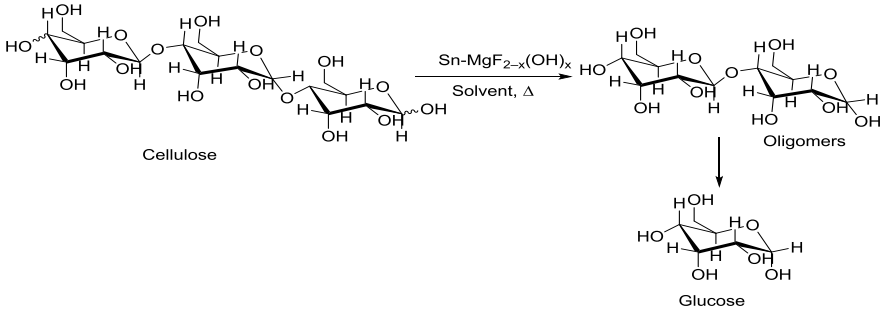 	77
6	**Synthesis of vitamin E** 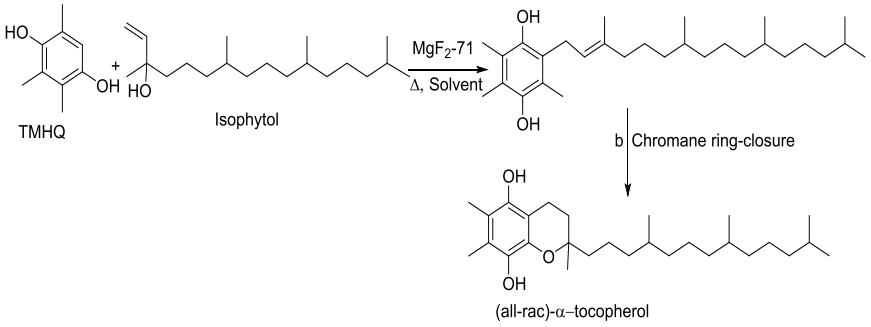 	78
7	**Electrophilic substitution using benzyl alcohols** 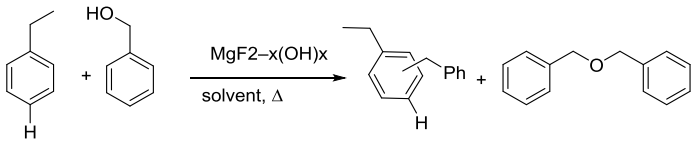 	79
8	**1,4-Michael addition for 2-methylcyclohexane-1,3-dione** 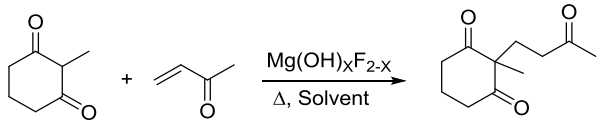 	80
9	**Suzuki coupling using 4-bromoanisole** 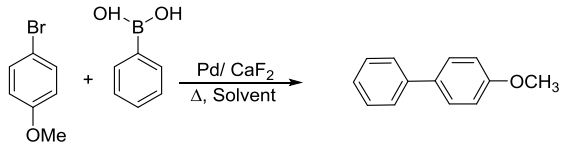 	81

10	**Oxidative dehydrogenation of propane** 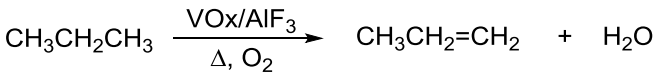	82
11	**Oxidation of ethylbenzene** 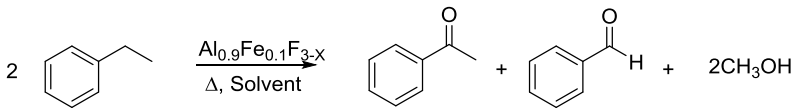	83
12	**Ammoxidation of 3-methylpyridine** 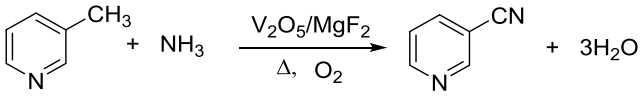	84
13	**Reduction of nitrobenzene** 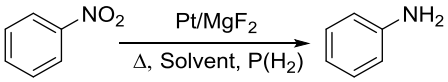	85

1.4. Palladium in catalysis

1.4.1. Palladium (Pd)

Palladium was discovered by William Hyde Wollaston in 1803, it behaves as a soft acid (low electronic orbital energy level for accepting electrons). Although Pd is considered as an expensive metal, currently compared to other noble metals (*i.e.*, platinum, gold or rhodium) its base price are 2 to 3-times lower [86]. Pd can adsorb over 900 times its volume of hydrogen forming a solid solution with hydrogen, *i.e.*, Pd *β*-hydride (Pd *β*-hydride is metallic Pd that contains a substantial quantity of hydrogen within its crystal lattice), which is expelled when heated. Another important property of Pd is that spontaneous dissociation of H_2 molecules on the surface.

The statistical data obtained from *SciFinder* showed that publication in the area of palladium based catalysis contributes more that 31% among all noble metals since 1950 (fig. 1.7 A). Also a special focus of a research community was observed in the area palladium based catalysis (fig. 1.7 B).

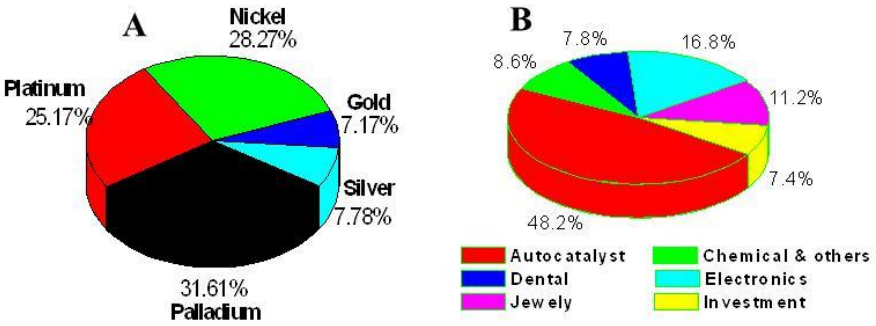

Figure 1.7. A) Contribution of different noble metals in scientific research and B) contributions of catalytic research in over-all palladium research since 1950.

1.4.2. Synthesis of supported palladium catalysts

Synthesis of the supported metal catalysts with desired active sites is often a challenging task because even minor alterations of the preparation conditions can have a significant effect on the catalyst properties. These factors often influence the demands like high activity, high selectivity and long lifetime of the catalysts in the catalytic reaction. Method of preparation, use of different metal precursors (chloride, nitrate, acetates, complexes and ligands) and additives (precipitating or reducing), supports (high or low surface area) and thermal treatments can alter the chemical features and performance of the final catalyst because they can influence considerably the nature and size of the metal particles and their interactions with the support, which determine the catalytic behavior of the supported catalyst [87]. Typically the supported heterogeneous catalysts are prepared using the different available methods like as follows.

A. Impregnation and drying

Generally, an impregnation process is related the introduction of the dissolved aqueous metal precursors onto the supports [88], after which the solvent will be eliminated by drying. For palladium based catalysts preparation, H_2PdCl_4, $Pd(NO_3)_2 \cdot 2H_2O$, Na_2PdCl_4, K_2PdCl_4, $Pd(NH_3)_4Cl_2$, $Pd(OOCCH_3)_2$, $Pd(acac)_2$ and $Pd(NH_3)_4(NO_3)_2$ are commonly used precursors [89].

B. Precipitation and co-precipitation

The formation of a precipitate from a homogeneous solution may occur as a result of physical transformations such as temperature or solvent evaporation, but

mostly by chemical processes such as addition of acid or base, presence of impurities as well as use of complex forming agents.

C. Deposition-precipitation

The deposition-precipitation is similar to the precipitation method except that the precipitate after its immediate formation deposits on the support, which is present in the reaction vessel.

1.4.3. Applications of supported palladium catalysts

Palladium is used as essential tool for many applications like organic synthesis, catalysis, polymers and materials. In share, this extensive scope is due to its ability to participate in catalytic transformations, as well as its high functional group tolerance. Palladium catalysis has impacted nearly every area of organic synthesis. The supported palladium catalysts are used in industry for hydrogenation [90], dehydrogenation [91], hydrodehalogenation [92], petroleum cracking [93], water gas shift [94], steam reforming [95], and oxidation reactions [96]. In addition Pd catalysts also enables important coupling reactions like Heck, Suzuki, Stille, Sonogashira and Buchwald-Hartwig cross-couplings, Wacker process, Tsuji-Trost allylation [97]. Pd-based catalytic methods often proceed under mild conditions which offer high yields, with excellent levels of chemo-, stereo-, and regioselectivity. The catalytic performance of Pd catalyst is strongly dependent on interactions between active support and metal nanoparticles, the method of preparation, precursor materials and additives, thermal pretreatment, co-components. The most conventional supports for Pd-based hydrogenation catalysts are silica, γ-alumina and charcoal. These porous supports provide large surface areas in the order of 200 - 400 m^2/g for SiO_2 and γ-Al_2O_3 and 1000 m^2/g for activated charcoal.

The extensive use of the Pd as catalyst is due to its high activity and selectivity. Additionally, it also has several advantages such as

- Use of minimum quantity of catalysts,
- No special infrastructure facility
- Excellent selectivity leads to high product yield
- Highly stable nature of the catalysts under reaction conditions,
- Generally pretreatment procedure is not require

The support stabilizes the Pd crystallites against sintering or leaching. They can also have intrinsic catalytic activity, related to their Brønsted or Lewis

acidity/basicity. In addition, metal-support interactions, activity and stability of catalyst and deactivation of catalyst help in deciding the choice of support for optimal catalyst performance.

1.4.4. Role of supports in palladium catalysis

The performance of catalysts is often changed by the use of different supports because of their different physical and chemical properties like thermal stability, acid-base properties, high surface area, oxygen storage capacity and reducibility. Generally the selection of the support is done on the basis of type of reactions. For example, in oxidation reaction, the selection of a particular support for the Pd particles is based on the point of zero charge (PZC) of the support [98]. The increasing order of PZC of the some common supports is a follows: MoO_3 > Nb_2O_3 > SiO_2 > TiO_2 > CeO_2 > ZrO_2 > Co_3O_4 > Al_2O_3 > activated carbon ≈ carbon black> graphene oxide. MoO_3 or NbO_3 have high acidic PZC, i.e., a negatively charged surface is good for adsorption of cationic metal precursors, whereas carbon supports with high PZC are useful to support the metal particles in the reduced state.

In case of aerobic oxidation of alcohols, frequently oxides are used for supporting palladium. Due to high PZC of oxides the catalytically active species Pd^{2+} is stabilized over oxide support. Hence the supports like TiO_2, CeO_2, ZrO_2, Co_3O_4 and Al_2O_3 have been used for stabilization of both cationic and anionic species. Along with the stabilization of catalytically active species the oxygen donating capacity of support is important for oxidation reactions. Among all supports, CeO_2 shows higher tendency to donate oxygen, hence it is more active for oxidation reaction.

Similarly in case of hydrogenation reaction, the Pd nanoparticles which are more stable over neutral support and supports with least PZC values show better catalytic activity and stability. Hence activated charcoal, carbon black and graphene oxide are used even industrially as support for hydrogenation reactions. However, sometimes, modifications in the preparation conditions, thermal pretreatments can also dominate the role of supports.

In general, palladium nanoparticle on different support behaves differently due to change in their properties and stability of catalytically active species. Apart from the conventional support, the supports like metal fluorides have attracted to catalytic research. The metal fluorides supports are known for stabilization of active palladium species due to metal–support interactions. It is interesting to study the activity of

palladium supported on different metal fluorides for various industrially important catalytic reactions like hydrogenation, oxidation and epoxide ring opening.

1.5. Research scope and objectives of the thesis

Considering the role of supported Pd in various heterogeneous catalytic reactions, the objective of this thesis is to generalize the one pot sol-gel synthesis route of Pd supported on alkaline earths metal fluorides. The synthesized catalysts were used as heterogeneous catalyst for various organic reactions of academic as well as industrial interest. To achieve above mentioned objectives, Pd supported on alkaline earth metal fluorides exhibiting varying Lewis acidic/ basic properties have been investigated in the present study. The detailed objectives of the thesis are as follows:

- Synthesis of palladium supported on metal fluorides like, $MgF_XOH_{(2-X)}$, $SrF_X\ OH_{(2-X)}$, and $BaF_X\ OH_{(2-X)}$ using one pot sol-gel method
- Characterization of synthesized catalysts using various physico-chemical techniques
- Study of catalytic activity of synthesized catalysts for the important reactions like hydrogenation, oxidation and alcoholysis of epoxides and understanding of mechanism by *in-situ* FTIR studies.

1.6. Outline of the thesis

This section deals with the chapter wise arrangement of the work performed during the Ph.D. tenure.

Chapter 1 briefly introduces the general concept of catalysis and heterogeneous catalysis. This also explains the types and properties of heterogeneous catalysts with special attentions towards metal-support interactions. A synthesis pathways and properties and catalytic applications of metal fluorides are also discussed with special consideration to MgF_2, SrF_2 and BaF_2. With a brief introduction of Pd, the methods of synthesis and catalytic application of palladium catalyst are discussed.

Chapter 2 describes the synthesis, characterizations of Pd supported sol-gel synthesized magnesium fluoride catalysts and its applications for catalytic hydrogenation. The study in this chapter is divided into two sections, First **(2A)** section mainly deals with synthesis and characterizations of Pd supported magnesium

hydroxyl fluoride catalysts using different concentration of aq. HF. Further these catalysts are used for catalytic olefin hydrogenation under ambient reaction conditions. Further, *in-situ* mechanism study using FTIR spectroscopy for catalytic hydrogenation is also discussed. Later **Section 2B** showed the applications of Pd supported on magnesium fluoride as novel catalyst for catalytic hydrogenation of vegetable oils under solvent and solvent free conditions.

Chapter 3 deals with the synthesis and characterization of sol-gel synthesized Pd supported on barium hydroxyl fluoride catalyst and its applications in selective catalytic aerobic oxidations of alcohols under base-free conditions. Various reaction parameters are studied to optimize reaction conditions so as to achieve maximum conversion and selectivity. Aerobic oxidation is studied using various alcohols in order to study the substrate scope. Further, i*n-situ* mechanism study using FTIR spectroscopy for catalytic aerobic alcohol oxidation is also discussed.

Chapter 4 describes the synthesis and characterization of sol-gel synthesized Pd supported on strontium hydroxyl fluoride catalyst and its applications in alcoholysis of epoxides under mild conditions Various reaction parameters are studied to optimize reaction conditions so as to achieve maximum conversion and selectivity. Alcoholysis of epoxides is studied using various epoxides in order to study the substrate scope.

Chapter 5: This chapter presents the summary and conclusions of the thesis work.

1.7. References

[1] J. J. Berzelius, *J. Ber. Chem*., **1835**, *15*, 237.

[2] W. Ostwald, *Ann. Naturphil*., **1910**, 9.

[3] J. Sinfelt, *Surf. Sci.*, **2002,** *500*, 923.

[4] G. Ertl, H. Knozinger and J. Weitkamp, *Handbook of Heterogeneous Catalysis*, Wiley- VCH, Weinheim, **1997**.

[5] V. Smil, *Nature*, **1999**, *400*, 415.

[6] B. E. Leach, *Applied industrial catalysis*, Academic press, Inc. New York, **1983**.

[7] S. Brunauer, P. Emmett, E. Teller, *J. Am. Chem. Soc*., **1938**, *60*, 309.

[8] G. Parshall, S. Ittel, *Homogeneous Catalysis*, John Wiley, New York, **1992**.

[9] R. L. Burwell Jr., G. L Haller, K. C. Taylor, J. F. Read, *Adv. Synth. Catal.*, **1969**, *29*, 1.

[10] A. P. Kieboom, J. Moulijn, P. W. N. M. van Leeuwen, R.A. van Santen,

Catalysis: An Integrated Approach, *Stud. Surf. Sci. Catal*., Elsevier, Amsterdam, Ed. 2, **1999**.

[11] S. M. George, *Chem. Rev.*, **1995**, *3*, 475.

[12] C. L. Pieck, M. B. Gonzalez, J. M. Parera, *Appl. Catal. A*, **2001**, *205*, 305.

[13] R. Szostak, *Molecular Sieves*, Blackie Academic & Professional, London, Ed. 2, **1998.**

[14] W. O. Haag, R. M. Lago, P. B. Weisz, *Nature*, **1984**, *309*, 589.

[15] H. Widdecke, P. Hodge, *Synthesis and Separations Using Functional Polymers*, John Wiley & Sons, **1988.**

[16] S. M. George, *Chem. Rev.*, **1995**, *95*, 475.

[17] A. S. K. Hashmi, G. J. Hutchings, *Angew. Chem. Int. Ed*., **2006**, *45*, 7896.

[18] K. Sekizawa, H. Widjaja, S. Maeda, Y. Ozawa, K. Eguchi, *Catal. Today*, **2002**, *59*, 69.

[19] R. A. Sheldon, I. Arends, U. Hanefeld, *Green Chemistry and Catalysis*, Wiley-VCH Verlag GmbH & Co. KGaA, Weinheim, **2007**.

[20] S. Rudiger, E. Kemnitz, *Dalton Trans.*, **2008**, 1117-1127.

[21] J. Lucas, F. Smektala, J. I. Adam, *J. Fluorine Chem.*, **2002**, *114*, 113.

[22] M. Ahrens, G. Scholz, S. Redmer, E. Kemnitz, *Solid State Sci.*, **2007**, *9*, 833.

[23] S. A. Pollack, M. Robinson, *Electronics Lett.*, **1988**, *24*, 320.

[24] G. G. Amatucci, N. Pereira, *J. Fluorine Chem*., **2007**, *128*, 243.

[25] B. Coq, F. Medina, D. Tichit, A. Morato, *Catal. Today*, **2004**, *88*,127.

[26] D. J. Sung, D. J. Moon, S. Moon, J. Kim, S.-I Hong, *Appl. Catal. A,* **2005**, *292*, 130.

[27] A. Tressaud, *Functionalized inorganic fluorides: synthesis, characterization and properties of nanostructured solids*, John Wiley & Sons, **2010**.

[28] M. F. Best, U.S. Patent No. 5,268,196, **1993**.

[29] J. Haber, M. Wojciechowska, *J. Catal.*, **1988**, *110*, 23.

[30] R. H. Hina, R. K. Al-Fayyoumi, *J. Mol. Catal. A,* **2004**, *207*, 27.

[31] N. Herron, D. L. Thorn, R. L. Harlow, F. Davidson, *J. Am. Chem. Soc.*, **1993**, *115*, 3028.

[32] W. Kleist, C. Haessner, O. Storcheva, K. Koehler, *Inorg. Chim. Acta*, **2006**, *359*, 4851.

[33] E. Kemnitz, J. M. Winfield, *Advanced Inorganic Fluorides: Synthesis,*

characterization and Applications, Elsevier Amsterdam, **2000**, 367.

[34] A. K. Ghosh, R. A. Kydd, *Catal. Rev.-Sci. Eng*., **1985**, *27*, 539.

[35] V. R. Choudhary, *Ind. Eng. Chem., Prod. Res. Dev*., **1977**, *16*, 12.

[36] O. Boese, W. E. S. Unger, E. Kemnitz, S. L. M. Schoeder, *Phys. Chem. Chem. Phys*., **2002**, *4*, 2824.

[37] (a) T. Skapin, E. Kemnitz, *Catal. Lett.*, **1996**, *40*, 241; (b) R. I. Hegde, M. A. Barteau, *J. Catal.*, **1989**, *120*, 387; (c) L. E. Manzer, *Science*, **1990**, *249*, 31.

[38] (a) T. Skapin, E. Kemnitz, *J. Non-Crys. Solids*, **1998**, *225*, 163. (b) H. Bozorgzadeh, E. Kemnitz, M. Nickkho-Amiry, T. Skapin, J. M. Winfield, *J. Fluorine Chem.*, **2001**, *107*, 45; (c) H. Bozorgzadeh, E. Kemnitz, M. Nickkho-Amiry, T. Skapin, J. M. Winfield, *J. Fluorine Chem.*, **2001**, *110*, 181.

[39] C. J. Brinker, G. W. Scherer, *Sol Gel Science: The Physics and Chemistry of the Sol Gel Processing*, Academic Press, San Diego, **1990**.

[40] (a) A. C. Pierre, G. M. Pajonk, *Chem. Rev.*,**2002**,*102*, 4243; (b) A. P. Wight, M. E. Davis, *Chem. Rev.*, **2002**,*102*, 3589.

[41] D. P. Debecker, P. H. Mutin, *Chem. Soc. Rev.*, **2012,** 41, 3624.

[42] H. D. Gesser, P. C. Goswami, *Chem. Rev.*, **1989,** 89, 765

[43] A. C. Pierre, G. M. Pajonk, *Chem. Rev.*, **2002,** *102*, 4243.

[44] C. J. Brinker, G. W. Sherer, *Sol-Gel Science, Academic Press*, San Diego, **1990,** 20

[45] H. X. Mai, Y. W. Zhang, R. Si, Z. G. Yan, L. Sun, L. P. You, C. H. Yan, *J. Am. Chem. Soc*., **2006**, *128*, 6426.

[46] S. Fujihara, *Recent Res. Dev. Mater. Sci.*, **2002**, *3*, 619.

[47] E. Kemnitz, D. H. Menz, *Prog. Solid State. Chem.*, **1998**, *26*, 97.

[48] E. Kemnitz, U. Groß, S. Rüdiger, C. S. Shekar, *Angew. Chem. Int. Ed.*, **2003**, *42*, 4251.

[49] S. K. Rüdiger, U. Groß, M. Feist, H. A. Prescott, S. C. Shekar, S. I. Troyanov, E. Kemnitz, *J. Mater. Chem.*, **2005,** *15*, 588.

[50] T. Krahl, R. Stösser, E. Kemnitz, G. Scholz, M. Feist, G. Silly, J.- Y. Buzare, *Inorg. Chem.*, **2003**, *42*, 6474.

[51] J. Krishnamurthy, U. Gross, S. Rüdiger, V. V. Rao, V. V. Kumar, A. Wander, C. L. Baily, N. M. Harrison, E. Kemnitz, *J. Phys. Chem., B*, **2006**, *111*, 8314.

[52] M. Ahrens, G. Scholz, S. Redmer, E. Kemnitz, *Solid State Sci.*, **2007**, *9*, 833.

[53] S. V. Kuznetsov, V. V. Osiko, E. A. Tkatchenko, P. P. Fedorov, *Russ. Chem. Rev.*, **2006**, *75*, 1065.

[54] S. Sakka, *Handbook of sol-gel science and technology*, Springer, **2005**, *1*.

[55] C. Zhao, S. Feng, Z. Chao, C. Shi, R. Xu, J. Ni, *Chem. Commun*., **1996**, 1641.

[56] D. Dambournet, A. Demourgues, C. Martineau, S. Pechev, J. Lhoste, J. Majimel, A. Vimont, J.-C. Lavalley, C. Legein, J.-Y. Buzare, F. Fayon, A. Tressaud, *Chem. Mater.*, **2008**, *20*, 1459.

[57] A. K. Ghosh, R. A. Kydd, *Catal. Rev. Sci. Eng*., **1985**, *27*, 539.

[58] M. Wojciechowska, M. Zielinski, M. Pietrowski, *J. Fluorine Chem.*, **2003**, *120*, 1.

[59] M. Wojciechowska, R. Fiedorow, *J. Fluorine Chem*., **1980**, *15*, 443.

[60] J. Krishna Murthy, U. Gross, S. Rüdiger, E. Kemnitz, J. M. Winfield, *J. Solid State Chem.*, **2006**, *179*, 743.

[61] M. Wojciechowska, K. Nowinska, W. Kania, A. Nowacka, *React. Kinet. Catal. Lett.*, **1975**, *2*, 229.

[62] M. Wojciechowska, M. Pietrowski, S. Lomnicki, B. Czajka, *Catal Lett*., **1997**, *46*, 63.

[63] (a) A. Maliowski, W. Juszczyk, J. Pielaszek, M. Bonarowska, M. Wojciechowska, Z. Karpinski, *Chem. Commun*., **1999**, 685; (b) J. K. Murthy, U. Groß, S. Rüdiger, E. Kemnitz, *Appl. Catal.*, A, **2004**, *278*, 133.

[64] H. Berndt, H. B. Zahed, E. Kemnitz, M. Nickkho-Armiy, M. Pohl, J. M. Winfield, *J. Mater. Chem*., **2002**, *12*, 3499.

[65] B. Coq, F. Medina, D. Tichit, A. Morato, *Catal. Today*, **2004**, *88*, 127.

[66] (a) B. Coq, J. M. Cognion, F. Figueras, D. Tournigant, *J. Catal*., **1993**, *141*, 21; (b) P. K. Ramarao, K. S. Ramarao, A. H. Padmasri, *Cattech*, **2003**, *7*, 218.

[67] A. Hess, E. Kemnitz, A. Lippitz, W. E. S. Unger, D. -H. Menz, *J. Catal*., **1994**, *148*, 270; (b) S. Rüdiger, G. Eltnany, U. Groß, E. Kemnitz, *J. Sol-Gel Sci. Technol.*, **2007**, *41*, 209; (c) G. Eltnany, *Ph. D. Thesis*, Humboldt University of Berlin, **2007**; (d) P. T. Patil, *Ph. D. Thesis*, Humboldt University of Berlin, **2008**.

[68] K.-U. Niedersen, K. Fiedler, E. Kemnitz, *J. Fluorine Chem.*, **2005**, *126*, 1017.

[69] E. Kemnitz, K.-U. Niedersen, *J. Catal.*, **1995**, *155*, 283.

[70] O. Bose, B. Adamczyk, K. Fiedler, E. Kemnitz, *Catal. Lett.*, **1998**, *54*, 211.

[71] (a) H. Yang, H. Quan, M. Tamura, A. Sekiya, *J. Mol. Catal. A: Chem.*, **2003**, *233*, 99; (b) H. Lee, H. S. Kim , H. Kim, W. S. Jeong, I. Seo, *J. Mol. Catal. A: Chem.*, **1998**, *136*, 85.

[72] Y. Zhu, K. Fiedler, S. Rüdiger, E. Kemnitz, *J. Catal.*, **2003**, *219*, 8.

[73] J. Krishna Murthy, U. Groß, S. Rüdiger, E. Kemnitz, *Appl. Catal. A*, **2004**, *278*, 133.

[74] S. Rudiger, E. Kemnitz, *Dalton Trans.*, **2008**, 1117.

[75] A. Negoi, S. Wuttke, E. Kemnitz, D. Macovei, V. I. Parvulescu, C. M. Teodorescu, S. M. Coman, *Angew. Chem. Int. Ed.*, **2010**, *49*, 8134.

[76] I. Agirrezabal-Telleria, Y. Guo, F. Hemmann, P. L. Arias, E. Kemnitz, *Catal. Sci. Technol*., **2014**, *4*, 1357.

[77] S. Wuttke, A. Negoi, N. Gheorghe, V. Kuncser, E. Kemnitz, V. Parvulescu, S. M. Coman, *ChemSusChem*, **2012**, *5*, 1708.

[78] S. M. Coman, S. Wuttke, A. Vimont, M. Daturi, E. Kemnitz, *Adv. Synth. Catal.*, **2008**, *350*, 2517.; (b) S. Wuttke, S. M. Coman, G. Scholz, H. Kirmse, A. Vimont, M. Daturi, S. L. M. Schroeder, E. Kemnitz, *Chem Eur. J.*, **2008**, *14*, 11488.

[79] N. S. Candu, S. Wuttke, E. Kemnitz, S. M. Coman, V. I. Parvulescu. *Appl. Catal. A*, **2011**, *391*, 169.

[80] H. A. Prescott, Z-J. Li, E. Kemnitz, J. Deutsch, H. Lieske, *J. Mater. Chem.*, **2005**, *15*, 4616.

[81] (a) S. S. Pröckl, W. Kleist, K. Köhler, *Tetrahedron*, **2005,** *61*, 9855; (b) P. T. Patil, A. Dimitrov, J. Radnik, E. Kemnitz, *J. Mater. Chem.*, **2008**, *18*, 1632.

[82] K. Scheurell, G. Scholz, A. Pawlik, E. Kemnitz, *Solid State Sci.*, **2008,** *10*, 873.

[83] I. K. Murwani, K. Scheurell, E. Kemnitz, *Catal. Commun.*, **2008**, *10*, 227.

[84] V. N. Kalevaru, B. D. Raju, V. V. Rao, A. Martin, *Catal. Commun*., **2008,** *9*, 715.

[85] M. Pietrowski, M.Wojciechowska, *Catal. Today*, **2011**, *169*, 217.

[86] *http://www.platinum.matthey.com*

[87] A. Lycourghiotis, *Synthesis of Solid Catalysts*, Wiley-VCH Verlag GmbH & Co. KGaA, **2009**.

[88] J. A. Schwarz, C. Contescu, A. Contescu, *Chem. Rev*., **1995**, *95*, 477.

[89] M. Gurrath, T. Kuretzky, H. P. Boehm, L. B. Okhlopkova, A. S. Lisitsyn, V. A. Likholobov, *Carbon*, **2000**, *38*, 1241.

[90] (a) G. Brieger, T.J. Nestrick, *Chem. Rev*., **1974**, *74*, 567; (b) C.R. Lederhos, M. J. Maccarrone, J. M. Badano, G. Torres, F. Coloma-Pascual, J. C. Yori, M. E. Quiroga, *Appl. Catal. A*, **2011**, *396*, 170.

[91] E. Gbenedio, Z. Wu, I. Hatim, B. F. K. Kingsbury, K. Li, *Catal. Today*, **2010**, *156*, 93.

[92] L. Rodríguez, D. Romero, D. Rodríguez, J. Sánchez, F. Domínguez, G. Arteaga, *Appl. Catal. A.* **2010**, *373*, 66.

[93] J. A. Moulijn, P. W. N. M. van Leeuwen, R. A. van Santen, *Stud. Surf. Sci. Catal*., Elsevier, **1993**.

[94] Y. Bi, H. Xu, W. Li, A. Goldbach, *Int. J. Hydrogen Energy*, **2009**, *34*, 2965.

[95] L. S. F. Feio, C. E. Hori, S. Damyanova, F. B. Noronha, W. H. Cassinelli, C. M. P. Marques, J. M. C. Bueno, *Appl. Catal. A*, **2007**, *316*, 107.

[96] E. Abdellatif, S. E. Kazzouli, M. Bousmina, *J. Nanosci. Nanotechnol.*, **2014**, *14*, 2012.

[97] T. Punniyamurthy, S. Velusamy, J. Iqbal, *Chem. Rev.*, **2005**, *105*, 2329.

[98] J. R. Regalbuto, *Synthesis of Solid Catalysts*, Wiley-VCH Verlag GmbH & Co. KGaA, **2009**, 33.

Chapter 2

PALLADIUM SUPPORTED ON MAGNESIUM HYDROXYL FLUORIDES: SYNTHESIS, CHARACTERIZATION AND ITS CATALYTIC APPLICATIONS

Abstract

One pot synthesis of palladium supported on magnesium hydroxyl fluoride has been carried out by fluorolytic sol-gel method. The prepared catalysts were characterized using various physicochemical techniques. The sol-gel method has led to the formation of high surface area (>135 m^2/g), mesoporous (pore volume 0.19 - 0.23 cc g^{-1} and pore diameter 3-5 nm) catalysts with uniform dispersion of palladium of ~2 nm size on the surface. The catalysts synthesized using different concentrations of aqueous hydrofluoric acid showed change in surface as well as acidic properties. Very high dispersion of Pd on magnesium fluoride (47%) was obtained for 1% Pd loading.

The prepared catalysts were used for hydrogenation of various olefins in presence of other organic functionalities at room temperature and atmospheric hydrogen pressure. Various substituted olefins have been hydrogenated with almost 100% conversion and selectivity. The catalyst was recycled efficiently for five cycles without appreciable loss in the catalytic activity. There was no Pd leaching under reaction conditions which was confirmed by ICP-AES analysis. The in-situ FTIR studies indicated facile activation of hydrogen on the palladium supported on magnesium hydroxyl fluoride however the activation of olefin on the catalyst surface could not be observed.

As palladium supported on magnesium hydroxyl fluoride showed best catalytic activity for hydrogenation of olefins it was further used for hydrogenation of oils. The hydrogenation of castor oil under ambient reaction conditions using Pd-MgF_2-100 showed decrease in iodine value of hydrogenated products upto 4 without affecting hydroxyl value. Also the catalyst showed activity for hydrogenation of edible and nonedible oils under ambient conditions. The catalyst showed could be successfully recycled upto three cycles without Pd leaching as proved by ICP-AES studies.

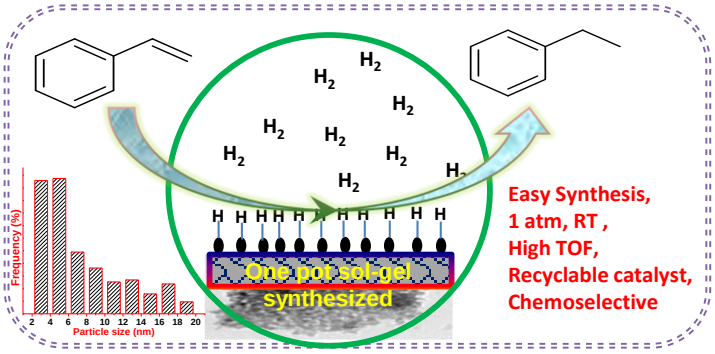

Section 2A: Palladium Supported on Magnesium Hydroxyl Fluorides: Synthesis, Characterization and Its Catalytic Applications for Selective Hydrogenation of Simple Olefins

2A.1. Introduction

A support plays a vital role in heterogeneous catalysis [1], hence a large number of supports have been explored for synthesis of efficient catalysts [2] which include carbon [3], metal oxides [4], polymeric materials [5] and magnetic nanoparticles [6]. Support not only helps adsorption and desorption of reactants and products but also has a substantial influence on the electron transfer [7], adsorption capacity [8], chemical and electronic structure of the active metal [9]. Recently, many efforts have been devoted to the design and fabrication of supported metal catalysts by changing the crystal structure, morphology and crystanality of supports [10]. The metal support interactions in catalysts depend on the characteristics of the support such as surface area, crystal facets, crystal size and acidity/basicity of the support [11].

Recently, Kemnitz et al. have reported metal fluoride based new type of nanoscopic, high surface area partly hydroxylated inorganic fluorides with bi-acidic (Lewis/Brønsted) characters for fluorination and related processes [12], such as synthesis of (all-rac)-[α]-tocopherol [13], Suzuki coupling [14], synthesis of menthol [15], Friedal-Crafts reaction [16], synthesis of vitamin K-1 and K-2 chromanol [17], oxidation of ethylbenzene [18], dehydrohalogenation of 3-chloro-1,1,1,3,-tetrafluorobutane [19], C-H bond activation [20], and glycerol acetylation [21]. Still there is an enormous scope for the exploration of these supports in various organic transformations by taking the advantages of their acidic and basic properties.

Palladium has been extensively used as catalyst in many organic transformations which include formation of C–C, C–O, C–N bonds, oxidation, and hydrogenation [22]. Among all reactions, hydrogenation of organic molecules is probably one of the most important reactions in synthetic chemistry [23]. Heterogeneous catalytic hydrogenations are significant reactions that find comprehensive industrial application in the production of pharmaceuticals, agrochemicals, fine chemicals, flavors, fragrances and dietary supplements. These

reactions are generally highly selective and easy to work up, the catalyst can often be recovered and recycled, and the processes are atom economical. Out of total catalytic reactions used to produce chemicals, hydrogenation contributes between 10–20% [24]. However it is well recognized that heterogeneous catalysts are more preferred from an industrial point of view [25], offering well-known benefits in terms of waste reduction, separation of the catalysts and recyclability [26]. Especially when palladium is present in form of nanoparticles (Pd-NPs), the catalytic activity is known to enhance considerably [27, 28]. This is closely linked to the development of suitable stabilizing agents and supporting materials such as metal oxides [29], ionic liquids [30], polymers [31], dendrimers [32] and carbonaceous materials [33]. Pd based catalysts including heterogeneous Pd catalysts (Pd/C) are widely used to hydrogenate organic functionalities, such as alkynes, alkenes, azide, nitro, benzyl ether, benzyl ester, aromatic halide, aromatic ketone, N-benzyloxycarbonyl (N-Cbz), and epoxide groups in organic syntheses [34].

A significant progress has been achieved in improving the catalytic activity, selectivity and substrate scope. The hydrogenation using Pd catalysts were carried out under drastic reaction conditions such as high pressure and high temperature leads to agglomeration of palladium and deactivation of catalyst. Further Pd leaching is another severe problem faced in many industrial processes and need to be addressed [35]. The replacement of expensive high energy consuming processes by inexpensive, low energy and environmentally benign processes is a desirable goal in hydrogenation reactions. Therefore hydrogenation under ambient temperature and pressure is ideal in industries. To explore metal fluorides as non-conventional support, palladium supported on nanoscopic magnesium fluorides have been prepared by a one pot fluorolytic sol-gel route and used it for selective hydrogenation of various olefins under ambient reaction conditions, the results of which are reported herein.

2A.2. Experimental

2A.2.1. Materials

All chemicals were procured from Aldrich chemical co. USA and used as received. Hydrofluoric acid with various concentrations (40, 71 and 100% HF alcoholic solution) were purchased from Merck chemicals, Germany and used as obtained. Solvents were freshly dried before use as per literature procedure [36].

2A.2.2. Catalyst synthesis

CAUTION: HF is a highly toxic and irritant compound causing severe burns if it comes in contact with the skin! So it is advised to use all safety wears.

Catalyst preparation was carried out under argon atmosphere using standard Schlenk technique. Series of palladium supported on magnesium hydroxyl fluoride catalysts were prepared from metallic magnesium using sol-gel method as follows: In 250 mL round bottom flask, metallic magnesium (1.56 g, 64 mmol) was dissolved in dry methanol (100 mL) at room temperature for 16 h to form the methanolic solution of magnesium methoxide. To this magnesium methoxide solution, stoichiometric amount (1:2 equivalent) of HF (130 mmol) of different concentrations (40, 71 and 100%) was added followed by addition of methanolic solution of palladium acetate (0.845 g, 3.77 mmol) corresponding to 1 wt% Pd loading. The mixture was allowed to react to form highly viscous opaque gray colored gels. The gel was aged for 12 h, and then dried under vacuum initially at room temperature for 3 h and at 60 °C for 3 h until was completely removed. The solid product was further dried at 250 °C for 5 h. Based on the concentration of aqueous HF used for synthesis; the catalysts are referred as Pd-MgF_2-40, Pd-MgF_2-71, Pd-MgF_2-100 indicating 40%, 71% and nonaqueous HF (100%) respectively. For comparison 1% Pd-MgO was synthesized using a similar procedure by adding millipore water instead of HF to the mixture of magnesium methoxide solution and methanolic palladium acetate solution corresponding to 1 wt% Pd loading followed by drying at room temperature and later at 250 ºC.

2A.2.3. Catalyst characterization

A. Powder X-ray Diffraction (PXRD) analysis

Crystallinity and phase purity of the samples were determined using powder X-ray diffraction (PXRD) analysis. Powder patterns were recorded on X'pert Pro PANalytical X-ray diffractometer with Ni-filtered Cu-Kα radiation (40 kV, 30 mA) in the 2θ range of 10 – 80 ° at a scan rate of 4 ° min^{-1} on glass substrate.

B. BET surface area measurements

The specific surface area (BET) of the samples was determined by acquiring adsorption-desorption isotherm (BET method) at 77 K for nitrogen gas using a

Autosorb Quanta Chrome corporation instrument. The micropore volume was estimated from the t-plot and the pore diameter was estimated using the Barret-Joyner-Halenda (BJH) model.

C. Ammonia –Temperature Programed Desorption (NH_3-TPD) analysis

NH_3-TPD measurements were performed on a Micromeritics AutoChem 2910 instrument. In a typical experiment, 0.1 g of catalyst was taken in a U-shaped, flow-thru, quartz sample tube. Prior to measurements, the catalyst was pre-treated in helium (30 cm^3 min^{-1}) at 250 °C for 1 h. A mixture of NH_3 in helium (10%) was passed (30 cm^3 min^{-1}) at 25 °C for 1 h. The sample was subsequently flushed with helium (30 cm^3 min^{-1}) at 100 °C for 1 h. The TPD measurements were carried out in the range 100–250 °C at a heating rate of 10 °C min^{-1}. Ammonia concentration in the effluent was monitored with a gold-plated, filament thermal conductivity detector (TCD). The amount of desorbed ammonia was determined based on the area under the peak.

D. Hydrogen chemisorption study

Hydrogen chemisorption studies were carried on a Micrometrics AutoChem 2910 instrument: 0.1 g of the catalyst was placed in a quartz tube and treated with O_2 (22%) – He (78%) gas mixture (30 $cm^3 min^{-1}$) at 250 °C for 2 h. A gas mixture of H_2 (5%) – Ar (95%) was then passed (50 cm^3 min^{-1}) through the quartz reactor at 50 °C for 1 h. The temperature was raised to 300 °C at heating rate of 10 °C min^{-1} and held at 300 °C for 30 min. The amount of hydrogen consumed was estimated and the reduction capacity of the catalyst was determined. A standard CuO powder was used to calibrate the amount of hydrogen consumption.

E. Energy Dispersive X-ray Analysis (EDAX) and Scanning Electron Microscopy (SEM)

The elemental composition on the catalyst surface and catalyst morphology was determined by EDAX analysis coupled with FEI Quanta, 200 3D SEM using an aluminium sample holder on carbon film.

F. High Resolution Transmission Electron Microscopy (HRTEM)

Palladium particle size was determined using HRTEM measurements on Tecnai F 30 instrument operated at an accelerating voltage of 200 kV. The TEM grids were prepared by dispersing the powder in 2-propanol using ultrasound. The suspension was dropped by the micropipette on a conventional carbon film with a thickness of about 20 nm supported by a copper grid. After complete evaporation of the 2- propanol from the specimen, the TEM imaging was performed.

G. X-ray Photoelectron Spectroscopy (XPS)

XPS was recorded using VG Micro Tech ESCA 3000 instrument at a pressure below 10^{-9} Torr. The samples were mounted on sample tubs. The wide scan C-1s, O-1s, F-1s, Pd-3d and Mg-2p core level spectra were recorded with a monochromatic Al Kα radiation (photon energy = 1486.6 eV) at pass energy of 50 eV and electron take off angle of 60 °. The core-level binding energies were aligned taking 'adventitious' of carbon binding energy as 284.6 eV. All peaks were fitted with Gauss-Lorentz peaks using XPSPEAK41 software to obtain peak information. A Shirley's base line was used in the fitting process.

H. Fourier transformed Infra-red Spectroscopy (FTIR)

Nicolet Nexus 670 FTIR instrument with DTGS detector was used to record the IR spectrum of the catalyst in range 4000-400 cm^{-1} with KBr pallet technique in transmission mode. In situ FTIR analysis was carried out using DRIFT accessory in Shimadzu FTIR 8300 spectrometer equipped with a mercury cadmium telluride (MCT) cryodetector. Data were collected in the 700 – 4000 cm^{-1} range at 4 cm^{-1} resolution averaged over 100 scans.

2A.2.4. Procedure for catalytic hydrogenation reaction

CAUTION: During bubbling in reaction the hydrogen is liberated, therefore all the reactions were carried out under fume hood and high safety concerns.

A two necked round bottom flask (25 mL) was charged with substrate (5.0 mmol), toluene (6 mL) and catalyst (10 wt% with respect to substrate). The reaction mixture was stirred at room temperature and hydrogen gas was bubbled through the reaction mixture at flow of 10 mL min^{-1}. The reaction was monitored by gas chromatographic analysis using Agilent 6890 Gas Chromatograph equipped with a

HP-5 dimethyl polysiloxane capillary column (60 m length, 0.25 mm internal diameter, 0.25 μm film thickness) with flame ionization detector. Products were confirmed by comparison with retention time of the authentic samples.

2A.2.5. Procedure for recyclability study of the catalyst

The recyclability of Pd-MgF_2-100 was tested for styrene hydrogenation under optimized reaction conditions (Styrene: 1.0 mmol; Catalyst: 0.01 g (10 wt %; 0.1 wt % Pd w. r. t. styrene); Toluene: 6.0 mL; H_2 bubbled; Temperature: RT (27 °C); Time: 3 h). After completion of the reaction catalyst was recovered by filtration, washed with toluene (10 mL), and finally dried at 110 °C for 30 min. The recycled catalyst was used for further catalytic cycles under identical conditions.

2A.2.6. Filtration method procedure

The filtration test was carried out to verify the Pd leaching in the reaction mixture under reaction conditions. A 0.05 g of catalyst was stirred with 0.5 g of styrene in 6 mL of toluene under typical reaction conditions i.e. bubbling hydrogen gas at room temperature (27 °C). After 1.5 h, catalyst was removed from liquid phase by filtration through Whatmann filter paper no. 1 and the reaction mixture was allowed to further react under reaction conditions without catalyst.

2A.2.7. Procedure for preparation of ICP samples

Catalyst sample was mixed with pure conc. HNO_3 acid solution (20% v/v) in 50 mL PFA beaker (ratio of acid solution to sample = ~50 by weight). The sample was heated in bomb at 100 °C in oven for 3 h. After cooling the sample the solution was taken out in volumetric flask. The solution was then diluted to 100 mL using milli Q water by using calibrated volumetric flask which was further subjected to ICP analysis. Metal leaching was studied by ICP-AES analysis of the catalyst before and after the three reaction cycles.

2A.3. Results and Discussion

2A.3.1. Catalyst synthesis

Palladium supported on magnesium hydroxyl fluoride was synthesized by the fluorolytic sol-gel route using magnesium methoxide as precursor (scheme 2A.1). During fluorolysis, in situ prepared magnesium methoxide was reacted with different

concentrations of hydrofluoric acid (HF), 100 % (alcoholic), 71 and 40% (aqueous) to get magnesium fluorides and hydroxyl fluorides. During the fluorolysis two competitive reactions namely hydrolysis and fluorolysis (fluorination) of metal methoxide take place. Depending on the concentration of HF the extent of fluorination/hydrolysis varied to give Pd-$MgF_{2-X}(OH)_X$ [37]. Although the fluorination is dominant, the hydrolysis of magnesium alkoxide becomes competitive with increasing water content in the medium resulting in a continuous change in the degree of fluorination [38]. By adding the palladium precursor during sol-gel synthesis of $MgF_{2-X}(OH)_X$, the one pot synthesis of palladium supported on magnesium hydroxyl fluoride was successfully achieved. According to the concentration of HF used (100, 71 and 40%) for the synthesis, the catalysts were denoted as Pd-MgF_2-100, Pd-MgF_2-71 and Pd-MgF_2-40 respectively. The non-aqueous sol-gel route resulted in the formation of clear sols and transparent gels whereas the aqueous route always resulted in opaque gels [38].

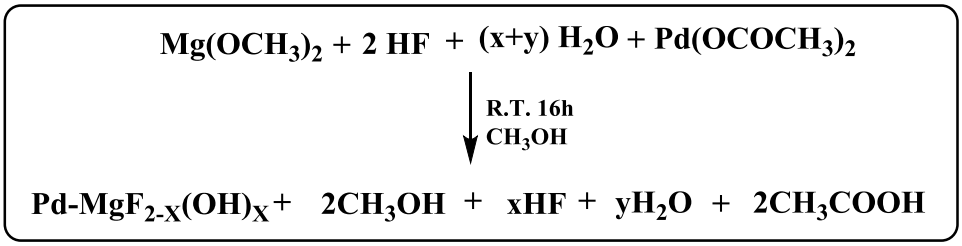

Scheme 2A.1. One pot sol-gel synthesis of different Pd-$MgF_{2-X}(OH)_X$ catalysts.

2A.3.2. Powder X-ray Diffraction

The PXRD patterns of all the catalysts as shown in fig. 2A.1 showed the presence of magnesium hydroxyl fluoride ($MgF_{2-X}(OH)_X$) phases. The PXRD patterns of the fluorinated catalysts showed broadening in peak pattern compared to pure tetragonal primitive lattice; this broadening of peaks indicated the disordered structure of the solids with small crystal size. There was no significant difference observed in XRD patterns of Pd-MgF_2-40 (fig. 2A.1-b), Pd-MgF_2-71 (fig. 2A.1-c) and Pd-MgF_2-100 (fig. 2A.1-d) which indicates that the MgF_2-structure of Pd-$MgF_{(2-X)}OH_X$ as formed tolerates water and the crystal phase does not change with the amount of water used. In another words, the crystal structure formation is not affected by the F/OH ratio. Moreover, this is clear evidence that the competitive hydrolysis reaction by water is suppressed in presence of the significantly stronger reactant HF. Hence fluorolysis strongly dominates over hydrolysis reaction. PXRD pattern of Pd-MgO

prepared for comparison also showed broad peaks confirming the nanoscopic nature of this catalyst too (fig. 2A.1-a). In line with former investigations the XRD patterns showed no deviation from the MgF_2 structure although magnesium hydroxyl fluoride phases ($MgF_{2-X}(OH)_X$), with low OH-content were formed.

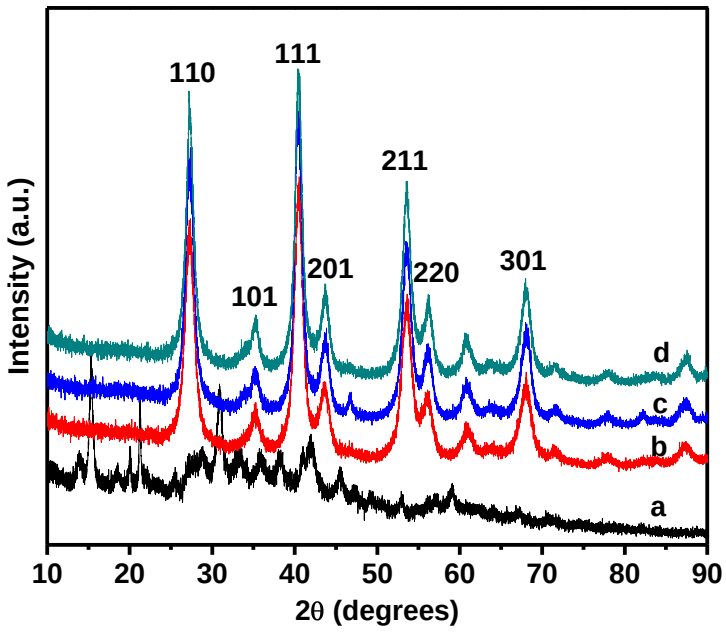

Figure 2A.1. Powder XRD patterns of a) Pd-MgO; b) Pd-MgF_2-40; c) Pd-MgF_2-71and d) Pd-MgF_2-100.

2A.3.3. FTIR

The prepared catalysts were characterized by FTIR spectroscopy as shown in fig. 2A.2. Due to the octahedral coordination of magnesium by fluorine and oxo/hydroxyl, all the catalysts expectedly exhibit Oh symmetry for an ordered structure with two infrared active modes. In fluorinated catalysts typically Mg-F and Mg-O stretches were observed at 460 and 552 cm^{-1} respectively [39]. The bands present at 3713 and 3432 cm^{-1} indicate the presence of isolated and bridging hydroxyl groups or adsorbed water molecules respectively. The band in the range of 2750-3200 and 1050-1150 cm^{-1} are assigned to C-H and C-O stretching vibration respectively. In case of Pd-MgO very weak vibrations were observed in the range of 3000-2750, 1463 and 1101 cm^{-1} indicating the presence of few methoxy functionalities as well as carbonate groups in the catalyst. The band at 1651cm^{-1} corresponds to O-H bending vibrations due to adsorbed water or surface O-H groups. The FTIR spectrum of Pd-

MgO showed peaks corresponding to magnesium carbonate at 1463, 2790-2925 and 3379 and 3697 cm^{-1} which matched well with literature reports [39].

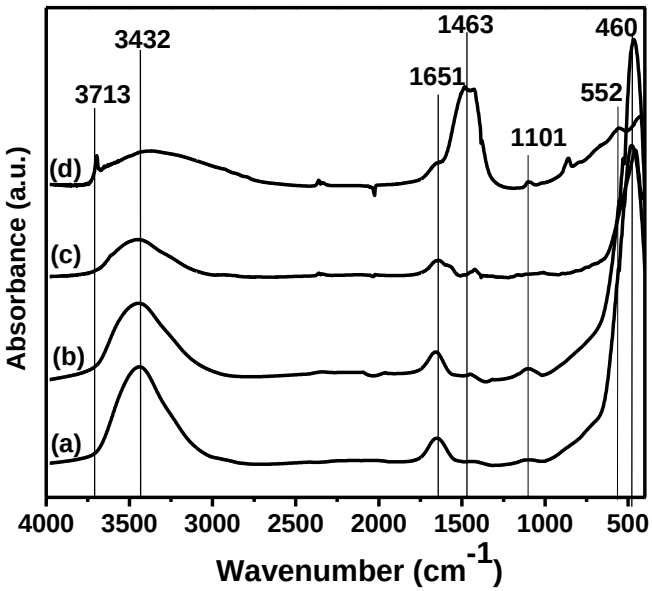

Figure 2A.2: FTIR spectra of (a) Pd-MgF_2-100; (b) Pd-MgF_2-71; (c) Pd-MgF_2-40; and (d) Pd-MgO.

2A.3.4. BET surface area

Nitrogen adsorption-desorption investigations were performed to study the effect of fluorination process on alteration of surface area, pore diameter and volume. The adsorption isotherms are plotted in fig. 2A.3 and resulting data from these are summarized in table 2A.1. All the catalysts showed very high surface area of around 136 m^2g^{-1} compared to 40-45 m^2g^{-1} for MgF_2 or MgO prepared by conventional method [40]. All the isotherms showed type IV character typical for mesoporous materials with a H1 type hysteresis loop and porous texture. The BET-surface area of all the catalysts showed decrease in order Pd-MgO > Pd-MgF_2-40 > Pd-MgF_2-71 > Pd-MgF_2-100. In Pd supported magnesium hydroxyl fluorides, the surface area changed with variation of the HF/H_2O ratio used for fluorination which affected the degree of fluorination/hydrolysis. The fluorinated catalysts showed mesoporous nature with a decreasing trend in pore size with decreasing HF concentration used for fluorolysis. The pore diameter for Pd-MgO falls in the mesoporous range. There was no trend observed in case of total pore volume studies. The pore volume for all the catalyst was found to be in the range of 0.19 - 0.23 $cm^3\,g^{-1}$.

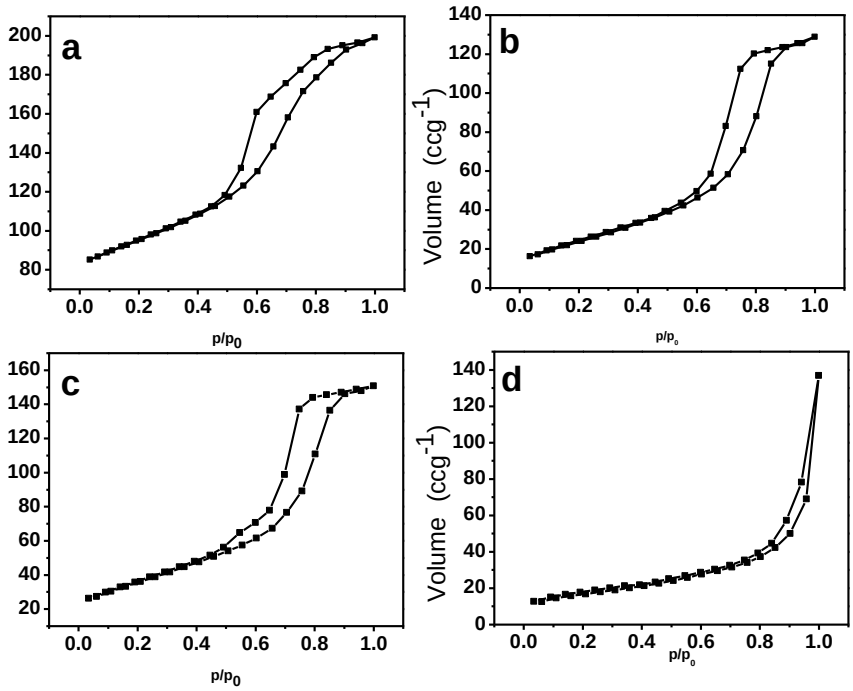

Figure 2A.3. BET surface area plot of (a) Pd-MgF_2-100; (b) Pd-MgF_2-71; (c) Pd-MgF_2-40 and (d) Pd-MgO.

2A.3.5. Ammonia Temperature programmed desorption (NH_3-TPD)

The total acidity as well as the strength of acidic sites on the surface of the catalysts were determined by NH_3 temperature programmed desorption (NH_3-TPD) technique and the plots are shown in fig. 2A.4. and the results are presented in table 2A.1. The extent of fluorination against hydrolysis was found to depend on the concentration of HF used and decreased with increase of the water content in HF. NH_3-TPD results indicated a decrease in total acidity of the catalysts in the order Pd-MgF_2-100 (0.328 mmol/g) > Pd-MgF_2-71 (0.208 mmol/g) > Pd-MgF_2-40 (0.173 mmol/g). The peak maxima for Pd-MgF_2-100 observed at 240 °C which decreased to 210 °C for Pd-MgF_2-71 and further decreased to 120 °C for Pd-MgF_2-40. This decrease can be correlated with the strength of acidity which decreased from Pd-MgF_2-100 to Pd-MgF_2-40. The peak maxima for Pd-MgF_2-40 (120 ºC) was observed in the same range of physisorbed NH_3. The similar peak (< 150 ºC) was not observed in other two samples (Pd-MgF_2-100 and Pd-MgF_2-71) which were analyzed under identical conditions, and confirms the weak acidity of Pd-MgF_2-40.

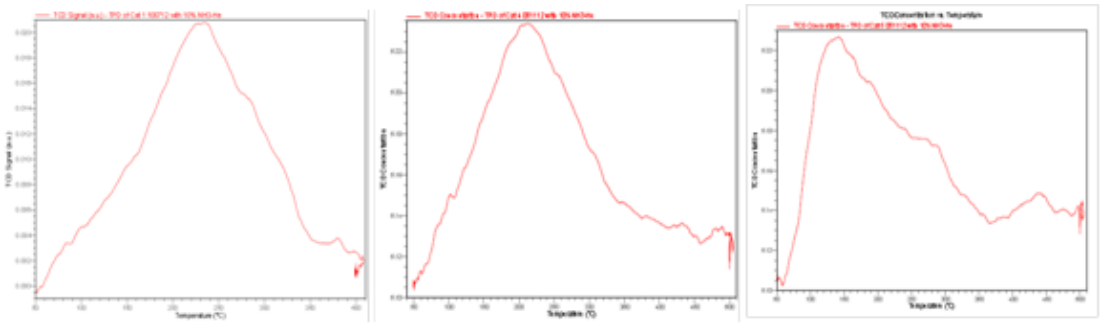

Figure 2A.4. NH_3-TPD plots of (a) Pd-MgF_2-100; (b) Pd-MgF_2-71 and (c) Pd-MgF_2-40.

2A.3.6. FTIR-Photoacaustic spectrum of adsorbed pyridine study

The type of acidity present on the catalyst surface was studied by FTIR-Photo acoustic spectroscopy (FTIR-PAS) of adsorbed pyridine (pKa = 5.25) as shown in fig. 2A.5. The spectra of Pd-MgF_2-100, Pd-MgF_2-71, Pd-MgF_2-40 indicated the presence of intense bands at 1445, 1490 and 1576 cm^{-1} which are characteristics for the Lewis acid sites. The strengths of Lewis acidity decreased in the order of Pd-MgF_2-100 > Pd-MgF_2-71 > Pd-MgF_2-40 which is in agreement with NH_3-TPD results. The origin of Lewis acidity on to the surface of the catalyst can be explained by the presence of 5 or 4 fold coordinated Mg surface sites (fig. 2A.6-a) and is attributed to the presence of more electron withdrawing fluorine atoms attached to five coordinated Mg sites as reported previously [41]. The peak at 1545 cm^{-1} showed comparatively higher intensity in Pd-MgF_2-40 as compared to other fluorinated catalysts. The Brønsted acidity may be generated due to the presence of Mg, which is coordinated by fluorine and hydroxyl groups. In such cases due to high electronegative fluorine atoms the bonded electrons migrate towards fluorine thus causing a weakening of strength of the O-H bond. The weak O-H bond can lose proton and behaves as Brønsted acid (fig. 2A.6-b). A steady decrease in the Lewis and increase in Brønsted acidity was observed for Pd-MgF_2-71 and Pd-MgF_2-40. As expected, Pd-MgO did not show any surface acidity. Thus, the Lewis acidity of the Pd-MgF_2-based catalysts decreased in the order Pd-MgF_2-100 > Pd-MgF_2-71 > Pd-MgF_2-40 > Pd-MgO. This order corresponds nicely to the rationalization first time given for pure magnesium hydroxyl fluoride [42]. It is commonly accepted that bonds in Mg-OH fragments are polarized in such a way that the Mg-O bond is significantly more polar than the O-H bond in pure $Mg(OH)_2$, thus resulting in cleavage of the Mg-O bond under the action of a

solvent like water. Consequently, MgO in water and $Mg(OH)_2$ are basic in nature. On the other hand, in chemically pure MgF_2 there are no OH-groups, consequently just Lewis acidity might be expected provided coordinative unsaturated Mg-surface sites are present.

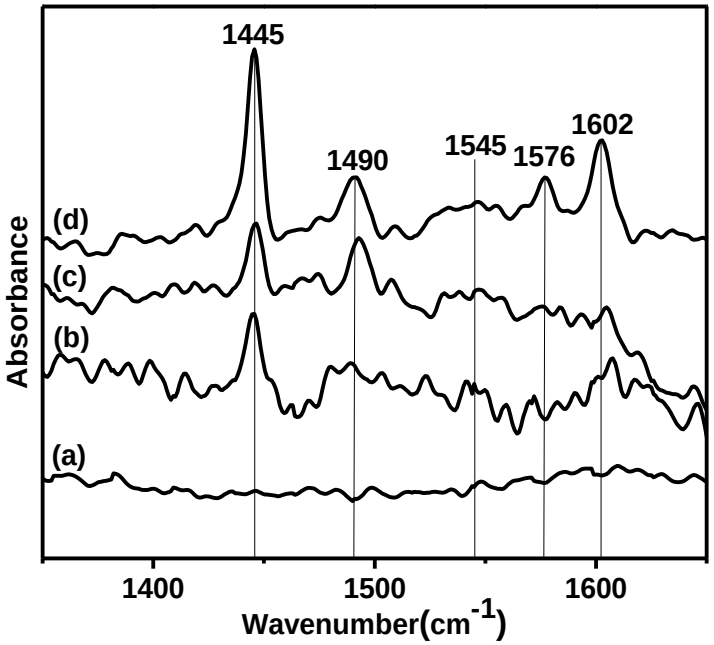

Figure 2A.5. FTIR-PAS of adsorbed pyridine on a) Pd-MgO; b) Pd-MgF_2-40; c) Pd-MgF_2-71 and d) Pd-MgF_2-100.

This condition is fulfilled in nanoscopic MgF_2 based on high surface area material providing a high degree of structural distortion though it is very limited in case of crystalline MgF_2. If however a very low amount of hydroxyl groups are introduced into MgF_2, the situation is different to that described above. As proven by MAS ^{19}F-NMR spectroscopy which showed the presence of the highly distorted $MgF_{(6-X)}(OH)_X$ octahedral building blocks in Pd-MgF_2-100, Pd-MgF_2-71, and Pd-MgF_2-40 samples [43]. It should be noted that the stoichiometric number X increases with decrease in concentration of HF used in the synthesis procedure. Thus, different to the situation of a Mg-O-H unit in MgO or $Mg(OH)_2$, in the Pd-MgF_2-samples the OH-groups are located in a fluorine rich structural environment. Due to the strong electron withdrawing nature of fluoride, the positive charge on the Mg^{2+} ion is further increased, thus inducing electron density shift from the O-H via the Mg-O bond. This strong polarization of the O-H bond in a fluorine rich structural environment alters the nature of the catalyst from basic to acidic as has been comprehensively discussed for the series of pure magnesium hydroxyl fluorides [41].

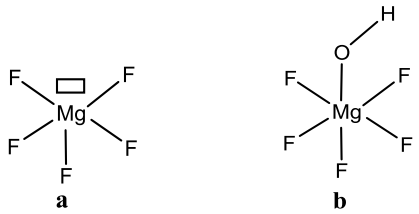

Figure 2A.6. Representative structures of a) generation of Lewis acidity due to presence of 5 fold coordination of Mg in MgF_2 and b) generation of Brønsted acidity due to presence of OH group in MgF_2.

2A.3.7. Hydrogen chemisorption

The palladium dispersion was determined by H_2 chemisorption studies and results are given in table 2A.1. According to literature reports PdO on heterogeneous metal fluoride supports gets reduced at low temperatures [44], hence the H_2 consumption profiles of the present samples were recorded from 50 °C to 300 °C. The amount of H_2 adsorbed on palladium supported catalysts varied from 2.22 x 10^{-5} to 1.58 x 10^{-5} mmol g^{-1}. Although there was no significant difference in surface area of support, the metal surface area and palladium dispersion has shown a decreasing trend in the order Pd-MgF_2-100 > Pd–MgF_2-71 > Pd–MgF_2-40. Pd-MgF_2-100 and Pd-MgF_2-71 exhibit approximately 47 and 46% Pd dispersion. This Pd dispersion is extremely high compared to palladium dispersed on commercial carbon of very high surface area (1400 m^2/g) which is reported to give only 30% dispersion for 1% Pd loading [45]. The higher Pd dispersion (~47%) on the MgF_2 catalyst having 136 m^2/g surface area compared to very high surface area carbon may be attributed to the in situ sol gel approach of synthesis leading to very high dispersion as well as decrease in the particle size of the palladium. The size of Pd particles determined from H_2-chemisorption studies was found to be in the range of 2.36-3.33 nm.

Table 2A.1. Surface characterization of catalysts by sorption techniques.

Entry	Catalysts	Physisorption (BET-Surface area)			Acidity(NH_3-TPD)		Chemisorption (H_2-TPR)			
		Surface area (m^2g^{-1})	Average pore diameter (nm)	Pore volume cm^3/g	NH_3 adsorbed (mmol/g)	Peak maxima (°C)	H_2 adsorbed (mmol/g) x 10^{-5}	Pd dispersion (%)	Metal surface area (m^2g^{-1})	Mean particle diameter (nm)
1	Pd-MgF_2-100	136	5.0	0.21	0.328	240	2.22	47.29	2.10	2.36
2	Pd-MgF_2-71	145	4.0	0.19	0.208	210	2.14	45.71	2.03	2.40
3	Pd-MgF_2-40	148	3.3	0.23	0.173	150	1.58	33.62	1.49	3.33
4	Pd-MgO	255	4.9	0.21	-	-	-	-	-	-

2A.3.8. XPS

The XPS was used to determine the effect of the support on the oxidation state of palladium of the as synthesized samples. The Pd-MgF_2-100 catalyst was compared with Pd-MgO and commercial 5% Pd-C (Sigma-Aldrich) as shown in fig. 2A.7. The binding energy (BE) of Pd in Pd-MgO and Pd/C was identical (336.9 eV) indicating Pd in zero oxidation state whereas in case of Pd-MgF_2-100 a peak was observed at 338.9 eV. The BE value of 338.9 eV corresponds to the presence of Pd^{2+} species on the surface origin of which may be palladium acetate used as Pd precursor. Commercial 5% Pd-C have shown two peaks at 336.9 and 342.2 eV corresponding to Pd^0 and Pd^{2+} respectively. The presence of Pd^0 and Pd^{2+} species indicates the presence of metallic Pd and PdO species respectively. There was no peak corresponding to PdO observed in Pd-MgF_2-100 and Pd-MgO indicating absence of PdO on these surfaces.

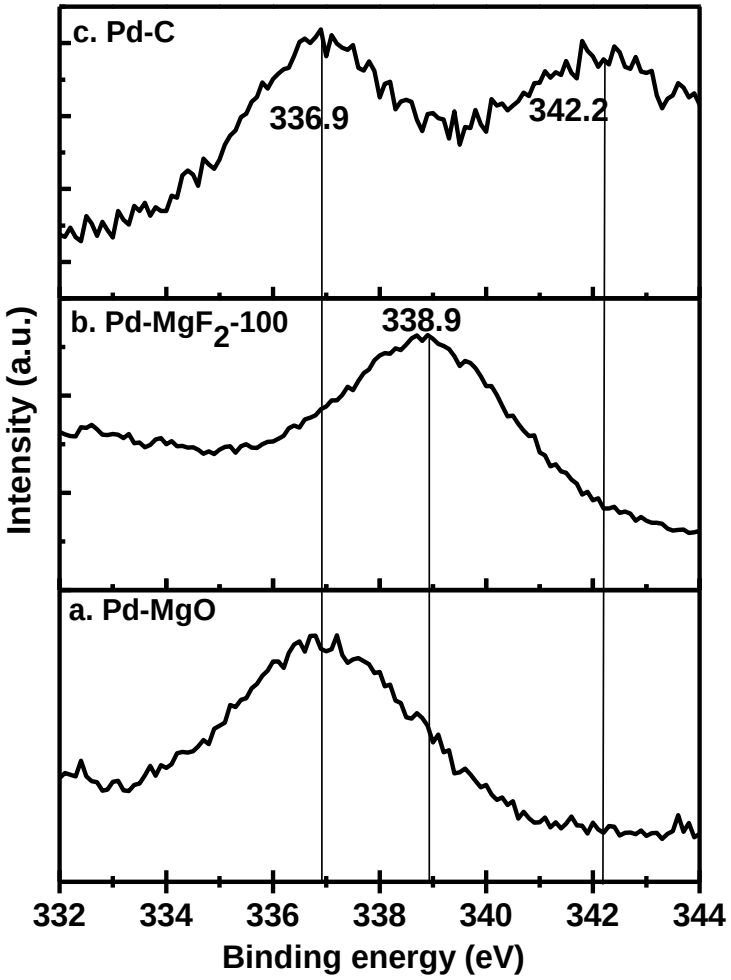

Figure 2A.7. X-ray photoelectron spectra of a) Pd-MgO; b) Pd-MgF_2-100 and c) Pd/C (commercial).

The considerable shift in binding energy of Pd^{2+} (338.9 eV) of Pd-MgF_2-100 from Pd^{2+} (338.6 eV) of palladium acetate [46] indicates a significant electron withdrawing effect caused by MgF_2 suggesting a strong metal support interaction. Obviously the fluoride rich structural environment in the highly distorted MgF_2-lattice withdraws electron density from the Pd inducing partial Lewis acidity at the precious metal [47]. Hence, partial positive charge on Pd in case of Pd-MgF_2-100 contributes additionally to the acidity of the catalyst which was also confirmed by NH_3-TPD studies.

2A.3.9. UV-DRS

To study the interaction of the palladium with MgF_2 support UV-DR spectra of the pre-reduced catalysts were recorded as shown in fig. 2A.8. The band at 283 nm matched with literature reported for $[Pd\text{-complex}]^{2-}$ species [48]. The bands around 325 nm are assignable to the d–d transition of Pd species [49]. The bands at 374 nm may correspond to a charge transfer band in Pd species in a strong electronegative environment. With increase in electronegativity of ligand, partial positive charge on metal increases which resulted in bathochromic shift in UV bands. The bands around 283, 325, and 374 nm in Pd-$MgF_{2-X}(OH)_X$ are less intense as compared to Pd-MgO. These results clearly confirmed strong metal-support interaction of Pd with magnesium fluorides and/or hydroxyl fluorides. These results are in line with results obtained by XPS analysis.

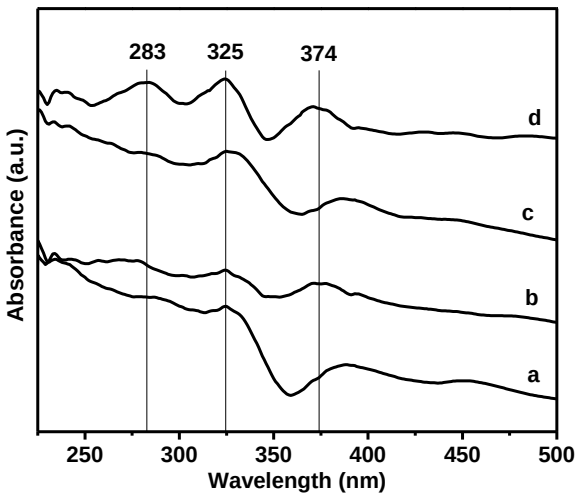

Figure 2A.8. UV-Vis spectra of a) Pd-MgF_2-100; b) Pd-MgF_2-71; c) Pd-MgF_2-40 and d) Pd-MgO.

2A.3.10. SEM and EDAX

SEM technique was used to observed the change in the morphology of the catalysts with change in the HF to water ratio used during the synthesis of Pd-$MgF_{2-x}(OH)_x$ and the images are shown in fig. 2A.9. The results clearly indicated the effect of dilution of HF on the textural properties of the final catalysts. HF concentration not only affected the crystallite size but also the morphology of the surface. It was found that the catalyst particle size decreased with decrease in HF concentration, Pd-MgF_2-100 showed very large crystals whereas Pd-MgF_2-71, Pd-MgF_2-40, and Pd-MgO showed sheet like structures of variable size along with few very small crystallites.

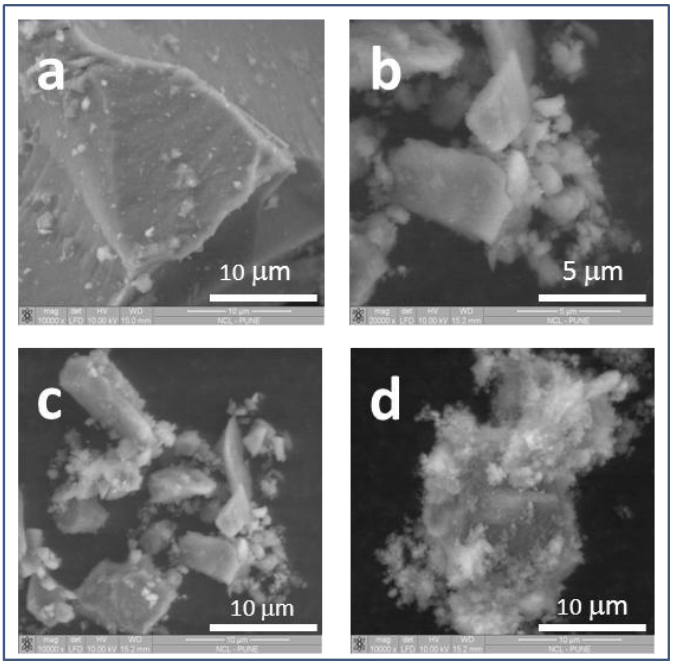

Figure 2A.9. SEM images of catalysts (a) Pd-MgF_2-100; (b) Pd-MgF_2-71; (c) Pd-MgF_2-40 and (d) Pd-MgO.

Table 2A.2. Elemental analysis of catalysts by EDAX.

Entry	Catalyst	Elemental Composition			
		Pd	Mg	F	O
1	Pd-MgF_2-100	0.99	39.57	55.70	3.74
2	Pd-MgF_2-71	1.20	39.34	54.26	5.21
3	Pd-MgF_2-40	0.93	39.02	51.20	8.85
4	Pd-MgO	0.89	58.20	0.0	40.91

Furthermore the surface composition of all the catalysts was determined using EDAX analysis as given in table 2A.2 which showed the presence of almost 1 wt% palladium on the surface indicating uniform dispersion as well as availability of all the loaded palladium on the surface for the reaction.

2A.3.11. HRTEM

The particle size of magnesium hydroxyl fluoride and palladium nanoparticle was estimated using HRTEM analysis as represented in fig. 2A.10. Previously we have shown that $MgF_{2-X}(OH)_X$ prepared by fluorolytic sol gel route leading to the formation of nanoscopic MgF_2 with a particle size in the range of 6-10 nm [50]. The particle size distribution studied by HRTEM clearly showed that the majority of particles had ~5 nm diameter, though the particle size distribution spreads up to 20 nm. The palladium particles were found to be in 111 plane as identified by measuring d spacing (d_{111} = 0.223 nm). The d spacing for MgF_2 confirmed the presence of 110 (0.326 nm) and 111 (0.222 nm) planes. In case of the Pd-MgO catalyst, d spacing confirmed formation of 111 plane of Pd (d_{111} = 0.223 nm) as well as MgO (d_{111} = 0.243 nm) which indicates a semi-crystalline nature of MgO.

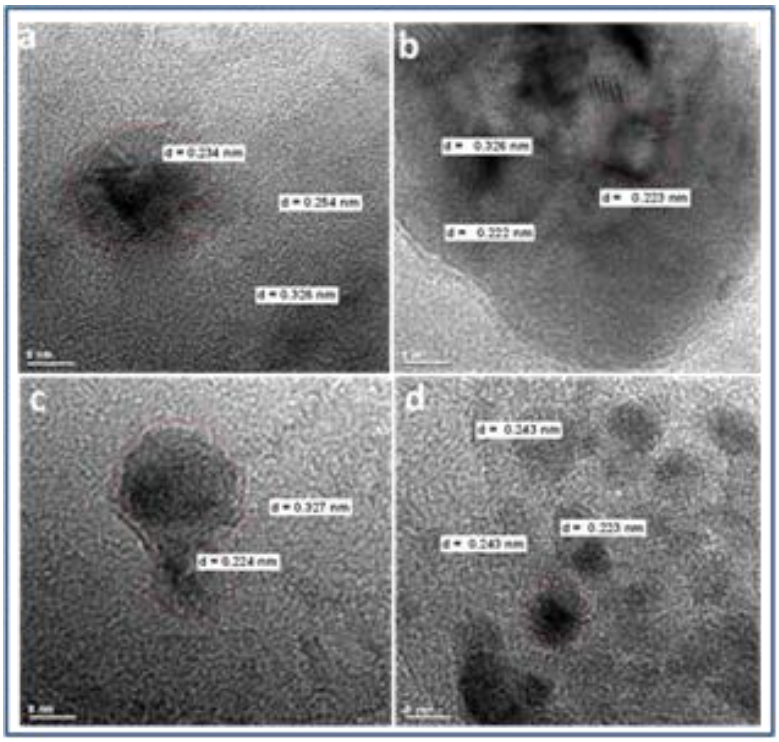

Figure 2A.10. TEM images of catalysts a) Pd-MgF_2-100; b) Pd-MgF_2-71; c) Pd-MgF_2-40 and d) Pd-MgO.

The formation of small Pd particles is attributed to the fluorolytic sol-gel preparation which enabled very high dispersion and small particle size. There was no appreciable difference observed in particle size distribution for all catalysts. The catalysts showed very high metal dispersion as compared to literature reports [44]. The high metal dispersion on relatively low surface area catalysts was due to the formation of palladium metal nanosheets on the surface of sol gel synthesized magnesium fluorides. In case of fluorinated catalyst palladium showed nanosheets like structure while in case of magnesium oxide spherical nanoparticle formation was observed.

2A.3.12. Catalytic activity for olefin hydrogenation

The catalytic activity of the palladium supported magnesium hydroxyl fluoride was evaluated for hydrogenation of olefins initially with styrene as model substrate (scheme 2A.2). The hydrogenation was carried out at room temperature and atmospheric pressure by bubbling hydrogen gas through the reaction mixture.

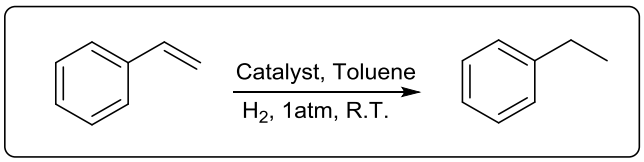

Scheme 2A.2. Hydrogenation of styrene.

Table 2A.3. Results of styrene hydrogenation.[a]

Entry	Catalyst	Conv.[b] (%)	Sel.[b] (%)	Rate constant[c] (s^{-1})
1	Blank	<1	100	-
2	5% Pd-C	4	100	-
3	Pd-MgO	7	100	-
4	Pd-MgF_2-40	44	100	2.12×10^{-3}
5	Pd-MgF_2-71	71	100	10.60×10^{-3}
6	Pd-MgF_2-100	~100	100	11.93×10^{-3}

[a] **Reaction conditions**: Styrene: 1.0 mmol; Catalyst: 0.01g (10 wt %; 0.1 wt % Pd with respect to styrene); Toluene: 6.0 mL; H_2 bubbled; Temperature: RT (27 °C); Time: 3 h. [b]Conversion and selectivity were determined based on GC, [c] Rate constants were determined by assuming reaction to follow 1st order kinetics for 10 minutes of time.

When the reaction was carried out under identical conditions for comparison without catalyst, with Pd-MgO and commercial 5 wt% Pd-C catalyst very poor styrene conversions <1, 7, and 4% respectively were obtained (table 2A.3, entry 1-3). When the reaction was carried out using Pd-MgF_2-40 catalyst, 44% styrene conversion was obtained after 3 h. (table 2A.3, entry 4) which increased to 71% with Pd-MgF_2-71 (table 2A.3, entry 5) and further increased to 100% using Pd-MgF_2-100 under identical reaction conditions (table 2A.3, entry 6). All the reactions were selective towards catalytic hydrogenation of olefinic double bonds. The aromatic ring hydrogenation was not observed in any of the reactions. Pd-MgF_2-100 showed 100% conversion with maximum rate constant of 11.9 x 10^{-3} s^{-1}.

2A.3.13. Catalyst loading effect

The effect of catalyst loading on styrene hydrogenation was studied using Pd-MgF_2-100 catalyst as shown in fig. 2A.11. When the catalyst loading with respect to styrene was gradually increased from 2 wt% to 20 wt% the conversion after 1 h gradually increased from 6% to 65%. The increase in catalyst loading increases the conversion without affecting selectivity. However to balance between catalytic loading and catalytic activity 10 wt% catalyst loading was used for further reactions.

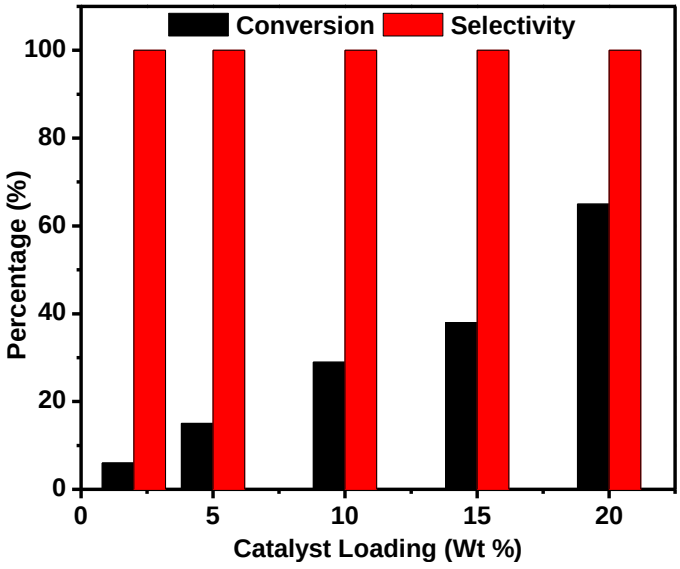

Figure 2A.11. Effect of catalyst loading on styrene hydrogenation.

Reaction conditions: Styrene: 1.0 mmol; Catalyst: 0.01g (10 wt % w.r.t. styrene); Toluene: 6.0 mL; H_2: bubbled, Temperature: RT (27 °C); Time: 1 h.

2A.3.14. Substrate scope

To study the wider applicability of the catalyst for olefin hydrogenation various substrates were studied and the results are shown in table 2A.4. In case of styrene the reaction was completed within 3 h with 100% selectivity for ethylbenzene (table 2A.4, entry 1). When cyclohexene, cyclooctene, and n-hexene were hydrogenated under identical conditions, the time required for complete conversion to desired hydrogenated products was longer compared to styrene indicating lower reactivity of the substrates (table 2A.4, entry 2-4). To expand the hydrogenation study to disubstituted olefins, indene and α-methylstyrene were screened, however lower activity compared to styrene was obtained (15 and 8% conversion after 1 h). The lower activity may be due to the higher order of substitution of these olefins leading to steric crowding (table 2A.4, entry 5-6). To study the hydrogenation of olefins in presence of other reducible functional groups, 2-butenal was hydrogenated with 100% selectivity for olefin hydrogenation without reduction of carbonyl moiety (table 2A.4, entry 7). In case of 2-alkenol olefinic hydrogenation is competitive with isomerization reaction. To study selectivity pattern in such substrates, 3-phenylpropenol was selected as representative substrate which on reaction showed 100% conversion with > 99% selectivity for 2-phenylpropanol (table 2A.4, entry 8). When olefin in presence of a carboxylic group like methyl acrylate and acrylic acid were hydrogenated, 100% conversion with almost complete selectivity for methyl propanoate and propanoic acid respectively (table 2A.4, entry 9 - 10) were obtained. The high conversion indicated stability of catalysts in presence of carboxylic group and electron withdrawing groups activating the olefinic C=C bond for catalytic hydrogenation. The effect of bulkier groups and electron withdrawing reducible carbonyl groups was studied using benzalacetophenone as substrate. The conversion decreased to 65% without affecting the selectivity of 1,5-diphenylpentanone. The lowered activity indicates a negative effect of steric crowding due to the presence of phenyl rings (table 2A.4, entry 11). The geometrical isomers, *cis* and *trans* stilbene were hydrogenated at slightly elevated temperature (80 °C) due to higher steric hindrance of the bulkier phenyl group. *Trans*-stilbene showed lower activity compared to *cis* isomer. This may be due to higher relative stability of *trans* isomers compared to *cis* isomers (table 2A.4, entry 12-13). Further on, the effect of the substituent on phenyl ring of styrene was examined by

atalytic hydrogenation of 4-vinylanisole. The reaction showed 95% conversion with 99% selectivity for olefin hydrogenation (table 2A.4, entry 14).

Table 2A.4. Catalytic hydrogenation of various olefins using Pd-MgF_2-100.[a]

Entry	Substrate	Time (h)	Conv. (%)	Sel. (%)	Normalized‡ TOF (h^{-1})
1	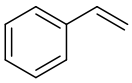	1	29	100	634
		3	~100	100	
2		1	7	100	197
		12	~100	100	
3		1	13	100	301
		8	~100	100	
4		1	9	100	243
		10	~100	100	
5	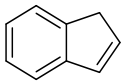	1	15	100	266
		6	~100	100	
6	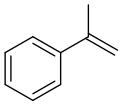	1	8	100	150
		12	~100	100	
7	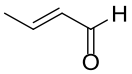	1	13	99	411
		9	~100	99	
8	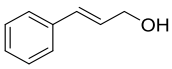	1	6	99	108
		12	~100	99	
9	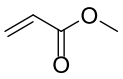	1	17	99	230
		6	~100	99	
10	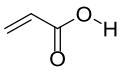	1	24	99	369
		5	100	99	
11	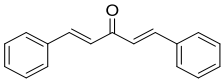	1	16	99	178
		6	65	99	
12#	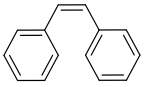	1	18	99	232
		6	89	99	
13#	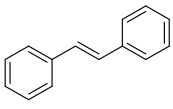	1	15	99	185
		6	66	99	
14#	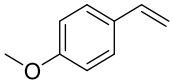	1	18	99	302
		6	95	99	
15#	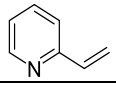	1	12	99	252
		12	78	99	

[a]**Reaction conditions:** Alkenes: 1.0 mmol; Catalyst: Pd-MgF_2-100, (10 wt% w.r.t. substrate, 0.1 wt% of Pd); Solvent: Toluene 6.0 mL; H_2: bubbled; Temperature: RT (27 °C); # 80 °C. ‡Normalized TOF was determined based on metal surface area

When 2-vinylpyridine was used as substrate to study olefinic hydrogenation in a heterocyclic system, 78% conversion with 99% selectivity (table 2A.4, entry 15) was achieved at 80 °C after 12 h. This substrate screening study showed sterically hindered olefins to be less reactive for catalytic hydrogenation. The catalyst showed selectivity for only olefinic hydrogenation in presence of other reducible functional groups such as carbonyl and carboxylic group. Also sterically hindered olefins need elevated temperatures for hydrogenation.

2A.3.15. Catalyst recycles study

The recyclability of the catalyst was tested using styrene hydrogenation as the model reaction under conditions as given in table 2A.3. After completion of each reaction the catalyst was separated, washed, dried and used for the next run and the results are summarized in fig. 2A.12. The catalyst could be recycled very efficiently for five cycles without appreciable decrease in styrene conversion.

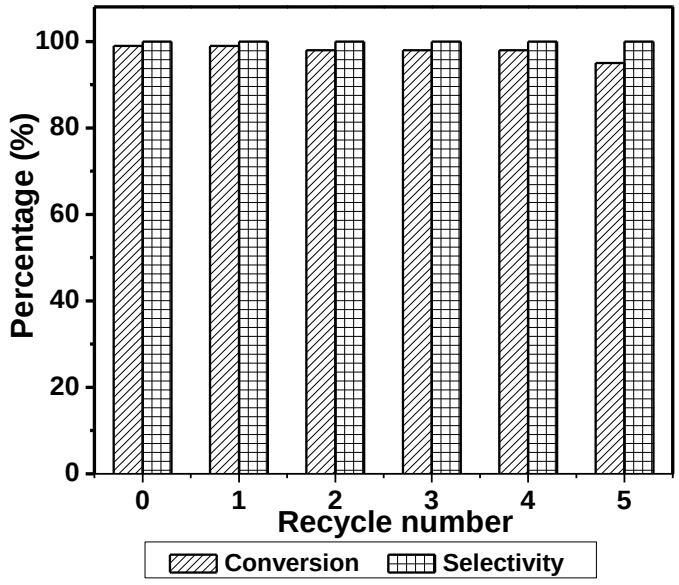

Figure 2A.12. Recyclability study of the catalyst.

Reaction conditions: Styrene: 1.0 mmol; Catalyst: 0.01g (10 wt %; w. r. t. styrene); Toluene: 6.0 mL; H_2: bubbled; Temperature: RT (27 °C); Time: 3 h.

2A.3.16. Catalyst filtration test and TEM analysis of recycled catalyst

The Pd leaching was confirmed using filtration test, where the catalyst was separated from reaction mixture by filtration after 1.5 h (57% styrene conversion) and reaction (filtrate) was continued without catalyst as shown in fig. 2A.13. However, even when the reaction was carried out for additional 3 h there was no increase in the

styrene conversion which confirmed no Pd leaching from the catalyst. Additionally, Pd leaching was also tested by ICP-AES analysis and showed no Pd leaching in the reaction medium (Pd metal detection limit 5 ppm).

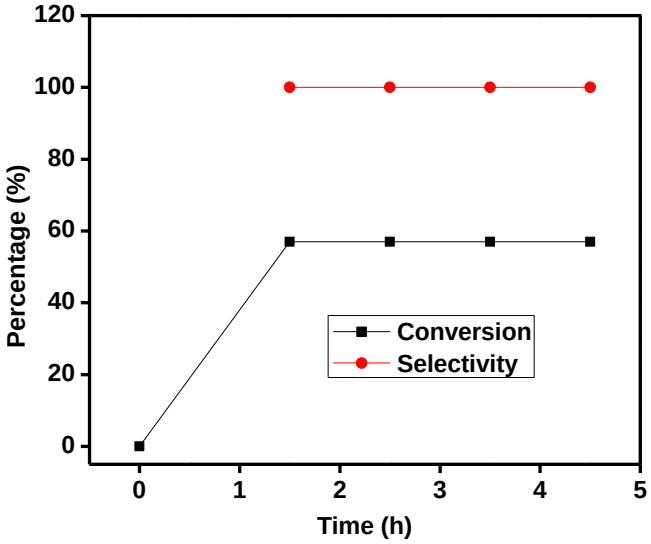

Figure 2A.13. Catalytic results of filtration test of catalyst.

Reaction conditions: Styrene: 1.0 mmol; Catalyst: 0.01g (10 wt % w.r.t. styrene); Toluene: 6.0 mL; H_2: bubbled; Temperature: RT (27 °C); Time: 3 h.

The TEM image of Pd-MgF_2-100 catalyst after 5th recycle revealed the slight agglomeration of Pd particles as shown in fig. 2A.14. In the fresh catalyst (as shown in fig. 2A.11) formation of Pd sheets was observed whereas in the recycled catalyst Pd particles of ~6 nm were observed indicating partial agglomeration.

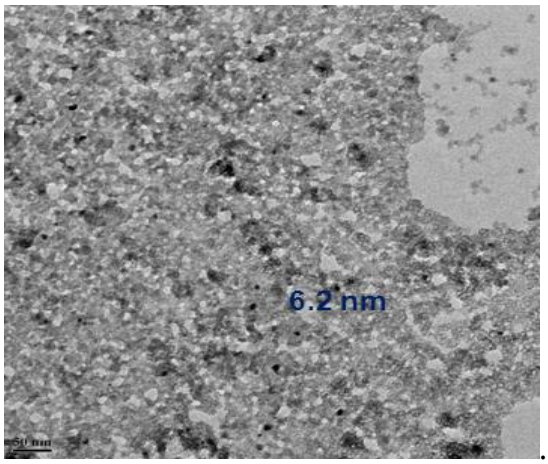

Figure 2A.14. TEM image of recycled catalyst after 5th recycle.

However there was no decrease in the catalytic activity in successive cycles indicating that even Pd particles on MgF_2 are equally active for hydrogenation of styrene under ambient conditions of pressure and temperature.

Kantam *et al.* recently reported the use of palladium supported on lanthanum modified nano magnesium oxides, Pd/La-MgO, as efficient catalyst for chemoselective hydrogenation of olefinic double bonds at room temperature and atmospheric pressure. However, 10% Pd loading had been used for this transformation. As the surface area of the support was low (~35 m^2/g) the palladium particles obtained were larger, e.g. in the range of 28-32 nm [51]. In another report, Asefa *et al.* have used Pd encapsulated in PAMMAM dendrimers supported onto silica microspheres. The reported activity was very high for room temperature hydrogenation of olefins, nitroaromatics as well as carbonyl compounds with very low palladium loading and very high TOF (24000 h^{-1}). However, the hydrogenation was effective only at higher pressures and the catalyst preparation involved multistep preparation [52].

The results obtained in the present study are superior compared to previous reports indicating positive effect of magnesium hydroxyl fluorides as support on catalytic activity of palladium nanoparticles. The results obtained in case of Pd-MgF_2-100 can be correlated with acidity of catalyst, size of the palladium nanoparticles, hydrogen adsorption capacity of catalyst and partial charge on Pd, and strong metal support interaction. When the Pd-MgF_2-100 catalyst was compared with other catalysts it showed distinct characteristics high specific surface acidity equivalent to 0.328 mmol of NH_3 and high hydrogen adsorption capacity equivalent to 2.22 x 10^{-5} mmol g^{-1} of catalyst. Due to high hydrogen adsorption capacity of the catalyst, it exhibited high metal dispersion up to 47% which led to smaller metal particle formation and higher metal surface area.

2A.3.17. *In situ* FTIR study and plausible reaction mechanism

To study the effect of support on palladium catalyzed hydrogenation reaction *in situ* FTIR studies were carried out by passing hydrogen and styrene on the catalyst surface in diffused reflectance mode and monitoring the formation of species on the catalyst surface as represented in fig. 2A.15. Initially only styrene was passed on the catalyst surface at room temperature with flow of nitrogen gas to study the activation of styrene (fig. 2A.15-c). However the activation of styrene could not be observed on the catalyst surface as no significant shift in olefinic C=C band (1600 cm^{-1}) and C-H stretching frequency (in range 2873-3085 cm^{-1}) was observed when compared with authentic styrene from FTIR database (fig. 2A.15-a). This confirmed only

physisorption of styrene on the catalyst surface. Then, hydrogen gas was passed on the catalyst surface which was already saturated with physisorbed styrene and instantaneous formation of ethyl benzene was observed on the catalyst surface with corresponding decrease in intensity of styrene peaks (fig. 2A.15-d). When styrene and hydrogen were passed together over the catalyst surface (fig. 2A.15-e) instantaneous ethyl benzene formation was observed along with very low intense peaks for styrene which clearly indicated facile activation of hydrogen on palladium under ambient reaction condition and further reaction with physisorbed styrene on the catalyst surface. Previously, Wojciechowska *et al.* have used Pt-MgF_2 for chemoselective hydrogenation of chloronitrobenzene. Pt/MgF_2 was prepared by precipitation using magnesium carbonate as Mg precursor and Pt loading by conventional impregnation method [53].

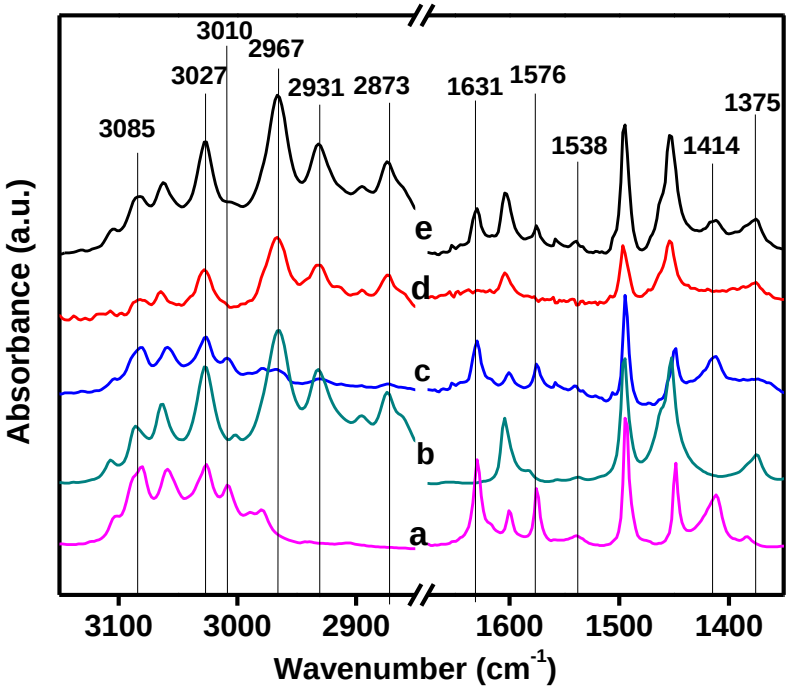

Figure 2A.15. *In situ* FTIR difference spectra for styrene hydrogenation on Pd-MgF_2-100, a) styrene; b) ethylbenzene; c) catalyst + styrene in nitrogen flow; d) catalyst + styrene in nitrogen flow + hydrogen and e) catalyst + styrene in hydrogen flow.

Chemoselective hydrogenation of nitro group was due to activation of nitrobenzene on Pt-MgF_2 as well as on MgF_2 which was proved by *in situ* FTIR studies [53]. Although in the present case sol-gel synthesized Pd-MgF_2 was used, no activation of the substrate (olefin) on the catalyst surface could be detected, but

instead, facile hydrogenation of olefin under ambient reaction conditions was observed.

Therefore based on FTIR studies, the plausible mechanism for hydrogenation of styrene on Pd-MgF_2-100 is represented in scheme 2A.3. As indicated by FTIR results, initial activation of hydrogen takes place on palladium (step 1) followed by the interaction of styrene with activated hydrogen (step 2) forming ethylbenzene that liberates to regenerate the catalyst (step 3).

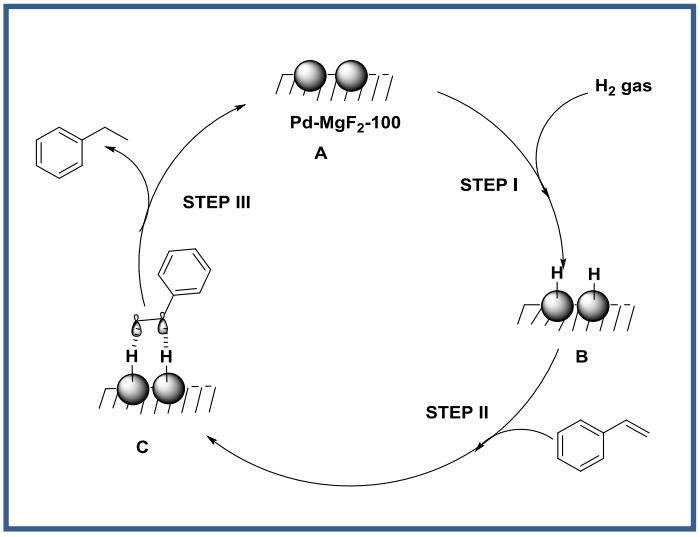

Scheme 2A.3. The proposed reaction mechanism for styrene hydrogenation using Pd-MgF_2-100 catalyst.

2A.4. Conclusions

Palladium supported on nanoscopic magnesium fluorides was synthesized using facile one-pot fluorolytic sol–gel method. The catalysts showed high surface areas upto ~135 m^2g^{-1}, metal dispersion up to 47% and sheet like structures of palladium particles. The catalyst showed high metal-support interaction between palladium and magnesium fluorides. The total acidity of the catalyst was associated degree of fluorination and HF used for synthesis of catalyst. Further the catalyst showed chemoselective hydrogenation of olefins under ambient reaction conditions and bubbling of hydrogen gas. The catalyst was recycled efficiently up to five cycles without appreciable loss in catalytic activity. There was no palladium leaching during the reaction as confirmed by ICP-AES. Activation of styrene was not observed on the catalyst surface by in situ FTIR studies, which indicated a facile activation of hydrogen on palladium giving very high activity under ambient conditions.

Section 2B: Hydrogenation of Triglycerides Using Palladium Supported on Magnesium Hydroxyl Fluorides as Catalyst

2B.1. Introduction

Vegetable oils are triglycerides extracted from the plants. Triglycerides are the esters of free saturated/unsaturated fatty acids and glycerin. Basically, many vegetable oils are consumed directly, or indirectly as ingredients in foods, pharmaceuticals, flavoring agents, etc. Many agro-industries are based on oils and its value added products. The reactions like oxidation, sulfonation and hydrogenation are widely used for valorization of various edible and non-edible oils. Among all these processes hydrogenation of oils is one of the very important process.

Hydrogenation of fats and oils is a very important operation in the industrial process of producing vegetable tallow, vegetable fats, margarines, and starting components for the cosmetic and chemical industry such as emulsifiers, soaps, creams, pastes, and similar products [54]. The unsaturated triglycerides possess low stability and exhibit autoxidation in presence of air or oxygen. Further hydrogenation provides high stability to unsaturated triglycerides which prevents from thermal decomposition and development of rancidity and improves the properties of final products [55]. The partial hydrogenation process delivers the desired softening and melting characteristics to oils that are important in the products like shortenings, margarines or confectionery fats. The properties of the final hydrogenated products are mainly depend on reaction condition as well as on the catalyst used [56].

Various metal based catalysts (Ni, Pd and Pt) have been developed for hydrogenation of fatty acids and triglycerides. Since late 19^{th} century, nickel and its alloys have been widely used as catalyst under high hydrogen pressure up to 300 psi and high temperature up to 180 °C [57]. Although Ni-based catalysts have relatively low cost but they require high energy consuming conditions such as high temperature and pressure as well as special material for construction of reaction vessel. Another drawback of nickel based catalyst is its toxicity. According to regulations in Russia the content of nickel cannot exceed 10 ppm in hydrogenated fats [58]. In addition, in presence of moisture and oxygen, Ni based catalysts shows deactivation due to

formation of nickel soaps (nickel salts of fatty acids) which leads to development of novel non-nickel based catalyst [59].

In 1906, Pd was used as catalyst for vegetable oil hydrogenation in the first margarine plants but was not used extensively due to its less availability and higher cost [60]. Further in 1960s, Pd based catalysts were used for the hydrogenation and isomerization of C=C bond in oleochemical research [61, 62] which concluded Pd catalysts are more effective than nickel catalysts at lower temperatures and forms selectively *trans* isomer in oils [63]. Furthermore various palladium based catalysts supported on different heterogeneous supports have been used for hydrogenation.

Palladium supported on low surface area activated carbon was used for catalytic hydrogenation of oils, which showed lower hydrogenation rate and higher trans-isomerization rate as compared to palladium supported on high surface area materials. This indicated the necessity of porous support for higher catalytic activity due to fine dispersion on palladium [64]. Further Pd supported on mesoporous TiO_2 and Al_2O_3 have shown high initial activity which decreased rapidly due to active metal blocking with impurities from the feed and water adsorption on the hydrophilic surface [65]. Again, Pd on structured mesoporous SBA-15 was used for hydrogenation of sunflower and canola oils; however these catalysts are costly and require special efforts for development [66]. In another report, Perez-Cadenas and co-workers have used carbon-based monoliths as catalyst supports for selective hydrogenation of edible oils because of highly tunable properties of carbonaceous materials [67]. In addition to the discussed literature few more catalyst systems have been used for oil hydrogenation such as Rh/TPPTS complexes [68], Cu/SiO_2 [69], Ni/SiO_2 [70], Pd/SiO_2 [71], Ni/Ru mixture [72], and Ni/Al_2O_3 [73].

Considering the previous reports, the oil hydrogenation catalyst needs following properties

- Highly dispersed metal nanoparticles which are resistant to sintering and leaching from support.
- High accessibility for the reagent molecules to active metal nanoparticles.
- Oil-support interactions for other side reactions
- Resistance of the catalyst and the mixture with oil to spontaneous ignition.

As describe in previous section Pd-MgF_2-100 has shown very high efficiency for selective hydrogenation of olefin at room temperature and atmospheric pressure of

hydrogen. We have extended the application of this catalytic system for one of the very important industrial application of oil hydrogenation.

2B.2 Experimental

2B.2.1. Materials

All chemicals including solvents were procured from Aldrich Chemical Co. USA and used without further purification. Solvents were purchased from Merck Chemicals, Germany and used as obtained. Wij's solution (ICl, 0.1 M solution in glacial acetic acid) was procured from Molychem Pvt. Ltd, India and used as obtained. Sodium thiosulfate, potassium iodide, starch and phenolphthalein were purchased from Rankem, India and were used as received. The various oils were obtained from local market.

2B.2.2. Typical procedure for hydrogenation of oils in solvent

CAUTION: During bubbling unreacted hydrogen gas is liberated, therefore all the reactions were carried in fume hood.

Two necked round bottom flask (50 mL) was charged with substrate (2.0 g), solvent (10 mL) and catalyst (0.2 g, 10 wt% with respect to substrate). The reaction mixture was stirred at room temperature with a flow of hydrogen gas (10 mL min^{-1}). After a particular time the reaction was stopped and the solvent was removed under high vacuum. Further the catalyst was separated from reaction mixture using hot centrifugation process. The product was isolated and analyzed by determining parameter like iodine number, hydroxyl value, acid number, melting points and specific gravity.

2B.2.3. Procedure for hydrogenation of oils under solvent free conditions

In a 50 mL high pressure autoclave (Amar reactors, India), 15.0 g oil and 1.5 g catalyst was added. The hydrogen gas was allowed to pass for 1 min under 1 atm pressure to remove all air from autoclave. Further the autoclave was filled with hydrogen gas to obtain the desired pressure. The reaction pressure was maintained using a pressure reservoir of hydrogen and filled whenever neccessary. The reaction was monitored by the consumption of hydrogen gas during the reaction. The rate of consumption of hydrogen gas was found to decrease near completion of reaction. The catalyst was separated from reaction mixture using hot centrifugation process and

product was isolated and analyzed for iodine number, hydroxyl value, acid number, melting points and specific gravity.

2B.2.4. Procedure for recyclability study of the catalyst

The recyclability of Pd-MgF_2-100 was tested for castor oil hydrogenation under optimized reaction conditions (Castor oil: 15.0 g; Catalyst: 1.5 g (10 wt % or 0.1 wt % Pd with respect to castor oil, Solvent: Methanol (10 mL)); H_2 pressure: 1 atm; Temperature: RT (27 °C); Time: 3 h). After completion of the reaction catalyst was recovered by filtration, washed with methanol (5 mL X 3 times), petroleum ether (5 mL X 3 times) and acetone (5 mL) and finally dried at 110 °C for 30 min. A new reaction was then carried out with fresh castor oil under the same reaction conditions. The Pd-MgF_2-100 catalyst was recycled 3 times using similar procedure.

2B.2.5. Analysis of hydrogenated oils [74]

A. Estimation of Iodine number of the triglycerides

Fixed quantity of hydrogenated product was placed in stoppered flask of 250 mL capacity with 25 mL carbon tetrachloride. The flask was shaken well until it dissolves. Further 25 mL of Wij's solution was added in flask and shaken gently with stopper. Then the flask was kept for 1 h in dark before analysis. Furthermore 10 mL aq. KI solution (10 wt %) was added with 100 mL water. Whilst shaking the contents of flask, it was titrated against sodium thiosulfate solution (0.1 M aqueous solution) until the appearance of yellow color. The freshly prepared starch indicator (1 mL, 1 wt% aq.) was added towards the end of the titration. The appearance of blue color indicated end-point of titration. The volume of sodium thiosulfate required for the end point (*a*) was determined. Similarly one titration was carried out without sample to determine blank reading against sodium thiosulfate (0.1 M) and was referred as *b*). The iodine number was calculated using the following formula:

$$\text{Iodine value} = \frac{(b-a) \times 0.01269 \times 100}{\text{Weight of sample in g}} \quad \text{---------- (}\textit{equation 2B.1)}$$

Where, a = Burette reading for sample.
b = Burette reading for blank.

B. Estimation of hydroxyl value of the triglycerides

An accurately weighed amount of hydrogenated product and 5 mL acetic anhydride-pyridine reagent was taken in 250 mL conical flask attached with air condenser. The flask was placed in water bath of temperature (95-100 °C) for 1 h. The flask was swirled vigorously until all the solid material is melted and is thoroughly mixed into the solution. Then the flask was removed from the water bath and cooled to room temperature. Further 10 mL water was added through the air condenser and the flask was heated using water bath for 10 minutes to complete the hydrolysis of the excess acetic anhydride reagent. Then 25 mL neutralized n-butanol was added to the flask and the condenser was removed. The above solution was titrated against methanolic KOH using phenolphthalein as an indicator until appearance of faint pink color. A blank reading was measured without hydrogenated product. The volume of potassium hydroxide solution required for the end point (*a*) was determined. Similarly the blank reading was taken without product of the reactions and titrated against KOH solution (0.1 M) *Vs* required (*b*). The hydroxyl value was calculated using the following formula:

$$\text{Hydroxyl value} = \frac{\text{(b-a) X } \textit{Normality of} \text{ KOH X 56.1}}{\text{Weight of sample in g}} + \text{Acid value} \quad \text{-- (}\textit{equation 2B.2)}$$

Where, a = Burette reading for sample.
b = Burette reading for blank.

C. Estimation of acid value of hydrogenated oils

An accurately weighed quantity of hydrogenated product was placed in a 250 mL conical flask with 50 mL ethanol-ether solution. The flask was shaken until solid was completely dissolved. The solution was titrated with standardized sodium hydroxide using phenolphthalein indicator. The measured volume of sodium hydroxide was titrated. Finally the acid value was calculated using following formula:

$$\text{Acid value} = \frac{\text{Volume of NaOH in mL X 5.61}}{\text{Weight of sample in g}} \quad \text{--- (}\textit{equation 2B.3)}$$

2B.3. Results and Discussions

2B.3.1. Catalytic activity for triglyceride hydrogenation

The catalytic activity of the Pd-MgF_2-100 was evaluated for hydrogenation of triglycerides, initially with castor oil (scheme 2B.1).

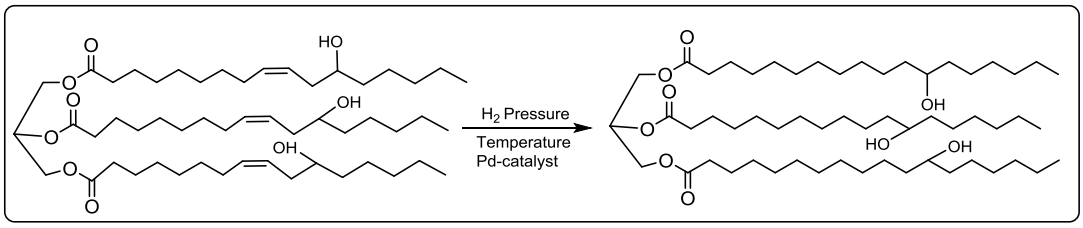

Scheme 2B.1. Hydrogenation of Castor oil using palladium based catalysts.

Palladium supported on sol-gel synthesized magnesium fluoride catalysts were used for catalytic hydrogenation of olefins. Triglycerides contain non-conjugated *cis*-C=C which on hydrogenation undergoes saturation. The conditions of hydrogenation reactions such as use of catalyst, hydrogen pressure, etc. affect the physical parameters such as melting point, specific gravity etc. of hydrogenated product and ultimately decides the quality of the formed product.

India is largest producer of castor oil in the world (~ 85% of total world production). Many Indian industries manufacture hydrogenated castor oils as value added product. Therefore the development in the present scenario of castor oil hydrogenation catalysis is of prime importance. Hence the hydrogenation of castor oil was attempted initially using all Pd supported magnesium hydroxyl fluoride catalysts.

The castor oil hydrogenation was carried out in methanol at room temperature and atmospheric pressure by bubbling hydrogen gas through the reaction mixture. Initially a series of Pd supported on sol-gel synthesized magnesium fluoride were screened for castor oil hydrogenation. The activity of the catalyst was compared with Pd-MgO catalyst. The conversion was determined by estimating iodine number of reactant and product. Castor oil shows iodine number of 84 which decreased to 75 after 3 h when Pd-MgO was used as catalyst (table 2B.1, entry 2). Further the reaction was carried out using fluorinated catalysts namely Pd-MgF_2-100, Pd-MgF_2-71 and Pd-MgF_2-40 which showed decrease in iodine number upto 50, 30 and 9.1 respectively (table 2B.1, entry 3-5). Pd-MgF_2-100 showed highest degree of saturation, thus the trend matched with the data for olefinic hydrogenation as described in chapter 2A. The higher catalytic activity of Pd-MgF_2-100 can be correlated to the higher acidity and metal support interactions between Pd and

support. The increase in degree of fluorination increases the activity of catalyst. Further steady decrease in iodine number was observed with increase in reaction time as described (table 2B.1, column 4). A reaction with Pd-MgF_2-100 catalyst under solvent free conditions showed a marginal decrease in iodine number of product upto 78. This may be due to formation of wax as solid product which disturbs the uniform stirring and hydrogen bubbling in reaction mixture. Among all fluorinated catalyst, Pd-MgF_2-100 showed best catalytic activity for castor oil hydrogenation, therefore it was selected for further catalytic studies.

Table 2B.1. Catalyst screening study for castor oil hydrogenation.[a]

Entry	Catalyst	Iodine number after 3 h	Iodine number after 8 h
1	Without catalyst	84	84
2	Pd-MgO	75	68
3	Pd-MgF_2-71	30	16
4	Pd-MgF_2-40	51	26
5	Pd-MgF_2-100	9	4

[a]**Reaction conditions**: Castor oil: 2 g; Catalyst: 0.2 g (10 wt %; 0.1 wt % Pd with respect to substrate); Methanol: 10 mL; H_2 bubbled; Temperature: RT (27 °C); Time: 3 h. [b] Conversion was determined based on iodine number.

2B.3.2. Catalyst loading effect using Pd-MgF_2-100

The effect of catalyst loading on castor oil hydrogenation was studied using Pd-MgF_2-100 catalyst as shown in table 2B.2. The hydrogenation of castor oil does not take place in absence of catalyst even after 12 h under ambient reaction conditions (table 2B.2, entry 1). When the catalyst loading with respect to castor oil gradually increased from 1 wt% to 15 wt% the iodine number after 3 h gradually decreased from 84 to 4 (table 2B.2, entry 2-6). Further the degree of hydrogenation was increased with increase in time (table 2B.2, column 4). Additionally a reaction was carried out under solvent free conditions in an autoclave which showed decrease in iodine number up to 8 at 80 °C. This may be due to effective stirring under molten condition of wax formed. However to balance between catalytic loading and catalytic activity 10 wt% catalyst loading was used for further reactions.

Table 2B.2. Catalyst loading effect using Pd-MgF_2-100.[a]

Entry	Catalyst loading (%)	Iodine number after 3 h	Iodine number (after time h)
1	Without catalyst	84	84 (12)
2	1	75	14 (48)
3	3	42	14 (20)
4	5	28	11 (7)
5	10	9	5 (6)
6	15	4	-
7[#]	10	8	-

[a]**Reaction conditions**: Castor oil: 2 gm; Catalyst: Pd-MgF_2-100; Methanol: 10 mL; H_2 bubbled; Temperature: RT (27 °C); Time: 3 h. [#]The reaction was carried under solvent free conditions at 80 °C in autoclave.

2B.3.3. Time profile study for castor oil hydrogenation using Pd-MgF_2-100

A time profile was studied to monitor the reaction progress with time. A linear decrease in iodine number was observed with increase in reaction time from 84 to 7.6 in 4 h. (fig. 2B.1).

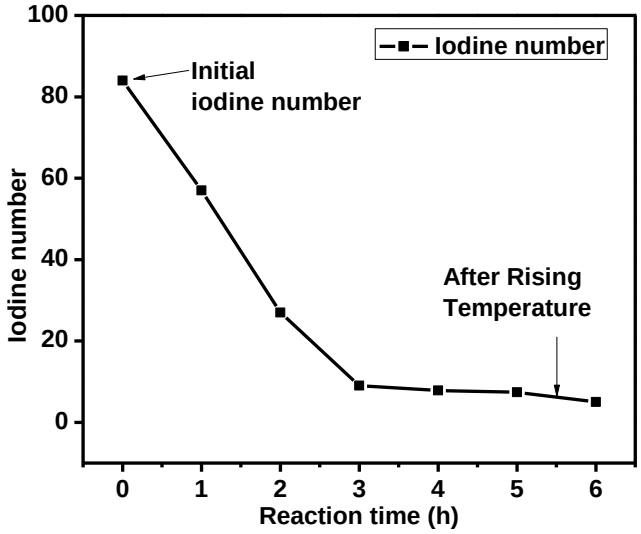

Figure 2B.1. Time profile study of castor oil hydrogenation using Pd-MgF_2-100. **Reaction conditions:** Castor oil: 2 gm; Catalyst (Pd-MgF_2-100): 0.2 g; Methanol: 10 mL; H_2 bubbled: 15 mL min^{-1}; Temperature: RT (27 °C); Time: 3 h.

Further continuation of reaction for 1 h showed the decrease in the iodine number upto 7.2 (~ 0.4 only). The reaction was continued further with heating at 65

°C, which led to decrease in iodine number up to 5 indicating almost complete hydrogenation of C=C present in castor oil.

2B.3.4. Castor oil hydrogenation under solvent free conditions

Considering the importance of solvent free conditions and industrial applications of hydrogenated castor oil, the reactions were studied under solvent free conditions. The reaction was carried out in 50 mL AMAR pressure reactor under 10 atm pressure of hydrogen gas under solvent free conditions using Pd-MgF_2-100 catalyst. Initially the catalyst loading effect was studied using 3, 5 and 10 wt% loading of catalyst with respect to substrate which showed iodine number of 29, 12 and 11 respectively of the final product. The degree of unsaturation was found to decrease rapidly with increase in catalyst loading. Hydroxyl value is one of the important parameter to determine the quality of hydrogenated castor wax. The hydroxyl value was also found to decrease from 161 to 120 with increase in catalyst loading (table 2B.3, entry 1-3). For maintaining the desired quality of the hydrogenated castor wax, the decrease in the hydroxyl value is not desirable. In view of this 5 wt% catalyst loading was considered as optimum for further studies of castor oil hydrogenation under solve free conditions.

To understand the effect of temperature on reaction profile and physical parameters of castor wax formed the reaction was carried out at 60, 90 and 100 °C (table 2B.3, entry 4-5). It was observed that the rate of reaction increased with rise in temperature which led to drop in iodine number and hydroxyl value of product. Considering the significance of retention of hydroxyl value of product and degree of hydrogenation of castor wax, a 90 °C was consider as optimum for further studies. When a time profile of reaction at 90 °C with 5 wt% of catalyst loading was studied, a decrease in degree of unsaturation was observed with increase in time of reaction also accompanied by significant decrease in hydroxyl value of castor wax (table 2B.3, entry 7-10). Further to understand the effect of amount of solvent, a couple of reactions using variable solvent proportions were studied. A reaction in methanol with methanol: castor oil ration 10:1 showed corresponding decrease in iodine number to 7 and hydroxyl value to 137 (table 2B.3, entry 11). Further a reaction with methanol: castor oil ration of 1:3 indicated the decrease in iodine number to 4 without decrease in hydroxyl value as compared to initial castor oil (table 2B.3, entry 12). This

concludes that concentration of solvent in reaction mixture not only affect to reaction rate but also hydroxyl value of the castor wax.

Table 2B.3. Hydrogenation of castor oil using Pd-MgF_2-100.[a]

Entry	Catalyst loading (Wt%)	Time (h)	Temp. (°C)	Iodine number	Hydroxyl Value	Melting point (°C)
			Catalyst Loading effect			
1	3	3	60	29	161	-
2	5	3	60	12	152	80.2
3	10	3	60	11	120	71.8
			Temperature effect			
4	5	3	60	28	152	-
5	5	3	90	10	145	76.9
6	5	3	100	7	137	72.9
			Time profile study			
7	5	1	90	57	151	-
8	5	2	90	37	150	-
9	5	3	90	10	145	76.9
10	5	5	90	5	98	76.1
			Reactions in solvent			
11[#]	10	3	RT	7	137	70.6
12[@]	10	4	RT	4	154	78.8

[a]**Reaction conditions**: Castor oil: 20 g, Catalyst: 1.0 g (5 wt%, Pd loading: 1 wt%); H_2 pressure: 10 atm, [#]Reaction with the ratio of methanol/ castor oil = 10. [@]Reaction with the ratio of methanol/ castor oil = 0.33.

2B.3.5. Parameters for quality of wax

The product obtained in lab using catalyst Pd-MgF_2-100 under solvent free conditions was compared with the commercial sample of castor wax obtained from Jayant Agrochemicals, Mumbai, India. The various standard parameters like appearance, melting point, iodine number, hydroxyl values, acid values and specific gravity were estimated for product samples obtained by hydrogenation. The results are tabulated in table 2B.4. All the parameters were found to be comparable with commercial sample.

Table 2B.4. Comparison between parameters of castor wax obtained from hydrogenation using Pd-MgF_2-100 catalyst with commercial wax

Entry	Parameters	Values	Commercial wax*
1	Appearance	White to creamish powder	White to creamish flecks
2	Melting point	81-83 ºC	83-85º C
3	Iodine number	5 max	5 max
4	Hydroxyl value	~ 138	160
5	Acid value	5 max	5 max
6	Specific gravity	1.050 g/ mL	1.027 g/ mL

*Sample obtained from Jayant Agrochemicals, Mumbai, India.

2B.3.6. Hydrogenation of various oils using Pd-MgF_2-100 catalyst

The hydrogenated vegetable oils are mainly used in foods in the form of margarine, vegetable ghee etc. All edible and non-edible oils are the unsaturated triglycerides having 1-3 number of C=C in each hydrocarbon chain in *cis* form. Hydrogenation of triglycerides containing 2-3 C=C in alkyl fragments results in triglycerides of monounsaturated fatty acids with both *cis* and *trans* C=C. It is well-known that the ratio of c*is*/*trans* isomers influences the physiological [75] and the physical properties of the hydrogenated fat, such as melting temperature, hardness, ability to form plastic mixtures with other fats, etc [76]. The trans fats have higher melting points which lead to blocking of arteries and further generated severe heart related problems (heart disorders like *arteriosclerosis*) in body. To avoid such problems, selective hydrogenation of *cis* C=C of edible oil without isomerization is of prime importance.

Furthermore the wider applicability of the Pd-MgF_2-100 catalyst was studied for hydrogenation of edible and non-edible oils at room temperature and atmospheric pressure of hydrogen gas in toluene (table 2B.5). In case of sunflower oil, the iodine number was decreased to 10 in 3 h (table 2B.5, entry 1). Further similar oils like Soyabean ad Palm showed a decrease in iodine number upto 12 and 14 respectively under identical conditions (table 2B.5, entry 2-3). Due to demand of selective *cis*-hydrogenation of edible oils with respect to C=C, the hydrogenated product was

analysed on GC to determine the % of *cis*-products at *Godrej industries, Mumbai, India*. The methyl ester derivatives of hydrogenated product of soyabean and sunflower oil showed up to selectivity up to 70% and 81% respectively for *cis*-hydrogenation.

Table 2B.5. Hydrogenation of various oils using Pd-MgF_2-100.[a]

Entry	Oils	Time	Iodine number	
			Initial	Final
1	Sunflower oil	3	135	10
2	Soyabean Oil	3	128	12
3	Palm oil	3	52	14
4[#]	Sunflower oil	7	135	54
		16		33

[a]**Reaction conditions**: Oil: 2 g; Catalyst: Pd-MgF_2-100 (0.2 g, 10 wt% w.r.t. substrate); Solvent: Toluene 10 mL; H_2 bubbled (1 atm); Temperature: RT (27 °C); Time: 3 h. [#] Reaction was carried out without solvent followed by heating after 7 h to 80 °C.

Hydrogenation of sunflower oil was studied under solvent free conditions (table 2B.5, entry 4). It showed decrease in iodine number from 132 to 54 after 7 h. Due to formation of solid wax after partial hydrogenation of sunflower oil the rate of stirring was decreased hence to maintain the effective stirring, the reaction flask was heated at 80 °C. Further the decrease in iodine number of hydrogenated oil was estimated to be 33 after 16 h. Further the applicability of catalyst was extended to hydrogenation of fatty acid like oleic acid in methanol. The estimated iodine number of oleic acid decreased from 95 to 5 in 3 h. This indicated versatility of Pd-MgF_2-100 catalyst for hydrogenation of various oils and fatty acid under optimum conditions.

2B.3.7. Results of recyclability study for castor oil hydrogenation

The recyclability of the catalyst was tested for castor oil hydrogenation at room temperature and atmospheric pressure of hydrogen gas. After completion of each reaction the catalyst was separated using hot centrifugation which upon washing with solvents [methanol (10 mL) and acetone (10 mL)] followed by drying at 100 °C. The dried catalyst was further used for the next run and the results are summarized in fig. 2B.2. The catalyst could be recycled very efficiently for three cycles without

appreciable decrease in activity under identical conditions. Further the Pd leaching was confirmed by ICP-AES analysis.

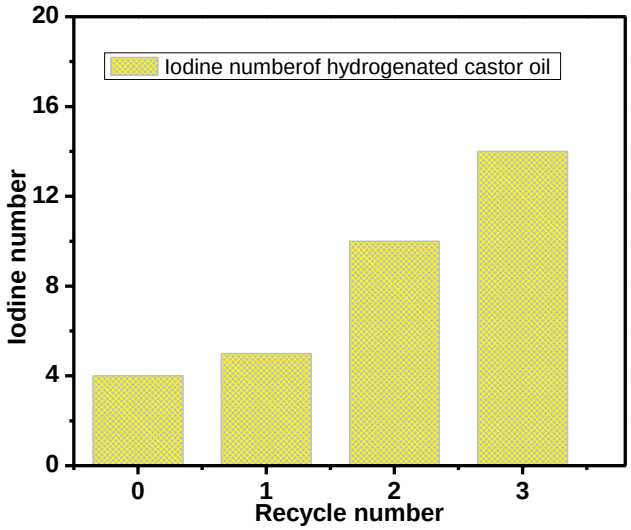

Figure 2B.2. Catalytic recycle study using Pd-MgF_2-100 catalyst**.**

[a]**Reaction conditions**: Castor oil: 2 g; Catalyst: Pd-MgF_2-100 (0.2 g, 10 wt% w.r.t. substrate); Methanol: 10 mL; H_2 bubbled (1 atm); Temperature: RT (27 °C); Time: 3 h.

There are several catalytic systems based on the Pd known in literature among which Pd supported on mesoporous materials such as SiO_2, Al_2O_3 and TiO_2 have been used for selective hydrogenation of oils and fats. These catalyst resulted in decrease in iodine number up to <5, but problems like metal blocking, and metal poisoning were observed. Furthermore several Pd supported on activated carbons and modified carbon supported catalytic systems have been studied. Although these catalysts showed high activity, due to pyrophoric nature they are less preferred with respect to other catalytic supports. Considering industrial need of novel catalytic support, metal fluorides can act as better and safer support due to their intrinsic properties as discussed in Section 2A. Although preliminary studies were done in this chapter 2B for oil hydrogenation using sol-gel synthesized Pd-MgF_2-100, a detailed investigation of palladium supported metal hydroxyl fluoride catalyst for their use in industries is under progress.

2B.4. Conclusions

The catalytic hydrogenation of various edible and non-edible oils was studied over Pd supported magnesium hydroxyl fluoride catalysts. Among a screened series of catalyst, Pd-MgF_2-100 showed excellent behavior under ambient pressure and high pressure conditions at room temperature and solvent free conditions. In case of castor oil hydrogenation, the iodine value of hydrogenation product could be reduced to 4 without affecting the hydroxyl value of product considerably. The hydroxyl number of the castor wax can be retained at 90 °C with 5 wt% loading of catalyst and by controlling the reaction time. The reaction parameters can be tuned easily to obtain desired properties of castor wax. The catalyst can be recycled efficiently even up to three cycles without appreciable loss in the catalytic activity. There was no Pd leaching during the reaction as confirmed by ICP-AES analysis. Furthermore the catalyst could be useful for hydrogenation of several vegetable oils along with fatty acids under ambient reaction conditions.

2.5. References

[1] (a) R. Si, M. F. Stephanopoulos, *Angew. Chem. Int. Ed.*, **2008**, *47*, 2884; (b) L. J. Liu, Z. J. Yao, Y. Deng, F. Gao, B. Liu, L. Dong, *ChemCatChem*, **2011**, *3*, 978; (c) J. F. Liu, W. Chen, X. W. Liu, K. B. Zhou, Y. D. Li, *Nano Res*., **2008**, *1*, 46.

[2] J. M. Campelo, D. Luna, R. Luque, J. M. Marinas, A. A. Romero, *ChemSusChem*, **2009**, *2*, 18.

[3] E. Garcia-Bordeje, M. F. R. Pereira, M. Ronningc, D. Chenc, *SPR Catalysis*, **2014**, *26*, 72.

[4] R. Ciriminna, A. Fidalgo, V. Pandarus, F. Beland, L. M. Ilharco, M. Pagliaro, *Chem. Rev.*, **2013**, *113*, 6592.

[5] E. Merino, E. Verde-Sesto, E. M. Maya, M. Iglesias, F. Sanchez, A. Corma, *Chem. Mater.*, **2013**, *25*, 981.

[6] Q. M. Kainz, O. Reiser, *Acc. Chem. Res.*, **2014**, *47*, 667.

[7] (a) X. Y. Liu, M. H. Liu, Y. C. Luo, C. Y. Mou, S. D. Lin, H. K. Cheng, J. M. Chen, J. F. Lee, T. S. Lin, *J. Am. Chem. Soc.*, **2012**, *134*, 10251; (b) K. Bramhaiah, N. S. John, *RSC Adv.*, **2013**, *3*, 7765.

[8] (a) S. J. Tauster, S. C. Fung, R. L. Garten, *J. Am. Chem. Soc.*, **1978**, *100*, 170;

(b) Z. H. Qin, M. Lewandowski, Y. N. Sun, S. Shaikhutdinov, H. J. Freund, *J. Phys. Chem. C*, **2008**, *112*, 10209.

[9] (a) J. Li, J. L. Chen, W. Song, J. L. Liu, W. J. Shen, *Appl. Catal. A*, **2008**, *334*, 321; (b) A. S. Ivanova, E. M. Slavinskaya, R. V. Gulyaev, V. I. Zaikovskii, O. A. Stonkus, I. G. Danilova, L. M. Plyasova, I. A. Polukhina, A. I. Boronin, *Appl. Catal. B*, **2010**, *97*, 57.

[10] Y. Li, W. Shen, *Chem. Soc. Rev.*, **2014**, *43*, 1543.

[11] Z. Ma, F. Zaera, *Design of Heterogeneous Catalysis: New Approaches Based on Synthesis, Characterization, and Modelling*, U. S. Ozkan ed, Wiley-VCH, Weinheim, **2009**, 113.

[12] (a) S. Wuttke, S. M. Coman, G. Scholz, H. Kirmse, A. Vimont; M. Daturi, S. L. M. Schroeder, E. Kemnitz, *Chem. Eur. J.*, **2008**, *14*, 11488; (b) E. Kemnitz, U. Gross, S. Rüdiger, S. Shekar, *Angew. Chem. Int. Ed*., **2003**, *42*, 4251.

13] S. M. Coman, S. Wuttke, A. Vimont, M. Daturi, E. Kemnitz, *Adv. Synth. Catal.*, **2008**, *350*, 2517.

[14] P. T. Patil, A. Dimitrov, J. Radnik, E. Kemnitz, *J. Mater. Chem.*, **2008**, *18*, 1632.

[15] A. Negoi, S. Wuttke, E. Kemnitz, D. Macovei, V. I. Parvulescu, C. M. Teodorescu, S. Coman, *Angew. Chem. Int. Ed.*, **2010**, *49*, 8134.

[16] N. Candu, S. Wuttke, E. Kemnitz, S. M. Coman, V. I. Parvulescu, *Appl.Catal. A*, **2011**, *391*, 169.

[17] S. M. Coman, V. I. Parvulescu, S. Wuttke, E. Kemnitz, *ChemCatChem*, **2010**, *2*, 92.

[18] I. K. Murwani, K. Scheurell, E. Kemnitz, *Catal. Commun.*, **2008**, *10*, 227.

[19] K. Teinz, S. Wuttke. F. Börno, J. Eicher, E. Kemnitz, *J. Catal.*, **2011**, *282*, 175.

[20] H. G. Prechtl, M. Teltewskoi, A. Dimitrov, E. Kemnitz, T. Braun, *Chem. Eur. J.*, **2011**, *17*, 14385.

[21] S. B. Troncea, S. Wuttke, E. Kemnitz, S. M. Coman, V. I. Parvulescu, *Appl. Catal. B: Environ.*, **2011**, *107*, 260.

[22] T. W. Lyons, M. S. Sanford, *Chem. Rev.*, **2010**, *110*, 1147.

[23] J. F. Hartwig, *Organotransition metal chemistry from bonding to catalysis, University Science Books*, **2010**.

[24] F. Nerozzi, *Platinum Metals Rev.*, **2012**, *56*, 236.

[25] P. W. N. M. van Leeuwen, *Homogeneous catalysis, understanding the art, Kluwer Academic Publishers*, **2004**.

[26] M. J. Climent, A. Corma, S. Iborra, *Chem. Rev.*, **2011**, *111*, 1072.

[27] J. Tsuji, *Palladium reagents and catalysts, new perspectives for the 21st century*, John Wiley & Sons, **2004**.

[28] D. Astruc, *Nanoparticles and catalysis*, Wiley-VCH, **2008**.

[29] A. Binder, M. Seipenbusch, M. Muhler, G. Kasper, *J. Catal.*, **2009**, *268*, 150.

[30] J. Dupont, G. S. Fonseca, A. P. Umpierre, P. F. P. Fichtner, S. R. Teixeira, *J. Am. Chem. Soc.*, **2002**, *124*, 4228.

[31] M. Dell'Ana, M. Gagliardi, P. Mastrorilli, G. P. Suranna, C. F. Nobile, *J. Mol. Catal. A: Chem.*, **2000**, *158*, 515.

[32] R. Andres, E. de Jesus, J. C. Flores, *New J. Chem.*, **2007**, *31*, 1161.

[33] R. S. Oosthuizen, V. O. Nyamori, *Platinum Met. Rev.*, **2011**, *55*, 154.

[34] (a) S. Nishimura, *Handbook of Heterogeneous Catalytic Hydrogenation for Organic Synthesis*, Wiley-Interscience, New York, **2001**; b) P. N. Rylander, *Hydrogenation Methods*, Academic Press, New York, **1985**.

[35] (a) R. Narayanan, M. A. Ei-Sayed, *J. Am. Chem. Soc.*, **2003**, *125*, 8340; (b) S. W. Kim, M. Kim, W. Y. Lee, T. Hyeon, *J. Am. Chem. Soc.*, **2002**, *124*, 7642.

[36] B. S. Furniss, A. J. Hannaford, P. W. G. Smith, A. R. Tatchell, *Vogel's Textbook of Practical Organic Chemistry*, 5th ed., Longman Scientific & Technical, **1989**.

[37] M. H. Tran, H. Okhita, T. Mizushima, N. Kakuta, *Appl. Catal. A*, **2005**, *287*, 129.

[38] E. Kemnitz, S. Wuttke, S. M. Coman, *Eur. J. Inorg. Chem.*, **2011**, 4773.

[39] (a) Y. Diao, W. Walawender, C. S. Sorensen, K. J. Klabunde, T. Ricker, *Chem. Mater.*, **2002**, *14*, 362; (b) K. T. Ranjit, K. J. Klabunde, *Chem. Mater.*, **2005**, *17*, 65; (c) L. Andrews, X. U. Wang, M.E. Likhani, L. Manceron, *J. Phys. Chem. A*, **2001**, *105*, 3052.

[40] M. Zieliński, M. Pietrowski, M. Wojciechowska, *Polish J. Environ. Stud.*, **2009**, *18*, 965.

[41] S. Wuttke, C. Dietel, F. M. Hinterholzinger, H. Hintz, H. Langhals, T. Bein, *J. Phys. Chem. C*, **2010**, *114*, 5113.

[42] H. A. Prescott, Z. J. Li, E. Kemnitz, J. Deutsch, H. J. Lieske, *Mater. Chem.*, **2005**, *15*, 4616.

[43] S. Wuttke, S. M. Coman, G. Scholz, H. Kirmse, A. Vimont, M. Daturi, S. L. M. Schroeder, E. Kemnitz, *Chem. Eur. J.*, **2008**, *14*, 11488.

[44] M. Fadoni, L. Lucarelli, *Stud. Surf. Sci. Catal.*, **1999**, *120A*, 177.

[45] K. V. R. Chary, D. Naresh, V. Vishwanathan, M. Sadakane, W. Ueda, *Catal. Commun.*, **2007**, *8*, 471.

[46] V. I. Nefedov, Y. V. Salyn, I. I. Moiseev, A. P. Sadovskii, A. S. Berenbljum, A. G. Knizhnik, S. L. Mund, *Inorg. Chim. Acta*, **1979**, *3*5, L343.

[47] D. D. Eley, H. Pines, *Advances in Catalysis*, Academic Press Inc., U. S. **1993**.

[48] B. M. Choudary, S. Madhi, N. S. Chowdari, M. L. Kantam, B. Sreedhar, *J. Am. Chem. Soc.*, **2002**, *124*, 14127.

[49] (a) L. Rasmussen, C. K. Jorgensen, *Acta Chem. Scand*. **1968**, *22*, 2313; (b) Z. Zhang, W. M. H. Sachtler, H. Chen, *Zeolite*, **1990**, *10*, 784.

[50] J. Noack, F. Emmerling, H. Kirmse, E. Kemnitz, *J. Mater. Chem.*, **2011**, *21*, 15015.

[51] M. L. Kantam, R. Kishore, J. Yadav, M. Sudhakar, A. Venugopala, *Adv. Synth. Catal.*, **2012**, *354*, 663.

[52] A. V. Biradar, A. A. Biradar, T. Asefa, *Langmuir*, **2011**, *27*, 14408.

[53] (a) M. Zielinski, M. Wojciechowska, *Catal. Commun.*, **2012**, *18* 1; (b) M. Zielinski, M. Pietrowski, M. Wojciechowska, *ChemCatChem*, **2011**, *3*, 1653; (c) M. Zielinski, M. Wojciechowska, *Catal. Today*, **2011**, *169*, 175.

[54] (a) A. E. Bailey, *J. Am. Oil Chem. Soc*., **1949**, *26*, 596; (b) L. F. Albright, *J. Am. Oil Chem. Soc*., **1965**, *42*, 250.

[55] (a) J. W. Veldsink, M. J, Bouma, N. H, Schoon, A. A. C. M. Beenackers, *Catal. Rev. Sci. Eng.*, **1997**, *39*, 253; (b) W. T. Koetsier, F. D. Padley, *Hydrogenation of edible oils, technology and applications: In Lipid Technologies and Applications*; Marcel Dekker, New York, **1997**, 265.

[56] M. W. Balakos, E. E. Hernandez, *Catal. Today*, **1997**, *35*, 415.

[57] K. F. Mattil, F. A. Norris, A. J. Stirton, D. Swern, *Bailey's Industrial Oil and Fat Products*, 3 Ed.; John Wiley and Sons, New York, **1964**.

[58] V. A. Semikolenov, I. L. Simakova, G. V. Sadovnichij, *Chem. Ind. (Moscow)* **1996**, *N3*, 40.

[59] H. J. Beckmann, *J. Am. Oil Chem. Soc.*, **1983**, *60*, 282.

[60] I. L. Simakova, O. A. Simakova, A. V. Romanenko, D. Y. Murzin, *Ind. Eng. Chem. Res.*, **2008**, *47*, 7219.

[61] R. J. Grau, A. E. Cassano, M. A. Baltanas, *Catal. Rev. Sci. Eng.*, **1988**, *30*, 1.

[62] R. J. Grau, A. E. Cassano, M. A. Baltanas, *J. Am. Oil Chem. Soc*., **1990**, *67*, 226.

[63] V. I. Savchenko, I. A. Makaryan, *Platinum Met. Rev*., **1999**, *43*, 74.

[64] N. Hsu, L. L. Dlosady, L. J. Rubin, *J. Am. Oil Chem. Soc*., **1988**, *65*, 349.

[65] S. Lestari, P. Maki-Arvela, H. Bernas, O. Simakova, R. Sjoeholm, J. Beltramini, D. Y. Murzin, *Energy & Fuels*, **2009**, *23*, 3842.

[66] K. Belkacemi, A. Boulmerka, J. Arul, S. Hamoudi, *Top. Catal.*, **2006**, *37*, 113.

[67] A. F. Perez-Cadenas, F. Kapteijn, M. M. P. Zieverink, J. A. Moulijn, *Catal. Today*, **2007**, *128*, 13.

[68] N. Ravasio, F. Zaccheria, M. Gargano, *Appl. Catal. A*, **2002**, *233*, 1.

[69] R. Yang, M. Su, M. Li, J. Zhang, X. Hao, H. Zhang, *Bioresour. Technol*., **2010**, *101*, 5903.

[70] M. A. Ermakova, D. Y. Ermakov, *Appl. Catal. A*, **2003**, *245*, 277.

[71] (a) M. Plourde, K. Belkacemi, J. Arul, *Ind. Eng. Chem. Res.*, **2004**, *43*, 2382; (b) M. B. Fernández, G. M. Tonetto, G. H. Crapiste, M. L. Ferreira, E. Damiani, *J. Mol. Catal. A*, **2005**, *237*, 67.

[72] A. J. Wright, A. L. Mihele, L. L. Diosady, *Food Res. Int*., **2003**, *36*, 797.

[73] B. W. Hoffer, A. D. Langeveld, J. P. Janssens, R. L. C. Bonné, C. M. Lok, J. A. Moulijn, *J. Catal*., **2000**, *192*, 432.

[74] http://apps.who.int/phint/en/p/docf/

[75] G. R. List, *Lipid Technol*., **2004**, *16*, 173.

[76] D. V. Stinglei, R. J. Wrobel, *J. Am. Oil Chem. Soc*., **1961**, *38*, 201.

Chapter 3

PALLADIUM SUPPORTED ON BARIUM FLUORIDE: SYNTHESIS, CHARACTERIZATION AND CATALYTIC ACTIVITY FOR AEROBIC OXIDATION OF ALCOHOLS

Abstract

Palladium supported on barium hydroxyl fluoride was synthesized from metallic barium via barium methoxide using one pot fluorolytic sol-gel method. The synthesized material was characterized by PXRD, FTIR, nitrogen adsorption, NH_3-TPD, FTIR of adsorbed pyridine, SEM-EDAX and HRTEM. The SEM analysis indicated formation of rod shaped barium hydroxyl fluoride of upto 2-3 μm length and 0.2 – 0.4 μm width. TEM showed presence of nanoparticles of palladium and palladium oxides. The catalytic activity of palladium supported barium hydroxyl fluoride was evaluated for aerobic oxidation of benzyl alcohol in liquid phase under base-free conditions, using toluene as solvent. The catalyst showed selective formation of benzaldehyde at reflux temperature of toluene. No by-products formation such as benzoic acid and benzyl benzoate were observed. The in-situ FTIR studies for determination of reaction mechanism showed the reaction to follow Langmuir-Hinshelwood type mechanism. The catalyst was recyclable up to five cycles without loss in catalytic activity. The true heterogeneous nature of catalyst was confirmed by hot filtration test as well as ICP-AES study which showed no palladium leaching.

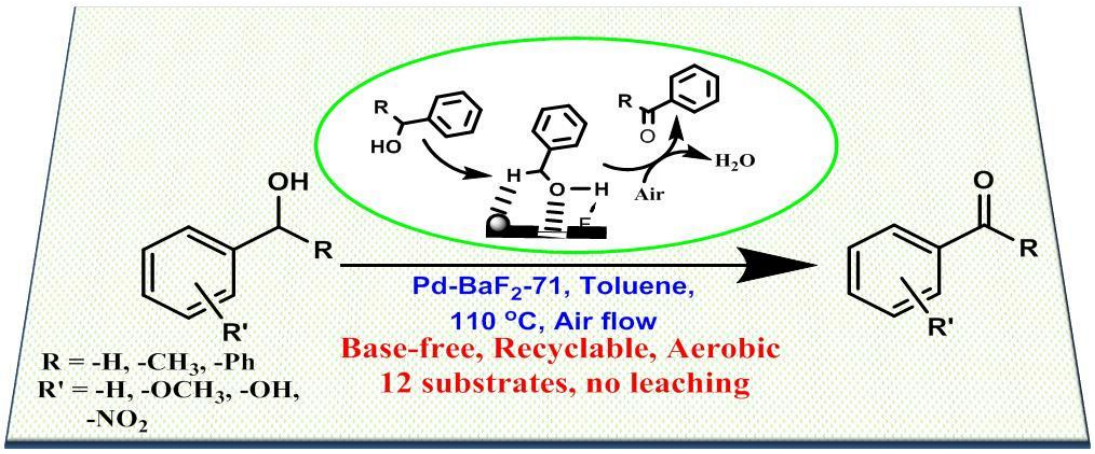

3.1. Introduction

Oxidation is one of the pivotal reactions in organic chemistry which is useful in industries for the productions of bulk chemicals. It is commonly used for conversion of oils and natural gas based feedstock to bulk chemicals [1]. Oxidation reaction is generally performed using stoichiometric amounts of inorganic oxidants which generate large quantities of inorganic salts as waste products [2]. Therefore, there is a pressing need for designing catalytic technologies employing benign oxidants, such as oxygen and/or hydrogen peroxide for the production of fine chemicals. In principle, catalytic oxidations can be performed with a large variety of oxidants. These oxidants need to be activated using catalyst. However, from an environmental viewpoint, oxidants which produce salts as by-products need to be eliminated and replaced by more environmental friendly technologies.

Oxidation of alcohols to corresponding aldehydes and carboxylic acids is one of the important methods in organic synthesis as they are widely used in the fine chemical industry. Aldehydes and ketones are the key raw materials for a wide range of pharmaceutical intermediates, fragrances and flavors [3]. Many processes with different reagents have been reported for this purpose including stoichiometric and catalytic methods. The stoichiometric oxidants, such as permanganate and dichromate are frequently used for this purpose, but these agents are expensive, toxic and produce large amount of wastes [4]. The heterogeneous catalytic oxidation using clean oxidants such as molecular oxygen, air or hydrogen peroxide lead towards green oxidations of alcohols. The use of heterogeneous catalyst systems would be superior to homogeneous counterparts owing to the easier separation of products and reuse of catalyst.

The utilization of abundantly available O_2 or air for the synthesis of many commodity chemicals is ever demanding owing to decrease in the cost of raw materials and no environmental pollution [5]. However, due to low reactivity of oxygen, its activation is the key step for all aerobic oxidation reactions [6]. To make oxygen react, it has to undergo excitation of inert ground triplet state ($^3O_2$) to highly reactive singlet state ($^1O_2$). However, such direct excitation ($^3O_2 \rightarrow {}^1O_2$) does not occur easily, hence it is necessary to select the appropriate medium to overcome this limitation. Many efforts have been taken using photosensitization with dye molecules (i.e. a spin−flip process) [7] or metal nanoparticles [8] for activation of oxygen

molecules. Particularly, supported transition metal nanoparticles have attracted much attention due to its quantum effect and variable properties [9].

For oxidation of alcohols a number of metal-based catalytic systems have been developed which allowed the use of air as oxidant. Among all used transition metal based catalysts, particularly Pd, Pt, Ru, Au based catalysts have shown promising activity [10]. Pd based catalysts have shown better activity for oxygen activation in aerobic oxidation due to labile redox nature [11] and partial electron transfer from Pd to O_2 ($Pd \rightarrow O_2$) [12]. The charge on Pd may offer a control for tuning its efficiency which is fundamentally important to optimize the design of the catalyst.

Various Pd catalysts like $PdCl_2$, $Pd(OAc)_2$ with equivalent or excess amount of base have been extensively studied for aerobic oxidation of alcohols. Previously, the $PdCl_2$-NaOAc system was employed in the oxidation of secondary alcohols using ethylene carbonate as solvent [13]. Further $PdCl_2$-Na_2CO_3 system with Adogen 464® as phase transfer catalyst (PTC) was used for oxidation of diols to lactones in chlorinated solvents [14]. However, the activities (TOFs) of these catalysts were found to be low [15]. Sheldon and coworkers achieved a high activity using water soluble palladium (II) bathophenanthroline catalyst [16]. Additionally with the nitroxyl radical TEMPO was used to prevent oxidation of the aldehyde to acid [17].

In heterogeneous catalysis, support plays a vital role in tuning activity and selectivity of reaction. Hence a large number of supports have been explored for synthesis of efficient catalysts [18], which include carbon [19], silica based structured supports [20], polymeric materials [21] and magnetic nanoparticles [22]. The co-operative effects of metal nanoparticles and supports are known for enhancement of catalytic activity. Recently, many efforts have been devoted to design the supported metal catalysts by changing the crystal structure, morphology and crystallinity of supports [23]. Although, there are large number of reports on aerobic oxidation via O_2 activation using Pd based catalysts such as Pd/C [24], Pd-hydrotalcites [25], Pd/TiO_2 [26], Pd/polymer [27], these catalysts suffer from drawbacks such as high catalyst loading, low catalytic activities, limited substrate scope and low stability. Hence there is large scope to find alternative support.

Metal fluorides are establishing as an important class of non-conventional support in heterogeneous catalysis [28]. Compared to conventional supports, metal fluorides have different properties like high ionicity, less absolute fundamental

absorption [29]. Among all metal fluorides, barium fluoride (BF) is one of the widely used dielectric fluorides with potential applications in microelectronic and optoelectronic devices [30], scintillators [31] and polymeric articles [32].

Previously barium fluoride was used as catalyst in very few reactions which include oxidative couplings of methane, where BaF_2 was used in combination with CeO_2. Barium fluoride was reported to activate O_2 by exchanging lattice fluoride with oxygen and resulted in formation of O_2^-/O_2^{2-} species at 800 °C [33]. It has also been used for selective dehydrochlorination [34] in gas phase reactions where it provides weak acidic and strong basic sites for activation of substrate at 200 °C. Hence it is interesting to explore further catalytic activity of barium fluoride as support in oxidation reaction.

Herein we have studied one pot synthesis of Pd supported on BaF_2 and its catalytic applications for aerobic oxidation of benzyl alcohols under base free conditions.

3.2. Experimental

3.2.1. Materials

All chemicals were purchased from Aldrich chemical Co. USA and used as received. Hydrofluoric acid (71% aqueous solution), and solvents were purchased from Merck chemicals, Germany and used as obtained.

3.2.2. Catalyst synthesis

Cautions: 1. HF is a highly toxic and irritant compound causing severe burns if it comes in contact with the skin.

2. Barium is highly reactive with methanol to generate hydrogen and heat hence the rate of reaction needs to be controlled initially by keeping reaction flask in ice bath.

Palladium supported on barium hydroxyl fluoride was prepared under inert atmosphere of argon using standard Schlenk technique by one-pot sol-gel method as follows: In 250 mL round bottom flask, metallic barium (2.0 g, 14.56 mmol) was dissolved in methanol (100 mL) at room temperature for 16 h to form the methanolic solution of barium methoxide. To the solution of barium methoxide, stoichiometric amount of hydrofluoric acid (71% aqueous solution, 0.7 mL, 30 mmol) was added followed by addition of methanolic solution (10 mL) of palladium acetate (0.0540 g,

0.24 mmol) corresponding to 1 wt% Pd loading in the final catalyst. The mixture was allowed to react to form highly viscous opaque gray colored gel. The gel was allowed to age for 16 h then dried under vacuum initially at room temperature for 3 h and then at 60 °C till complete removal of methanol. The solid product was further dried at 250 °C for 5 h in furnace. The synthesized catalyst was named as Pd-BaF_2-71.

3.2.3. Catalyst characterization

The synthesized Pd-BaF_2-71 catalyst was characterized using physicochemical techniques such as PXRD, FTIR, N_2-physisorption, NH_3-TPD, SEM-EDAX and TEM, the details of which are mentioned in chapter 2A, section 2A.2.6.

3.2.4. Catalytic reaction

A 50 mL two necked round bottom flask was charged with substrate (5 mmol), toluene (10 mL) and catalyst (10 wt% with respect to substrate). The reaction mixture was stirred at 110 °C and air was bubbled through the reaction mixture with flow of 10 mL min^{-1}. The reaction was monitored by gas chromatographic analysis using Agilent 6890 Gas Chromatograph equipped with HP-5 dimethyl polysiloxane capillary column (60 m length, 0.25 mm internal diameter, 0.25 μm film thicknesses) with flame ionization detector. Products were confirmed by comparison with retention time of authentic samples.

3.2.5. Catalyst recycle

The recyclability of Pd-BaF_2 was tested for benzyl alcohol oxidation under optimized reaction conditions (Benzyl alcohol: 1 mmol; Catalyst: 0.011 g (10 wt%; 0.1 wt% Pd with respect to benzyl alcohol); Toluene: 10 mL; Air flow: 10 mL min^{-1} Temperature: 110 °C; Time: 8 h). After completion of the reaction, catalyst was recovered by centrifugation followed by filtration and washing with solvents (toluene (5 mL x 2 times) and acetone 5 mL) and finally dried at 110 °C for 30 min. A new reaction was then carried out with fresh benzyl alcohol under the same reaction conditions. The Pd-BaF_2-71 catalyst was recycled for at least 5 times following the similar procedure.

3.2.6. Hot filtration test and ICP-AES analysis for Pd leaching

To verify the palladium leaching in the reaction mixture, the hot filtration test was carried out at room temperature. A 0.05 g of catalyst was stirred with 0.5 g of

benzyl alcohol in 10 mL of toluene under typical reaction conditions i.e. bubbling air with the flow of 10 mL min^{-1} at 110 °C. After 4 h, the reaction showed 58% benzyl alcohol conversion without affecting selectivity of benzaldehyde. At this point the catalyst was removed from liquid phase by filtration through Whatmann filter paper no. 1 and the reaction mixture was allowed to react further under mentioned reaction conditions.

The removed catalyst was tested using ICP-AES analysis as mentioned in section 2A for Pd content. The sample for ICP-AES analysis was prepared using procedure as given in chapter 2, section 2A.2.7.

3.3. Results and discussion

3.3.1. Catalyst synthesis

One pot synthesis of Pd-BaF_2-71 catalyst by fluorolytic sol-gel route using aq. hydrofluoric acid (71 %), resulted in fluorolysis and hydrolysis of Ba-OR bond and form Ba-F and Ba-OH bonds respectively [35, 36]. Though the molar ratio of Ba/HF was adjusted to 1:2, the hydrolysis of barium methoxide becomes competitive with fluorination because of water content in the fluorinating agent. This reaction generates the composition in which both fluoride and hydroxide are attached to barium in a solid structure and this led to the formation of barium hydroxyl fluorides [$BaF_{(2-X)}(OH)_X$]. The typical one pot sol gel synthesis of Pd-$BaF_{2-X}(OH)_X$ (henceforth mentioned as Pd-BaF_2-71) is represented in scheme 3.1. The addition of alcoholic solution of palladium acetate during fluorolysis gave light red color initially which upon aging turned to light gray. Typically the grey color of final gel indicates partial reduction of Pd^{II} to Pd^0 which may be due to the hydrogen liberated during the formation of barium methoxide from metallic barium.

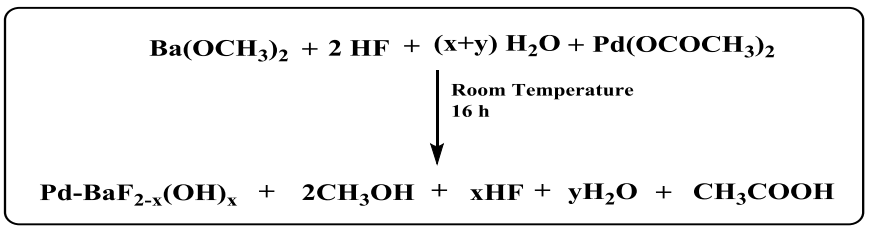

Scheme 3.1. Schematic representation for Pd-BaF_2-71 synthesis.

In contrast to the non-aqueous sol gel route which results in the formation of clear sols and transparent gels, the aqueous route results in opaque gels of grey color due to presence of partially reduced palladium nanoparticles [37]. The bulk and

surface structure of Pd-BaF_2-71 was analyzed using various characterization techniques.

3.3.2. Powder X-ray Diffraction Analysis (PXRD)

The metal fluorides are formed in different crystalline structures depending on their chemical composition. The diffraction peaks in PXRD pattern (fig. 3.1) can be indexed for barium fluorides (JCPDS 04-0452) and barium hydroxides (JCPDS 22-1054). The PXRD pattern showed two types of peaks. The sharp and high intense peaks correspond to reflections from barium fluoride while the broad and weak peaks may be due to reflections of barium hydroxide. Furthermore, presence of few less intense peaks at 2θ = 21.3, 27.5, 31.8 and 44.7 ° may be related to the reflection from mixed phase of barium hydroxyl fluoride.

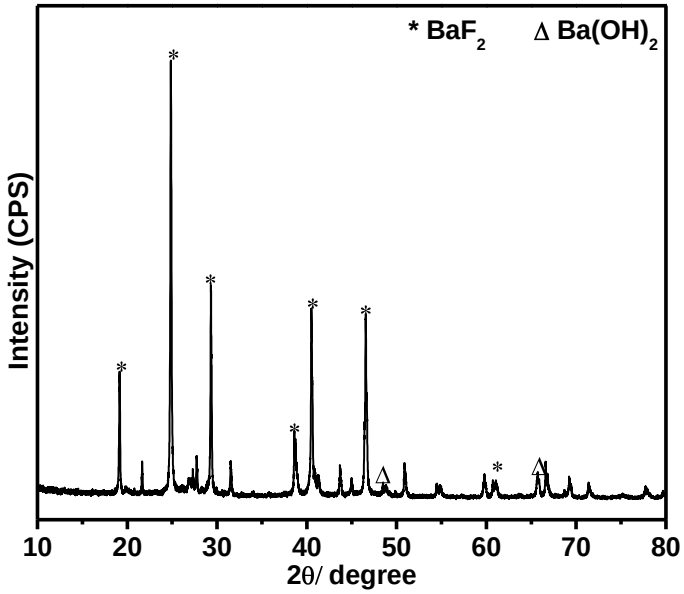

Figure 3.1. PXRD pattern of Pd-BaF_2-71.

However no diffraction for Pd_{111} (2θ = 40.01°) was detected which may be due to very low content of Pd (1 wt%) with high order of dispersion of Pd particles on the surface of catalyst.

3.3.3. FTIR spectra

The FTIR spectrum of Pd-BaF_2-71 catalyst is shown in fig. 3.2. Due to the octahedral coordination of magnesium by fluorine and oxo/hydroxyl, all the catalyst expectedly exhibit OH symmetry for an ordered structure with two infrared active modes. Fluorination of barium methoxide with aqueous hydrofluoric acid is

competitive reaction where fluorolysis and hydrolysis takes place simultaneously with variable rates. The fluorolysis led to the formation of Ba-F bond while hydrolysis forms Ba-O bonds. Typically ν(Ba-F) and ν(Ba-O) stretches were observed at 485 cm^{-1} and 732 cm^{-1} respectively [38].

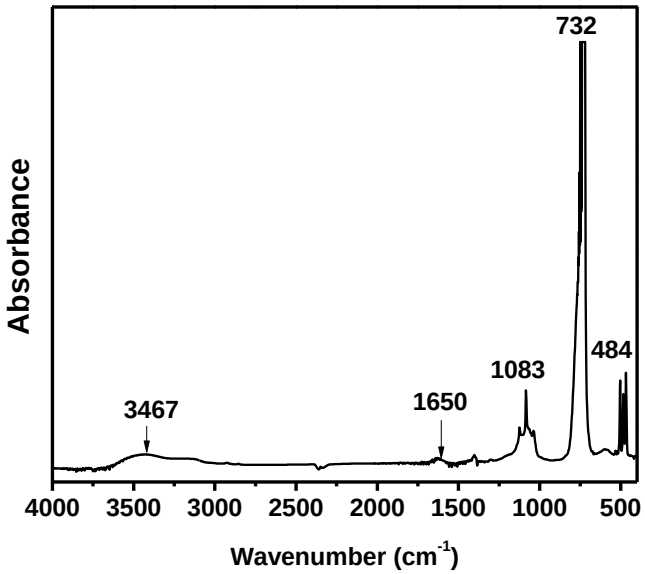

Figure 3.2. FTIR spectrum of Pd-BaF_2-71 catalyst.

The bands around 3467 and 1650 cm^{-1} corresponds to O-H stretching and bending vibrations respectively of surface hydroxyl groups. Along with these an additional band at 1083 cm^{-1} was observed which corresponds to ν(C-O) indicating presence of alkoxy residue in the final catalyst.

3.3.4. BET surface area

The N_2 adsorption-desorption isotherms of Pd-BaF_2-71 showed type IV character typical for mesoporous materials with a H1 type hysteresis loop and porous texture (fig. 3.3). The BET surface area of the catalyst was found to be only 8 $m^2\ g^{-1}$ with total pore volume of 0.018 cc g^{-1}. Typically the surface area of Pd-BaF_2-71 was very low compared to other metal fluorides like Pd-MgF_2-71 (140 m^2g^{-1}) and Pd-SrF_2-71 (58 m^2g^{-1}) prepared under identical conditions. Due to increase in atomic size of central metal (like Mg/Sr/Ba) the density of material increases which decrease the surface area. The average pore size was determined using Barrett-Joyner-Halenda (BJH) analysis and found to be 9.1 nm which confirms the mesoporous nature of the catalyst.

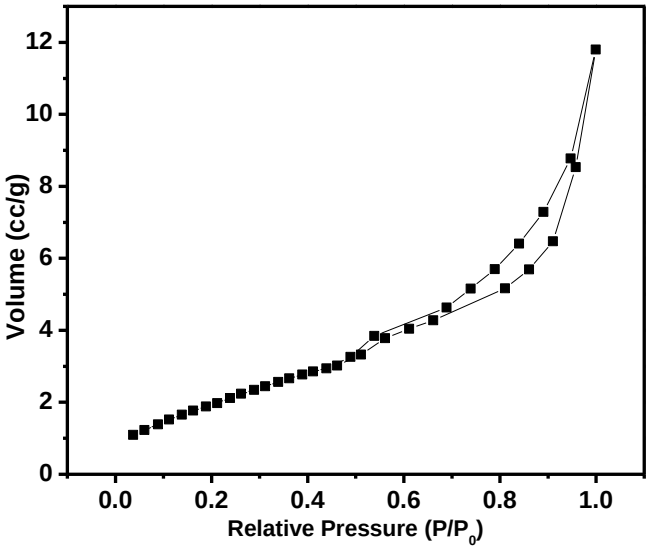

Figure 3.3. Nitrogen adsorption–desorption isotherm of Pd-BaF_2-71 catalyst.

3.3.5. Acid and base properties

The total acidity as well as the strength of acidic sites on the surface of the catalysts were determined by NH_3 temperature programmed desorption (NH_3-TPD) technique and the plot is shown in fig. 3.4.

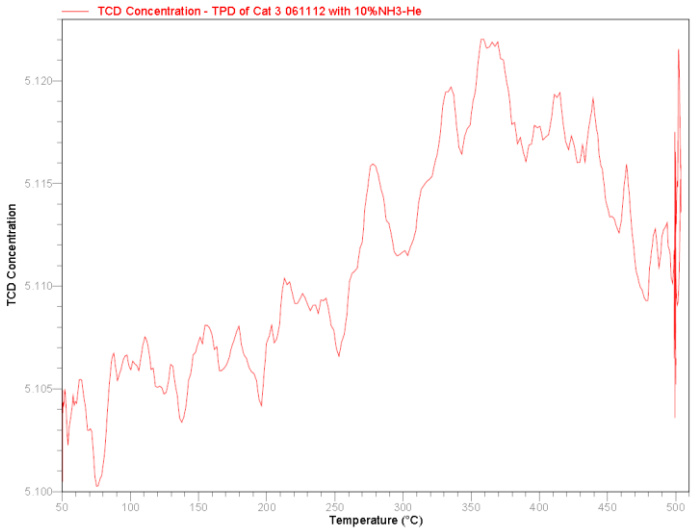

Figure 3.4. NH_3-TPD of Pd-BaF_2-71 catalyst.

In sol gel synthesis the extent of fluorination is depend not only on the concentration of HF used but also on the nature of metal alkoxide. Generally the acidity of metal fluoride increases down the group in periodic table similar to metal oxides. In alkaline earth metal fluoride series, MgF_2 was found to be acidic in nature which turned to basic nature in BaF_2. Therefore the NH_3-TPD measurements of Pd-BaF_2-71 catalyst showed very little desorption of NH_3 near 370 °C which showed the

pseudo acidic nature of catalyst. The FTIR studies of barium fluoride support were carried out using carbon monoxide as probe molecule to determine basic nature [34]. The studies indicated strong Brønsted basicity of barium fluoride.

3.3.6. X-ray photoelectron spectroscopy (XPS)

XPS was used to derive compositional information of the catalyst surface. XPS plots are shown in fig. 3.5.

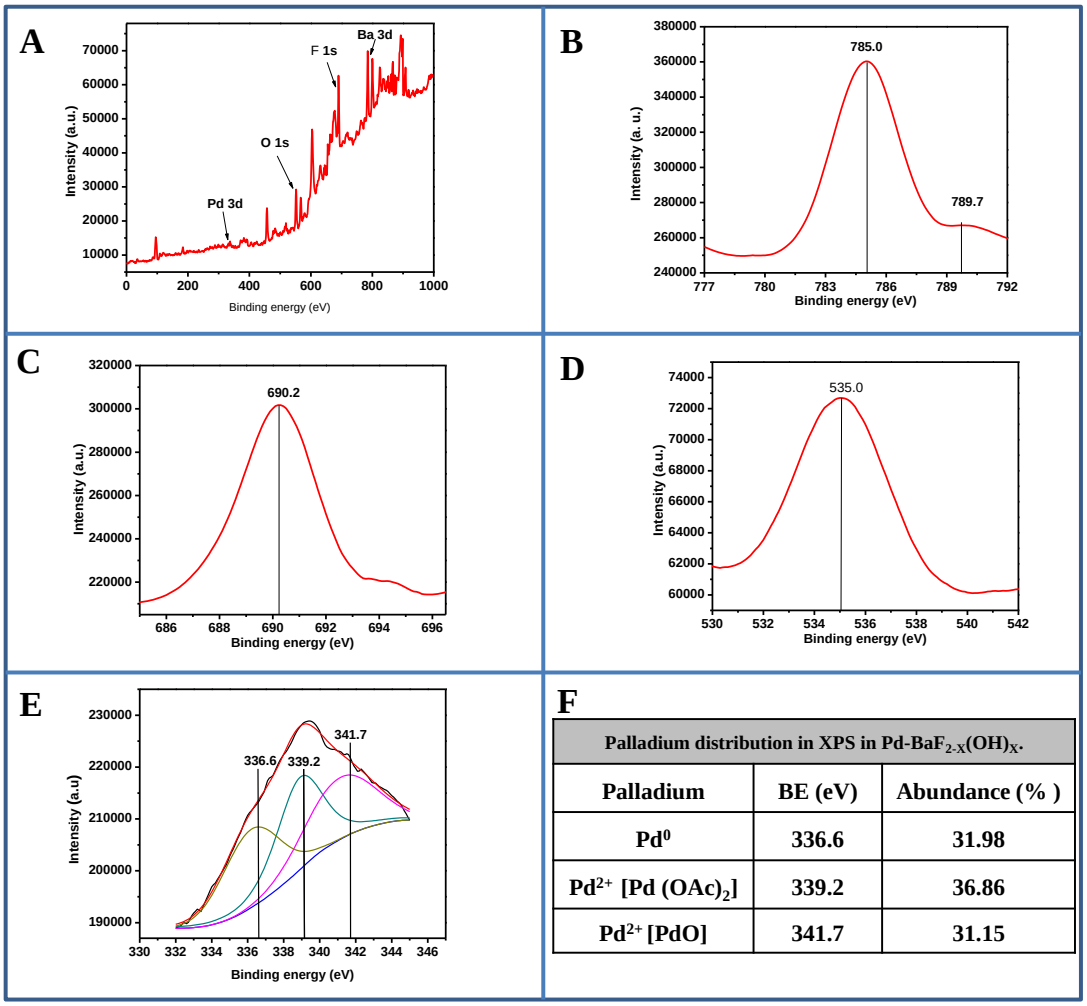

F

Palladium distribution in XPS in Pd-$BaF_{2-X}(OH)_X$.		
Palladium	**BE (eV)**	**Abundance (%)**
Pd^0	**336.6**	**31.98**
Pd^{2+} [Pd $(OAc)_2$]	**339.2**	**36.86**
Pd^{2+} [PdO]	**341.7**	**31.15**

Figure 3.5. X-ray photoelectron analysis of the Pd-BaF_2-71 (A) survey mode; (B) barium; (C) fluorine; (D) oxygen; (E) palladium and (F) relative abundance of Pd.

The XPS peaks were standardized with respect to carbon peak at 284.6 eV on surface. Due to non-conductive nature of barium fluoride some charging of sample was observed. The montage of survey scan after analysis of Pd-BaF_2-71 catalyst is shown (fig. 3.6-A). The peaks were annotated to Ba, F, O and Pd with their core level. The peak at 785.0 eV corresponds to $3d_{5/2}$ electron in Ba^{2+} species (fig. 3.6-B). The

peak at 690.2 eV can be related to 1s electron in F^- species (fig. 3.6-C). A peak at 535.0 eV can be related to 1s electron in oxide ion species (fig. 3.6-D).

Furthermore in order to determine the effect of the support on the oxidation state of palladium of the as synthesized samples, the region of Pd was studied (fig. 3.6- E). Palladium was found in two oxidation states namely Pd^0 and Pd^{2+}. The peak at 336.2 eV corresponds to presence of Pd^0 while peaks at 339.0 and 341.1 eV correspond to Pd^{2+} ($3d^{3/2}$). The peak at 339.0 indicated presence of palladium acetate species while the peak at 341.1 corresponds to presence of PdO species. The relative surface abundance of Pd: Pd^{2+} was found to be 1:2 (fig. 3.6-F).

3.3.7. SEM and EDAX

The SEM analysis showed rod shaped BaF_2 morphology with length in range of 50-1000 nm and diameter of the rod in range of 50 – 100 nm (fig. 3.7-A). The combined effect of higher electron density surrounding Pd nanoparticles and larger polarizability of BaF_2 lead to unidirectional growth of crystallite forming rods of barium hydroxyl fluorides. This unidirectional growth of crystallite resulted into formation of rod like structure of Pd-BaF_2-71 catalysts. The surface elemental composition was estimated using Energy Dispersive X-ray spectroscopy (EDX) which indicated 1.38 wt% of Pd on the surface of BaF_2 rods (fig. 3.7-B).

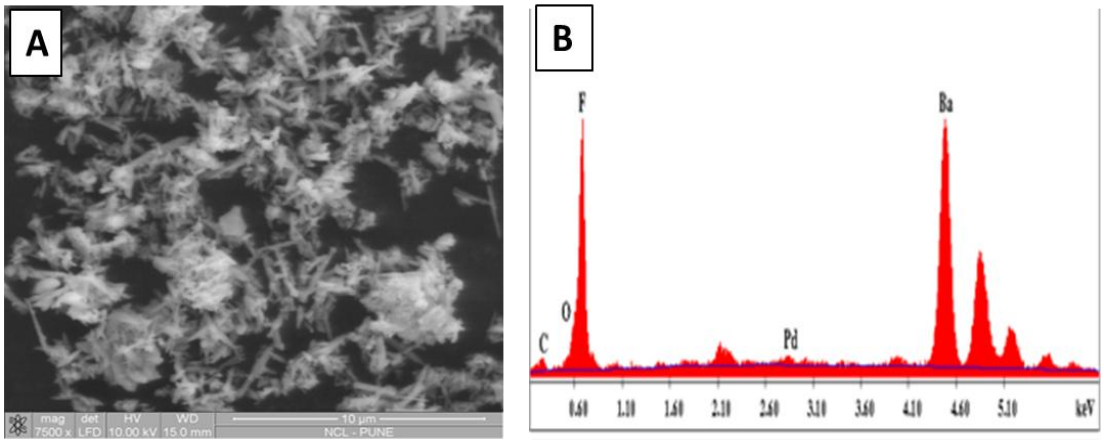

Figure 3.6. (A) SEM image and (B) EDAX analysis of Pd-BaF_2-71.

3.3.8. HRTEM

The HRTEM images were recorded to observe the actual shape and orientation of palladium nanoparticles and barium fluoride rods (fig. 3.8). The barium fluoride exhibited 111 planes (d_{111} =0.357 nm). The formation of very small Pd

particles mainly in the range of 2-10 nm was observed. The formation of small particles is attributed to the fluorolytic sol-gel preparation which enables very high dispersion. The palladium species were observed in two forms viz. Pd and PdO. The Pd particles exists in 111 plane (d_{111}= 0.223 nm) with size in range of 5-10 nm while PdO formed 100 plane (d_{100} = 0.302 nm) with size in range of 2-5 nm. Some agglomerated Pd nanoparticles were also observed (90-120 nm).

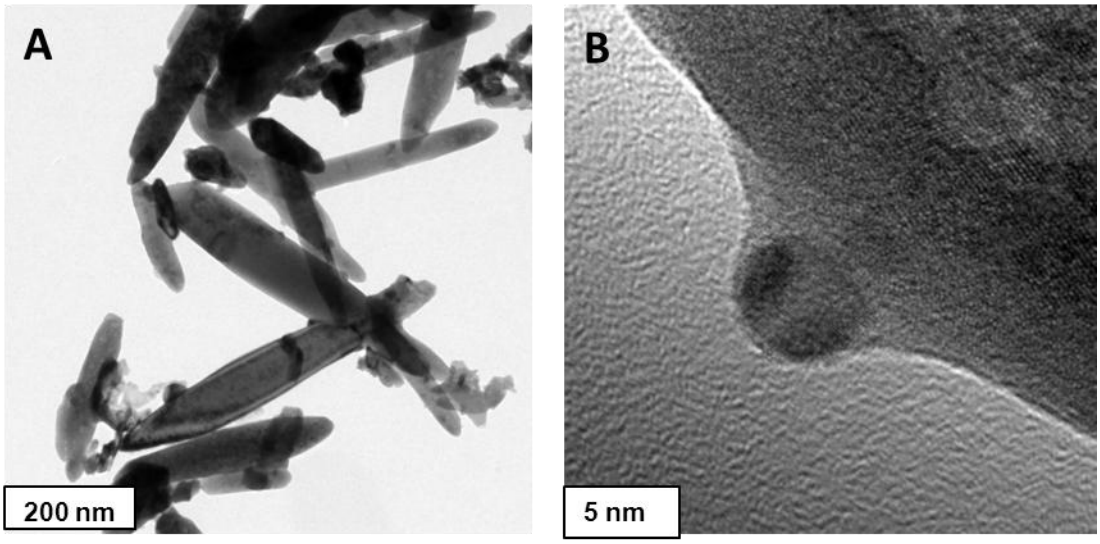

Figure 3.7. HRTEM images of Pd-BaF_2-71 catalyst at various resolutions (A) at 200 nm and (B) at 5 nm.

3.3.9. Catalytic activity

Selective oxidation of alcohols to corresponding carbonyl compound is one of the important reactions in organic synthesis. Among oxidation, aerobic oxidation is highly demanding because of its non-hazardous and cost-effective nature. In literature, Pd supported heterogeneous catalysts with equivalent amount of bases were used for catalytic aerobic oxidation of alcohols. Considering importance of aerobic oxidation using Pd based heterogeneous catalyst, it was studied for aerobic oxidation of alcohols under base free conditions using Pd supported on metal fluorides (scheme 3.2).

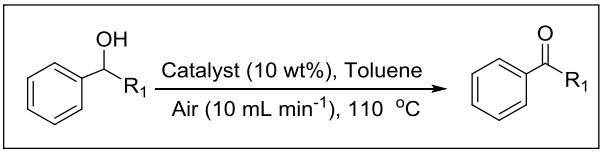

Scheme 3.2. Aerobic oxidation of alcohol.

The benzyl alcohol oxidation was carried out in toluene solvent at 110 °C with 10 wt% catalysts loading with respect to substrate under air flow of 10 mL min^{-1}. Initially, no conversion was observed for non-catalytic reaction even after 8 h (table 3.1, entry 1). Further the reaction was carried out with only BaF_2-71 to check the role of support, which resulted in poor conversion (>5%) of benzyl alcohol even after 8 h (table 3.1, entry 2). To study the effect of different metal fluoride as support for oxidation activity of Pd, benzyl alcohol oxidation was carried out using Pd-MgF_2-71, Pd-SrF_2-71, and Pd-BaF_2-71. The use of Pd-MgF_2-71 and Pd-AlF_3-71 showed almost no conversion (> 1%) whereas Pd-SrF_2-71 gave 40% conversion after 8 h with 80% selectivity for benzaldehyde (table 3.1, entry 3-5). When Pd-BaF_2-71 was used as catalyst it gave 100% benzyl alcohol conversion with 99% benzaldehyde selectivity (table 3.1, entry 6). This showed the high efficiency of Pd-BaF_2-71 for aerobic oxidation of benzyl alcohols.

Table 3.1. Results of catalytic aerobic oxidation of benzyl alcohol.[a]

Entry	Catalyst	Conv.[b] (%)	Sele.[b] (%)
1	Without catalyst	0	-
2	BaF_2-71	<5	-
3	Pd-AlF_3-71	<1	-
4	Pd-MgF_2-71	<1	-
5	Pd-SrF_2-71	40	80
6	Pd-BaF_2-71	100	>99

[a]**Reaction conditions**: Benzyl alcohol: 0.5 g (5 mmol); Catalyst: 0.05 g (10 wt%, 0.1 wt% of Pd,); S/Pd: 982; Solvent (Toluene): 10 mL; Time: 8 h.; Flow of air: 10 mL min^{-1}. [b]Conversion and selectivity were determined by GC analysis.

3.3.10. Parametric study using Pd-BaF_2-71 catalyst

A. Effect of temperature

The rate of the chemical reaction is function of temperature. When the aerobic oxidation of benzyl alcohol was carried out at various temperatures in toluene from 70 to 110 °C, the rate of reaction increased with increase in temperature (fig. 3.8). At 70 °C, no conversion of benzyl alcohol was observed even after 8 h, whereas conversion increased only up to 8% at 90 °C. However, with further increase in temperature to 110 °C showed 100 % conversion and 100% selectivity after 8h. This considerable

increase in rate of reaction can be attributed to increase in effective collision along with higher order of activation of reactant at higher temperature.

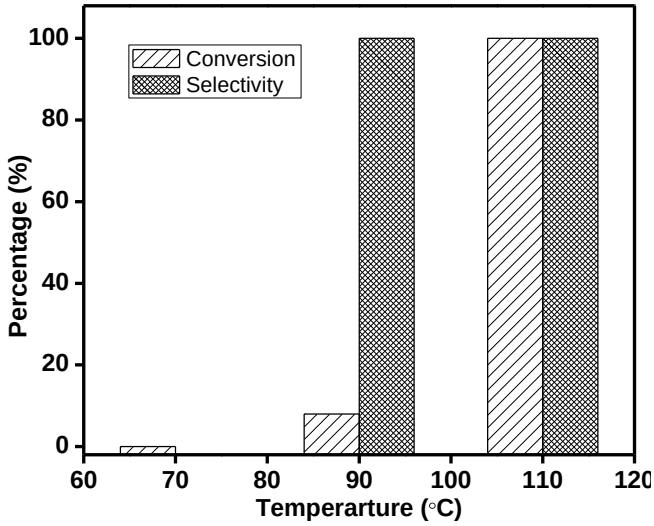

Figure 3.8. Effect of temperatures on benzyl alcohol oxidation using Pd-BaF_2-71.

Reaction conditions: BA: 0.2 g; Catalyst: 0.02 g; Solvent: 10 mL; Time: 8 h, Air flow: 10 mL min^{-1}.

B. Effect of catalyst loading

The rate of aerobic oxidation of benzyl alcohols was studied with catalysts loading ranging from 2 to 15 wt% as shown in fig. 3.9.

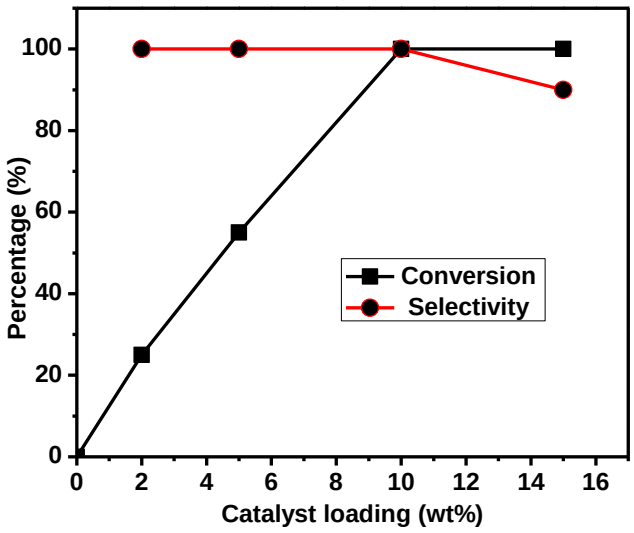

Figure 3.9. Effect of catalyst loading on benzyl alcohol oxidation using Pd-BaF_2-71.

Reaction conditions: BA: 0.2 g; Solvent: 10 mL; Temperature: 110 °C; Time: 8 h, Air flow: 10 mL min^{-1}.

The conversions of benzyl alcohol in toluene at 110 °C after 8 h was found to be 25, 55 and 100 % for 2, 5 and 10 wt% of catalyst loading respectively with >99% selectivity for benzaldehyde. Further increase in catalyst loading up to 15 wt% showed complete conversion of benzyl alcohol but a decrease in benzaldehyde selectivity up to 90% was observed due to over oxidation of benzaldehyde to benzoic acid.

C. Time profile study

The time profile of benzyl alcohol oxidation was monitored to study the kinetics of the reaction and formation of product with respect to time (fig. 3.10).

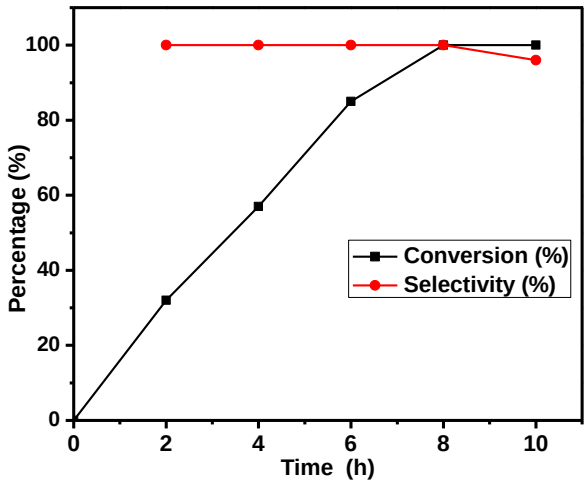

Figure 3.10. Time – profile study of benzyl alcohol oxidation using Pd-BaF_2-71. **Reaction conditions**: BA: 0.2 g; Catalyst: 0.02 g; Solvent: 10 mL; Temperature: 110 °C; Air flow: 10 mL min^{-1}.

The rate of benzyl alcohol oxidation was initially very high and showed conversion up to 32 % in 2 h. The conversion increased up to 57 and 85% after 4 and 6 h respectively without affecting the benzaldehyde selectivity. Further the rate of formation of product decreased slightly. The reaction showed 100% conversion in 8 h with >99% selectivity for benzaldehyde. On further continuation of reaction up to 10 h, a slight decrease in benzaldehyde selectivity up to 96% was observed. This shows the over oxidation of benzaldehyde to benzoic acid.

3.3.11. Substrate scope study

The wider scope of Pd-BaF_2-71 for aerobic oxidation was evaluated for various alcohols (table 3.2) under optimized reaction conditions (catalyst: 10 wt%

with respect to substrate; solvent: toluene (10 mL); temperature: 110 °C; time: 8 h; air flow: 10 mL min^{-1}). Initially benzyl alcohol was used as model substrate for oxidation, which showed 100% conversion and 99% selectivity (table 3.2, entry 1). Generally ring activated benzyl alcohols are known for formation of over oxidation products like benzoic acid, and corresponding esters. When Pd-BaF_2-71 was used for oxidation of 4-methoxy benzyl alcohol, it showed 100% conversion with >99% selectivity for corresponding aldehyde (table 3.2, entry 2). When vanillin alcohol was subjected for aerobic oxidation, it showed formation of vanilla aldehyde with >99% selectivity and completer conversion (table 3.2, entry 3). The vanilla flavor is produced by oxidation of vanillin alcohol using various catalysts. The catalytic aerobic oxidation of vanillin alcohol is ever demanding process [39]. Veratryl alcohol when screened for aerobic oxidation, veratraldehyde was produced with > 99% selectivity and 100% conversion of alcohol (table 3.2, entry 4). Veratraldehyde is used as commercial flavorant and odorant [40]. 4-nitrobenzyl alcohol was selectively oxidized to 4-nitrobenzaldehyde using Pd-BaF_2-71. The reaction showed 76% conversion of 4-nitrobenzyl alcohol in 8 h with >99% selectivity for 4-nitrobenzaldehyde (table 3.2, entry 5). 4-nitrobenzaldehyde is used as starting material for various pharmaceutical intermediate [41]. 2-Hydroxybenzyl alcohol on oxidation produced salicyaldehyde with 88% conversion and 99% selectivity (table 3.2, entry 6). The lowering in activity of reaction may be due of steric hindrance of hydroxyl group located at *ortho*-position. Salicyaldehyde is used as chelating agent in variety of chemical synthesis. Further secondary alcohols like 1-phenylethanol resulted in formation of acetophenone with 80% conversion and >99% selectivity (table 3.2, entry 7). Similarly, diphenylmethyl alcohol showed 100% conversion and 99% selectivity towards benzophenone (table 3.2, entry 8). Furthermore allylic alcohols like cinnamyl alcohol on oxidation exhibited exclusive formation of cinnamaldehyde with 82% conversion (table 3.2, entry 9). Furfuryl alcohol on oxidation showed formation of furfural with 89% conversion and 99% selectivity (table 3.2, entry 10). Furfural is an important renewable, non-petroleum based feedstock. Furfural is used to make other furan chemicals, such as furoic acid, via oxidation. The scope of the catalyst was further evaluated for oxidation of aliphatic alcohols. When simple alcohols like cyclohexyl alcohol and n-hexyl alcohol was subjected to aerobic oxidation, only 4 and 7% conversion was obtained respectively

(table 3.2, entry 11-12). The lower conversion of simple alcohols was obtained due to their low reactivity.

Table 3.2. Alcohols oxidation study using Pd-BaF_2-71 catalyst.

Entry	Substrate	Product	Conv.[b] (%)	Sel.[b] (%)	TON[c]
1	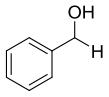	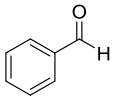	100	>99	982
2	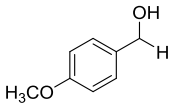	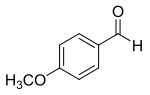	100	>99	768
3	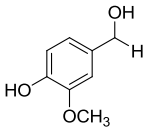	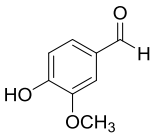	100	>99	688
4	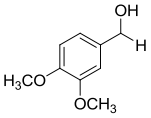	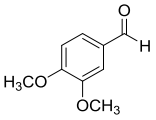	100	>99	631
5	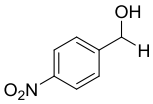	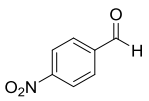	76	>99	527
6	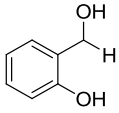	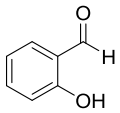	88	>99	695
7	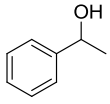	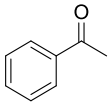	80	>99	752
8	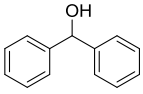	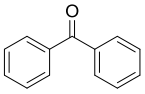	100	>99	609
9	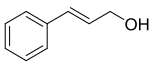	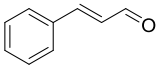	82	>99	649
10	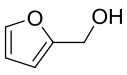	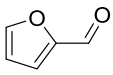	89	>99	962
11	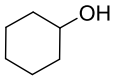		4	>99	4
12	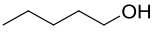	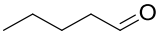	7	>99	7

[a]**Reaction conditions:** Substrate: 0.5 g; Catalyst (Pd-BaF_2-71): 0.05 g (10 wt %); Solvent (toluene): 10 mL; Time: 8 h, air flow: 10 mL min^{-1}.[b] Conversion and selectivity were determined by GC analysis based on alcohol; [c]Turn over number (TON) = [no. of moles of reactant converted/ no. of moles of Pd catalyst used].

3.3.12. Recycle study using Pd-BaF_2-71 catalyst

The recyclability of Pd-BaF_2-71 was studied under optimized reaction conditions for benzyl alcohol oxidation. However, even after 5th runs, the catalyst retained its activity with respect to conversion and selectivity of aldehyde (fig. 3.11).

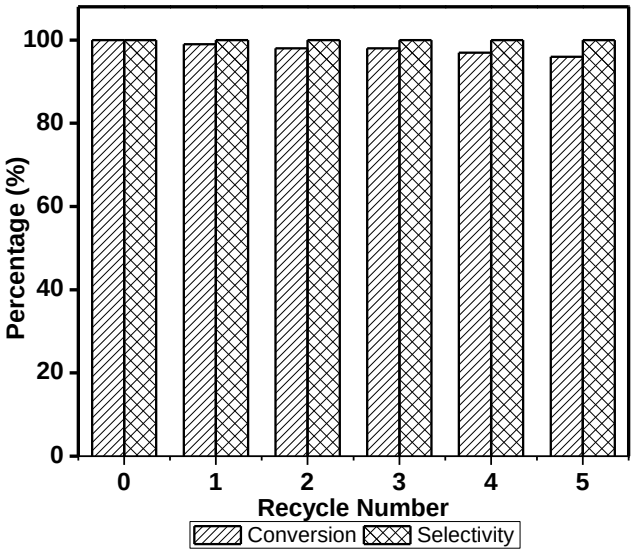

Figure 3.11. Recycle study of Pd-BaF_2-71 catalyst for oxidation of benzyl alcohol. **Reaction conditions**: BA: 0.2 g; Catalyst (Pd-BaF_2-71): 0.02 g (10 wt %); Solvent (toluene): 10 mL; Temperature: 110 °C; Time: 8 h; Air flow: 10 mL min^{-1}.

3.3.13. Hot filtration test and TEM study of recycled catalyst

Moreover, the catalyst showed excellent stability. Filtration test was used to check the Pd leaching in reaction mixture. In presence of catalyst, 58% conversion was obtained after 4 h. After the removal of catalyst by filtration the reaction was continued for 4 h which showed no further increase in conversion of benzyl alcohol even after additional 4 h absence of catalyst. This confirmed zero Pd leaching. Therefore Pd-BaF_2-71 acts as true heterogeneous catalytic system. This result was reconfirmed by ICP-AES analysis.

The TEM image of catalyst after 5th recycle showed no agglomeration of Pd on the catalyst surface (fig. 3.12). The Pd nanoparticle size was found to be in the same range (8-10 nm) when compared with the fresh catalyst (as shown in fig. 3.8). This confirms no agglomeration of Pd particles during the reaction and explains the reason for recyclability.

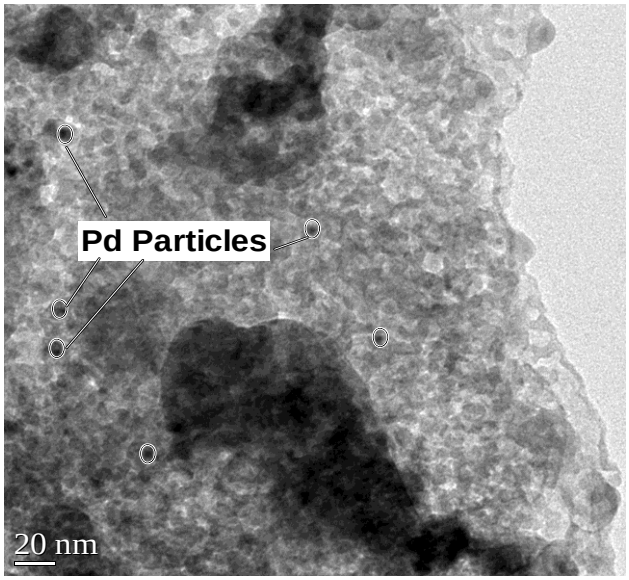

Figure 3.12. TEM image of Pd-BaF_2-71 catalyst after 5th catalytic recycle.

The oxidation of benzyl alcohol by palladium based catalyst was normally studied under high temperature in the range between 80-160 °C using equivalent amount of bases like sodium carbonate, potassium carbonate and expensive solvents such as trifluorotoluene. Karimi and co-workers [11] have used Pd anchored on SBA-15 using bipyridyl ligand for alcohol oxidation at 80 °C using 0.4 mol% of Pd in presence of equivalent amount of K_2CO_3. The catalyst showed 83% conversion of benzyl alcohol with 100% selectivity for benzaldehyde in 3.5 h in presence of O_2 gas. The high recyclability and no agglomeration of Pd nanoparticle were observed may be due to presence of anchored bi-pyridine based ligand systems. The method of preparation of anchored Pd catalyst was found to be tedious. Further Hutchings et al reported a novel bimetallic Au: Pd catalyst supported on supercritically synthesized CeO_2, which showed alcohols oxidation with conversion up to 98% at 160 °C under 10 bar pressure of O_2 using high Au and Pd loading upto 2.5 wt% each [42]. The catalyst showed high TOF up to 18000 h^{-1}. Furthermore Villa et al. used the carbonaceous material as support for bimetallic Au-Pd catalyst and used for alcohol oxidation at 60°C and 1.5 bar pressure of O_2 [43]. The catalyst showed conversion up to 94% but formation of other products like benzoic acid and benzyl benzoate was observed. Again, Pd supported on mesoporous Al_2O_3 synthesized using modified surfactant route showed high activity for aerobic oxidation of alcohols at 60 °C in air [44], where tetrammine palladium (II) nitrate complex was used as Pd precursor. Another modified palladium supported on amine grafted mesoporous molecular sieves (Pd/amine-grafted TUD-1) was used as catalyst for alcohol oxidation at 160°C

under atmospheric pressure of O_2 gas [45]. The catalyst showed selectivity up to 92% for benzaldehyde with 100% conversion.

Many researchers have reported comparable conversion but catalyst synthesis procedure and use of bases like K_2CO_3 require for oxidation which produces equivalent quantity of waste. While the solid base-catalysts like Pd supported hydroxyl appetite have shown better catalytic activity without base in presence of trifluorotoluene [46]. However Pd/Fe_3O_4, Pd/MnO_x and Pd/CeO_2 showed comparable activity but selectivity towards benzaldehyde was lowered in such cases [47]. With respect to these catalytic systems, Pd-BaF_2-71 was more favored due to its higher stability, reusability and due to very low Pd loading (1 wt%) and highly selective nature.

3.3.14. *In-situ* FTIR study for mechanism determination

The activation of oxygen and formation of intermediate species during the oxidation of benzyl alcohol (BA) was studied using *in situ* DRIFT spectroscopy (fig. 3.13). The catalyst was activated by heating at 250 °C for 3 h in DRIFT cell and cooled to 110 °C in the flow of helium. Typically FTIR of authentic BA showed (fig. 3.5-a) peaks at 3649 cm^{-1} (ν_{O-H} stretching), 3076 and 3039 cm^{-1} (ν_{C-H} aromatic stretching), 2932, 2883 and 2873 cm^{-1} (ν_{C-H} aliphatic stretching), 1493, 1457, 1425 and 1390 cm^{-1} ($\nu_{C=C}$ aromatic stretching), 1024 cm^{-1} (ν_{C-O} stretching) and 739 cm^{-1} (ν_{C-C} aromatic mono substituted) whereas the FTIR spectrum of authentic benzaldehyde (fig. 3.13-e) showed the peaks at 3076 and 3039 cm^{-1} (ν_{C-H} aromatic stretching), 2810, 2738 and 2694 cm^{-1} (ν_{C-H} aliphatic stretching), 1705 cm^{-1} ($\nu_{C=O}$ stretching), 1654, 1594 and 1457 cm^{-1} ($\nu_{C=C}$ aromatic stretching), 739 cm^{-1} (ν_{C-C} aromatic substitution). When BA was passed on the catalyst in the flow of helium to study the interaction of BA with the catalyst surface, it showed the instantaneous disappearance of O-H band at 3649 cm^{-1} of BA and the formation of very broad band around 3362 cm^{-1}. The disappearance of band may be attributed to strong interactions between hydroxyl proton and fluoride support. Further a small decrease in intensity of peak at 1024 cm^{-1} was observed which indicated decrease in concentration of benzyl alcohol on the catalyst surface (fig. 3.13-b). Simultaneously appearance of less intense peaks at 1713, 1594, 1457, 1173 and 824 cm^{-1} (fig. 3.13-b) indicated the formation of small amount of BZ on the catalyst surface. When oxygen was passed over adsorbed BA on catalyst surface at 110 °C for 20 minutes (fig. 3.13-c), the spectra showed

considerable increase in intensity of peak at 1713 cm^{-1} of $\nu_{C=O}$ which indicated further formation of BZ. This was also accompanied by supported by decrease in intensity of band at 1024 cm^{-1} of ν_{C-O} of BA which indicates decrease in BA concentration on the surface due to formation of BZ. The bands at 1270 and 824 cm^{-1} were observed (fig. 3.13-d) when O_2 was passed on the catalyst surface which may be assigned to ν_{O-O-H} stretching and bending vibration respectively indicating activation of oxygen on catalyst surface through intermediate peroxo species [33].

Further passing oxygen on adsorbed BA showed increase in the intensity of BZ peaks with complete diminishing of peak at 1024 cm^{-1} for BA (fig. 3.13-d). This spectral evidence indicates the instantaneous partial oxidation of benzyl alcohol even in absence of external oxygen. Therefore in the present case also the lattice oxygen takes part in formation of BZ initially and get replenished later by activation of oxygen.

Based on spectral observations the plausible mechanism for aerobic oxidation of alcohols is depicted in Scheme 3.3. First step includes the adsorption of BA on the surface of catalyst to generate alcoholate species B due to of the presence of weak acid sites on the surface of catalyst [34]. The proton transfer occurs from adsorbed alcohol to fluoride on the surface because of presence of strong basic site on the surface of barium hydroxyl fluorides in the second step [34]. The abstraction of alcoholic proton by fluoride of BaF_2 support clearly demonstrated the role of BaF_2 as proton abstracting agent and explains true base free nature of the catalyst. Further the formed alkoxide ions interact with unsaturated barium to form intermediate species C which shows intermolecular hydride transfer to form BZ which forms the hydrogenated catalyst intermediate species D. Additionally along with basic properties, barium fluoride is also known for the oxygen/hydroxyl ion transfer [33].

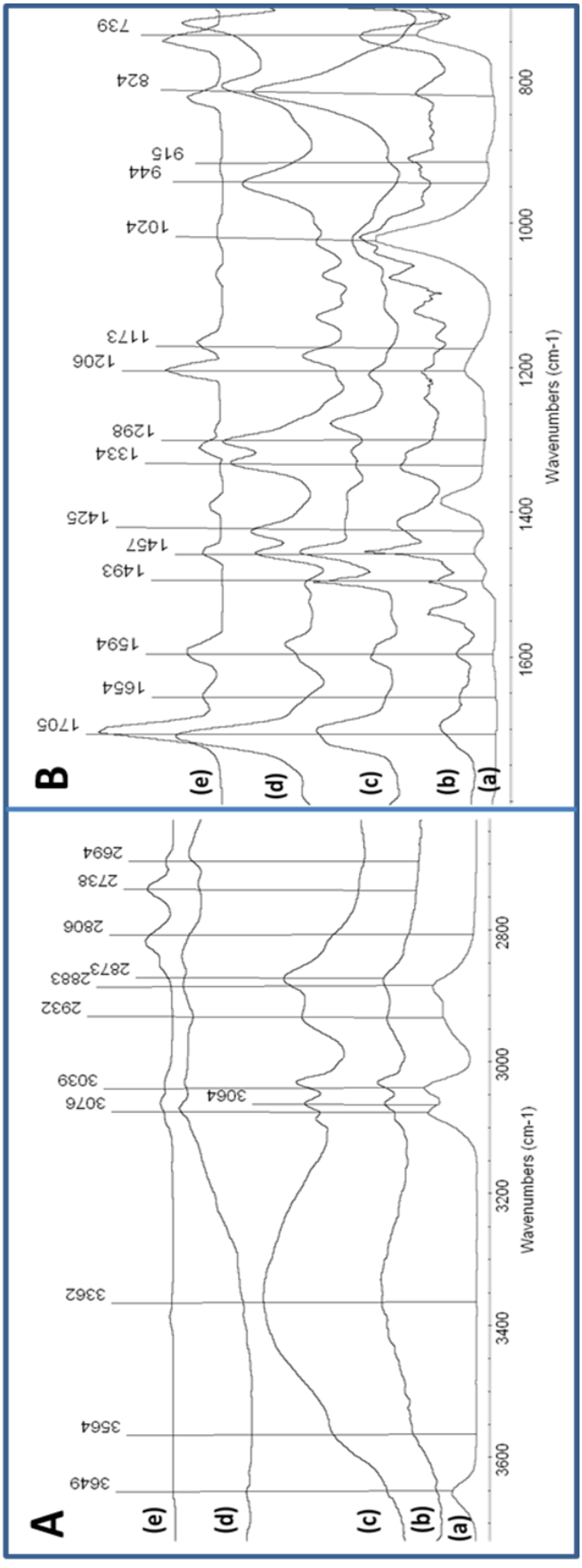

Figure 3.13. *In situ* FTIR study of oxidation of benzyl alcohol A) range 3660 - 2640 cm^{-1} B) range 1800 - 700 cm^{-1}. (a) FTIR spectrum of authentic BA; (b) catalyst + BA in helium flow; (c) catalyst + BA in oxygen flow after 20 min at 110 °C; (d) catalyst + BA in oxygen flow after 60 min at 110 °C and (e) FTIR spectrum of authentic benzaldehyde.

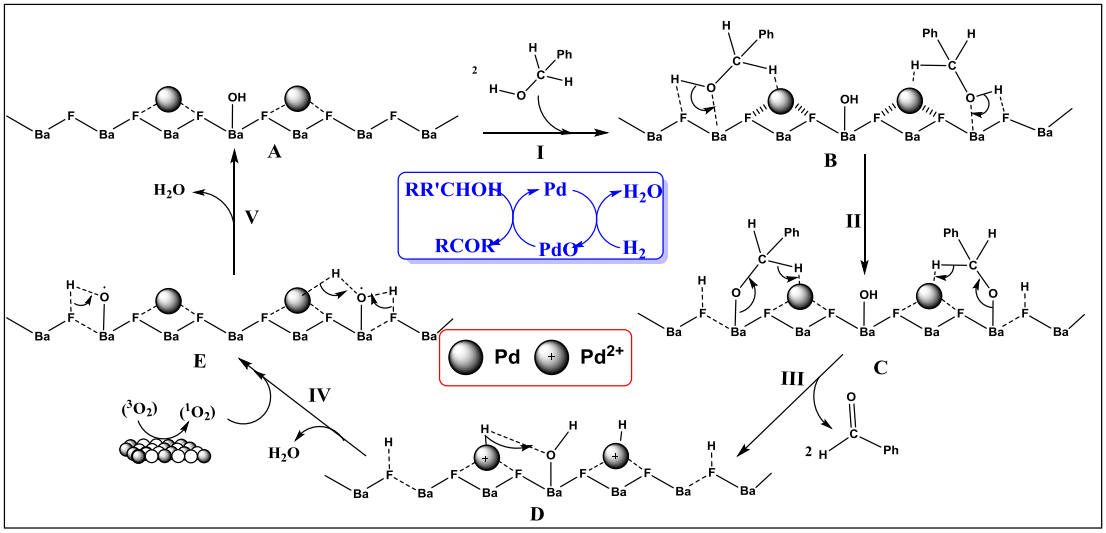

Scheme 3.3. Plausible mechanism of aerobic oxidation of alcohol on the surface of Pd-BaF_2-71 catalyst.

Hence liberation of water molecule take place using surface or lattice oxide/hydroxyl ions and hydride ion from palladium nanoparticle or proton attached to fluoride ion. This step is evident for the appearance of BZ peaks on the catalyst surface (fig. 3.13-b) even in absence of oxygen.

During the oxidative coupling of methane using BaF_2/CeO_2 catalyst Zhau et al. reported lattice oxygen participation in the reaction which generated the unsaturated barium species on the surface of catalyst with liberation of water molecule [33]. Similarly in the step IV of the reaction mechanism for aerobic oxidation of alcohols, the water molecule may liberate by combination of activated oxygen and hydrogen. Simultaneously palladium nanoparticles help for adsorption and activation of oxygen from air at reaction temperature. The activated singlet oxygen ($^1O_2$) migrates from Pd to unsaturated barium to form intermediate E. This promotes the formation of hydroxyl and/or hydronium ion on the surface of catalyst. Furthermore the species E undergoes dehydration to form the regenerated catalyst species A for further catalytic run. The activation of both BA and O_2 observed on the catalyst surface confirms the operation of Langmuir-Hinshelwood mechanism in this reaction. Further no peaks corresponding to carboxylic group were observed confirming no further oxidation to benzoic acid. This supports the selective nature of the catalyst for oxidation of alcohol to only aldehyde under reaction conditions.

The oxidation of alcohols to carbonyl compound on solid surfaces follows oxidative dehydrogenation pathways. In case of fluorinated support, it is anticipated that Lewis acidity decreases from AlF_3 to BaF_2 due to the increase in the ionic radius

and the decrease in the positive charge density with increase in Lewis basicity. Due to the basic nature of barium hydroxyl fluoride over other fluorinated catalyst the activation of alcohols occurs over the surface via de-protonation step which helps in the formation of adsorbed alkoxide species. The basic intrinsic property of barium fluoride support of transfer of oxide/ hydroxyl ion in co-operation with palladium nanoparticles for activation of dioxygen (O_2) species assisted oxidation of alcohols. Furthermore the Pd nanoparticles may be stabilized due to the non-covalent interaction of Pd and surface of the barium hydroxyl fluoride. The excellent catalytic activity of Pd-BaF_2 may be attributed to surface acid-base properties, electronic activation of oxygen using supported Pd species in addition with structural properties like rod shape of support.

3.4. Conclusions

The Pd-BaF_2-71 catalyst was successfully synthesized from barium metal using one pot fluorolytic sol-gel method which showed formation of rod shaped barium hydroxyl fluoride material on with uniform dispersion of Pd particles. It showed highly stable Pd and PdO nanoparticles of diameter in range of 2-10 nm on BaF_2-71 rods due to strong-metal support interactions. The catalyst showed high activity for aerobic oxidation of alcohols under mild base free conditions because of activation of substrate on basic surface. The catalyst was proved as efficient for aerobic oxidation of aromatic and allylic alcohol under base-free conditions. The reaction followed Langmuir-Hinshelwood mechanism for aerobic oxidation of alcohol as confirmed by *in-situ* FTIR studies.

3.5. References

[1] R. A. Sheldon, J. K. Kochi, *Metal–Catalyzed Oxidations of Organic Compounds,* Academic Press, New York, **1981**.

[2] R. A. Sheldon, I. W. C. E. Arends, U. Hanefeld, *Green Chemistry and Catalysis*, Wiley-VCH, Weinheim, **2007**.

[3] M. Hudlicky, *Oxidation in Organic Chemistry, ACS, Washington DC,* **1990**; (b) J. Clayden, N. Greeves, S. Warren, P. Wothers, *Organic Chemistry*, (Eds.), Oxford University Press, Oxford, **2001**.

[4] Y. Su, L. Wang, Y. Liu, Y. Cao, H. He, K. Fan, *Catal. Commun*., **2007**, *8*, 2181.

[5] (a) B. M. Trost, *Science*, **1991**, *254*, 1471; (b) R. A. Sheldon, *Green Chem*., **2000**, *2*, G1.

[6] A. J. Ingram, D. Solis-Ibarra, R. N. Zare, R. M. Waymouth, *Angew. Chem. Int. Ed.*, **2014**, *126*, 5754.

[7] C., Schweitzer, R. Schmidt, *Chem. Rev*., **2003**, *103*, 1685.

[8] R. Vankayala, A. Sagadevan, P. Vijayaraghavan, C. L. Kuo, K. C. Hwang, *Angew. Chem. Int. Ed*., **2011**, *50*, 10640.

[9] S. E. Davis, M. S. Ide, R. J. Davis, *Green Chem*., **2013**, *15*, 17.

[10] (a) A. Dijksman, I. W. C. E. Arends, R. A. Sheldon, *Plat. Met. Rev*., **2001**, *45*, 15; (b) J. Muzart, *Tetrahedron*, **2003**, *59*, 5789; (c) J. Muzart, *Chem. Asian J*., **2006**, *1*, 508.

[11] B. Karimi, S. Abedi, J. H. Clark, V. Budarin, *Angew. Chem. Int. Ed*., **2006**, *45*, 4776.

[12] J. F. Weaver, *Chem. Rev.*, **2013**, *113***,** 4164.

[13] T. F. Blackburn, J. Schwartz, *Chem. Commun.*, **1977**, 157.

[14] S. Alt-Mohand, F. Hénin J. Muzart, *Tetrahedron Lett.*, **1998**, *39*, 6011.

[15] T. Nishimura, T. Onoue, K. Ohe, S. Uemura, *J. Org. Chem.*, **1999**, *64*, 6750.

[16] G-J. ten Brink, I.W. C. E. Arends, R. A. Sheldon, *Science*, **2000**, *287*, 1636.

[17] G-J. ten Brink, I.W. C. E. Arends, R. A. Sheldon, *Adv. Synth. Catal.*, **2002**, *344*, 355.

[18] J. M. Campelo, D. Luna, R. Luque, J. M. Marinas, A. A. Romero, *ChemSusChem*, **2009**, *2*, 18.

[19] E. Garcıa-Bordeje, M. F. R. Pereira, M. Ronningc, D. Chenc, *SPR Catalysis*, **2014**, *26*, 72.

[20] R. Ciriminna, A. Fidalgo, V. Pandarus, F. Beland, L. M. Ilharco, M. Pagliaro, *Chem. Rev.*, **2013**, *113*, 6592.

[21] E. Merino, E. Verde-Sesto, E. M. Maya, M. Iglesias, F. Sanchez, A. Corma, *Chem. Mater.*, **2013**, *25*, 981.

[22] Q. M. Kainz, O. Reiser, *Acc. Chem. Res.*, **2014**, *47*, 667.

[23] Y. Li, W. Shen, *Chem. Soc. Rev.*, **2014**, *43*, 1543.

[24] T. Mallat, A. Baiker, *Chem. Rev.*, **2004**, *104*, 3037.

[25] T. Nishimura, N. Kakiuchi, M. Inoue, S. Uemura, *Chem. Commun*., **2000**, 1245.

[26] K.-M. Choi, T. Akita, T. Mizugaki, K. Ebitani, K. Kaneda, *New. J. Chem.*, **2003**, *27*, 324.

[27] D. I. Enache, J. K. Edwards, P. Landon, B. Solsona-Espiriu, A. F. Carley, A. A. Herzing, M. Watanabe, C. J. Kiely, D. W. Knight, G. J. Huchings, *Science*, **2006**, *311*, 362.

[28] S. Rudiger, U. Gross, E. Kemnitz, *J. Fluorine Chem*., **2007**, *128***,** 353.

[29] T. Justel, H. Nikol, C. Ronda, *Angew. Chem. Int. Ed.*, **1998**, *37*, 3084.

[30] R. Singh, S. Sinha, P. Chou, N. J. Hsu, F. Radpour, *J. Appl. Phys*., **1989**, *66*, 6179.

[31] A. J. Wojtowicz, *Nucl. Instrum. Methods A*, **2002**, *486*, 201.

[32] S. Sathyamurthy, E. Tuncer, K. L. More, B. Gu, I. Sauers, M. Paransparanathaman, *Appl. Phys. A*, **2012**, *e 106*, 661.

[33] X. P. Zhou, Z. S. Chao, W. Z. Weng, W. D. Zhang, S. J. Wang, H. L. Wan, K. R. Tsai, *Catal. Lett.*, **1994**, *29*, 177.

[34] K. Teinz, S. Wuttke, F. Börno , J. Eicher, E. Kemnitz, *J. Catal.*, **2011**, *282*, 175.

[35] Y. Diao, W. Walawender, C. S. Sorensen, K. J. Klabunde, T. Ricker, *Chem. Mater*., **2002**, *14*, 362.

[36] K. T. Ranjit, K. J. Klabunde, *Chem. Mater*., **2005**, *17*, 65.

[37] S. Wuttke, G. Scholz, S. Rudiger, E. Kemnitz, *J. Mater. Chem*., **2007**, *17*, 4980.

[38] R. A. Nyquist, R. O. Kagel, *Handbook of infrared and Raman spectra of inorganic compounds and organic salts: infrared spectra of inorganic compounds*. Academic press, **1972**.

[39] J. F. Stanzione, J. M. Sadler, J. J. La Scala, K. H. Reno, R. P. Wool, *Green Chem.*, **2012**, *14*, 2346.

[40] C. Flynn, M. Rohr, **1985**, U.S. Patent No. 4,547,315.

[41] B. M. Choudary, M. L. Kantam, A. Rahman, C. Reddy, K. Rao. *Angew. Chemie Int. Ed.*, **2001**, *40*, 763.

[42] P. J. Miedziak, Z. Tang, T. E. Davies, D. I. Enache, J. K. Bartley, A. F. Carley, A. A. Herzing, C. J. Kiely, S. H. Taylor, G. J. Hutchings, *J. Mater. Chem*.,

2009, *19*, 8619.

[43] A. Villa, N. Janjic, P. Spontoni, D. Wang, D. S. Su, L. Prati, *Appl. Catal. A*, **2009**, *364*, 221.

[44] S. E. J. Hackett, R. M. Brydson, M. H. Gass, I. Harvey, A. D. Newman, K. Wilson, A. F. Lee, *Angew. Chem. Int. Ed.*, **2007**, *46*, 8593.

[45] Y. T. Chen, Z. Guo, T. Chen, Y. H. Yang, *J. Catal*., **2010**, *275*, 11.

[46] K. Mori, K. Yamaguchi, T. Hara, T. Mizugaki, K. Ebitani, K. Kaneda, *J. Am. Chem. Soc*., **2002**, *124*, 11572.

[47] B. Qi, Y. Wang, L. Lou, Y. Yang, S. Liu, *Reac. Kinet. Mech. Catal.*, **2013**, *108*, 519.

Chapter 4

PALLADIUM SUPPORTED ON STRONTIUM FLUORIDE: SYNTHESIS, CHARACTERIZATION AND CATALYTIC ACTIVITY FOR ALCOHOLYSIS OF EPOXIDES

Abstract

Palladium supported on strontium hydroxyl fluoride has been synthesized by one-pot fluorolytic sol-gel method. The prepared catalyst was characterized by various physicochemical techniques including PXRD, BET-surface area measurements, acidity measurements, SEM and TEM etc. The sol-gel method has led to formation of high surface area (57 m^2g^{-1}), mesoporous (pore diameter = 13.0 nm) catalysts with uniform dispersion of Pd nanoparticles of size ~7 nm on surface of strontium hydroxyl fluoride. The catalyst was used for alcoholysis of epoxide to form β-alkoxy alcohols at room temperature. The epoxides were reacted with a range of alcohols under mild reaction conditions. The catalyst could recycle upto three catalytic cycles. The filtration test of catalyst indicated no Pd leaching which confirmed true heterogeneous nature of catalyst. Further the mechanism of alcoholysis was proposed on the basic of products of the catalytic reaction.

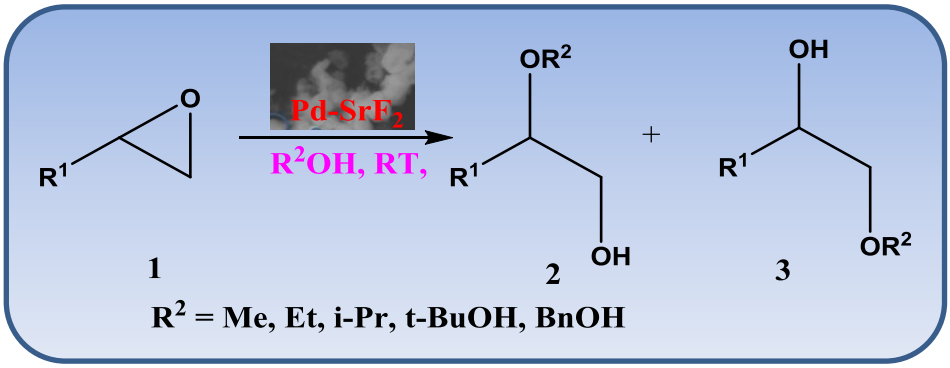

4.1. Introduction

Epoxides are resourceful and vital intermediates in organic synthesis and undergo ring-opening reactions to give β-substituted compounds with a variety of nucleophilic species [1]. Epoxide undergoes a variety of ring-opening reactions to give β-amino alcohols [2], 1,2-diacetates [3], carbonyl compounds [4], diols [5], β-alkoxy alcohols [6], and β-alkoxy sulfides [7]. These are convenient, practical and widely employed strategies for the synthesis of important classes of intermediates in organic chemistry. The opening of epoxides with alcohols is among important transformation in the synthesis of β-alkoxy alcohols which are mainly used as valuable organic solvents, versatile synthons, and intermediates [8].

A variety of organic reactions that are catalyzed by Brønsted acids such as H_2SO_4, HCl, HNO_3, CH_3COOH, etc. or Lewis acids like $AlCl_3$, $TiCl_4$, $FeCl_3$, $ZnCl_2$, etc. have been gradually replaced by heterogeneous catalysts with more efficiency [9]. The conventional minerals acids or bases have been used for alcoholysis of epoxides, which resulted in the formation of polymerized products with low regio-selectivity [10]. The use of conventional mineral acids in industrial processes is still widespread, leading to large amounts of inorganic wastes and often imposing drastic reaction conditions.

Various catalysts have been employed to accomplish this transformations including Lewis acids such as $FeCl_3$ [11], $Cu(BF_4)_2{\cdot}nH_2O$ [12], $InCl_3$ [13], $Mg(HSO_4)_2$ [14] and heterogeneous catalysts like polymer supported $FeCl_3$ [15] and $AlPW_{12}O_{40}$ [16]. Recently, the use of triflates $Yb(OTf)_3$ [17] and perchlorates $Fe(ClO_4)_3$ [18] have been reported along with other catalysts such as Cp_2ZrCl_2 [19], $K_5[CoW_{12}O_{40}]{\cdot}3H_2O$ [20], CBr_4 [21], tin(IV)porphyrinato trifluoromethanesulfonate [22], Amberlyst-15 [23] for the alcoholysis of epoxides. Although there are currently a number of methods available for epoxide ring opening, they have one or more disadvantages, such as long reaction time, high catalyst loading, high reaction temperature, tedious method of catalyst synthesis, and low selectivity. However in spite of high catalytic activity, perchlorates and triflates are less favored because of their explosive and expensive nature.

The use of harsh reaction conditions is necessary owing to poor nucleophilicity of alcohols, which led to decrease in regioselectivity of product [24].

Furthermore a significant and important progress has been made in the development of efficient catalytic methods which are successful under mild conditions [25].

The novel nanoscopic partially hydroxylated inorganic fluoride materials with bi-acidic (Lewis/Brønsted) properties were developed for catalytic applications [26]. The materials were synthesized using classical sol–gel route from metal alkoxide via fluorination with aqueous/nonaqueous HF which led to high surface area metal fluorides [27]. These types of catalysts have been already applied successfully for various catalytic applications viz. synthesis of (all-rac)-[α]-tocopherol [28], Friedal-Crafts reaction [29], Suzuki coupling reaction [30], synthesis of menthol [31], synthesis of vitamin K-1 and K-2 chromanol [32], oxidation of ethylbenzene [33], dehydrohalogenation of 3-Chloro-1,1,1,3,-tetrafluorobutane [34], catalytic C-H bond activation [35] and glycerol acetylation [36].

Recently the palladium supported catalyst was used for phenolysis of epoxides at high temperature in presence of bases [37]. The Pd supported on alkaline earth metal fluorides are known for its duel (acidic/basic) properties. These properties play an important role in determining not only activity but selectivity of the catalytic reactions. Therefore the study of synthesis and characterization of palladium supported strontium fluoride and its catalytic activity for alcoholysis of epoxides has been described in this chapter.

4.2. Experimental

4.2.1. Materials

All chemicals were purchased from Aldrich Chemical Co. USA and used as received. Hydrofluoric acid (71% aqueous solution) and solvents were procured from Merck Chemicals, Germany and used as obtained.

4.2.2. Catalyst synthesis

Cautions:
1. *HF is a highly toxic and irritant compound causing severe burns if it comes in contact with the skin.*
2. *Strontium is highly reactive with methanol to generate hydrogen hence the rate of reaction need to be controlled by keeping reaction flask in ice bath.*

Catalyst preparation was carried out under inert atmosphere of argon using standard Schlenk technique. In 250 mL round bottom flask, metallic strontium (2.103 g, 24 mmol) was treated with dry methanol (300 mL) at room temperature for 16 h in Schlenk flask to form strontium methoxide solution. A stoichiometric amount (Sr/F: 1/2) of 71% aqueous solution of hydrofluoric acid (5.3 mL, 48 mmol) was added to the solution of strontium methoxide followed by the addition of alcoholic solution of palladium acetate (0.630 g, 1 wt% loading of Pd metal, dissolved in 15 mL of methanol). This solution turned into a grey colored gel which was kept for 16 h for ageing. Then the grey gel was dried under vacuum at room temperature and 70 °C to remove solvents (methanol and water). The solid product was further calcined at 250 °C for 5 h. The prepared catalyst is referred hereafter as Pd-SrF_2-71 indicating 71% aqueous concentration of HF used for synthesis.

4.2.3. Catalyst characterizations

The Pd-SrF_2-71 was characterized using various physicochemical techniques as mentioned in chapter 2A, section 2A.2.6.

4.2.4. Typical procedure for catalytic reaction

In a sample tube equipped with a magnetic needle, an epoxide (1.0 mmol), alcohol (2.0 mL) and catalyst (10 wt % with respect to epoxide) was added. The reaction mixture was stirred at room temperature for the given time. The progress of the reaction was monitored by thin layer chromatography (TLC) and gas chromatography (GC). After the completion of the reaction the catalyst was separated by filtration and washed with alcohol and diethyl ether. The combined organic fractions were dried over anhydrous sodium sulfate and solvent was removed under reduced pressure. The reaction was monitored by gas chromatographic analysis using Agilent 6890 Gas Chromatograph equipped with a HP-5 dimethyl polysiloxane capillary column (60 m length, 0.25 mm internal diameter, 0.25 μm film thickness) with flame ionization detector. Products were confirmed by comparison with GC spectra of the authentic samples. Further the structure was confirmed by FTIR (Nicolet Nexus spectrometer equipped with DTGS detector), ^{1}HNMR (Bruker AC 200, 200MHZ spectrometer) spectral analysis and matched with the literature (only for representative reaction alcoholysis of cyclohexene oxide, styrene oxide and epichlorohydrin using ethanol).

4.2.5. Procedure for catalytic recycle study

To study the recyclability of the catalyst, after completion of the first reaction, the catalyst was separated using centrifugation followed by filtration through Whatmann filter paper (no. 1), washed with ethanol (5 mL X 3 times), and finally dried at 80 °C for 30 min. A fresh charge of reactants was taken with the dried catalyst and subjected under the similar reaction conditions. The same procedure was repeated for successive three catalytic run with same catalyst.

4.2.6. Procedure for filtration experiment study and ICP analysis

To verify the Pd leaching in the reaction mixture the filtration test was carried out at room temperature. A 0.05 g of catalyst was stirred with 0.5 g of cyclohexene oxide in 6 mL of ethanol under typical reaction conditions at room temperature. After 1 h, the catalyst was separated from liquid phase by centrifugation followed by filtration through Whatmann filter paper no. 1. Further the reaction was continued without catalyst at room temperature.

The separated catalyst was further tested for ICP-AES analysis to determine Pd content in the catalyst. The ICP-AES samples were prepared using similar procedure as mentioned in chapter 2 section 2A.2.7.

4.3. Results and discussion

4.3.1. Catalyst synthesis

The one pot synthesis of Pd-SrF_2-71 catalyst by fluorolytic sol-gel route using aq. HF (71%), resulted in simultaneous fluorolysis and hydrolysis of M-OR bond to form M-F and M-OH bonds respectively [38, 39]. Though the molar ratio of Sr:HF was adjusted to 1:2, the hydrolysis of strontium methoxide becomes competitive with the fluorination due of water content in the fluorinating agent. This reaction generates the composition in which both fluorine and hydroxide are attached to strontium in a solid structure and this led to the formation of strontium hydroxyl fluorides [$SrF_{(2-X)}(OH)_X$] material, which upon further addition of methanolic solution of palladium acetate forms Pd-$SrF_{2-X}(OH)_X$ (henceforth mentioned as Pd-SrF_2-71) catalyst as represented in scheme 4.1. The addition of alcoholic solution of palladium acetate led to formation of light red colored gel initially which upon aging turned to light gray. Typically Pd^{II} get partially reduced to Pd^0 due to dissolved hydrogen liberated during

the formation of strontium methoxide from metallic strontium to give gray color to the gel. In contrast to the non-aqueous sol gel route which results in the formation of clear sols and transparent gels, the aqueous route results in opaque gels of grey color due to presence of partially reduced palladium nanoparticles [40]. The bulk and surface structure of this material was characterized using various physicochemical techniques.

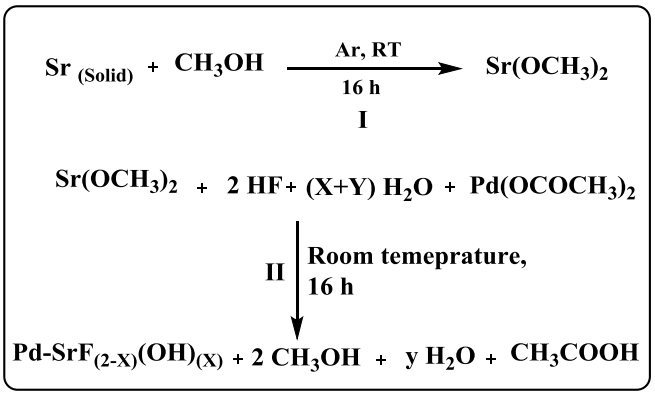

Scheme 4.1: Schematic representation for sol-gel synthesis of Pd-SrF_2-71 catalyst.

4.3.2. PXRD

The PXRD pattern of the prepared sample is shown in fig. 4.1. The diffraction peaks can be indexed as the peak corresponding to metal fluorides and metal hydroxides on comparison with strontium fluoride (JCPDS 06-0262) and strontium hydroxide (JCPDS 27-847).

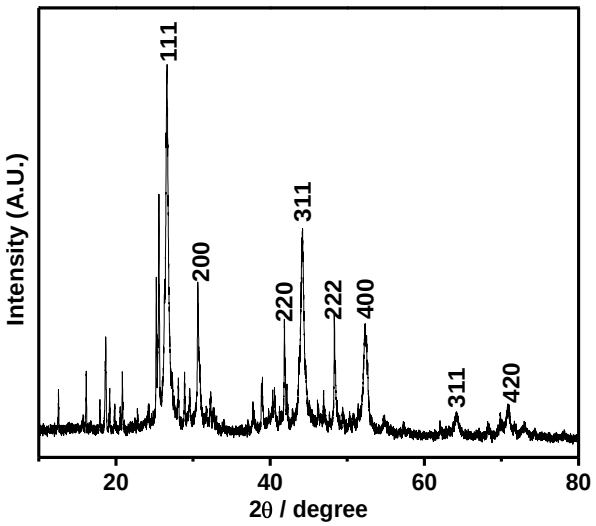

Figure 4.1. PXRD pattern of Pd-SrF_2-71 catalyst.

Furthermore, PXRD showed broad peaks which may corresponds to strontium fluoride and sharp peaks to strontium hydroxide. Additionally few less intense peaks

were observed, these peaks indicates the formation of mixed phases of strontium hydroxyl fluorides. However no diffraction for Pd_{111} was detected because of very low content of Pd with high order of dispersion of Pd particles over the surface of catalyst.

4.3.3. FTIR

The FTIR spectrum of the Pd-SrF_2-71 catalyst showed of the bands at 3450.1, 3007, 1631.5, 1402, 1083, 742.7, and 484.1 cm^{-1} (fig. 4.2). The high intense bands at 484.1 and 742.7 cm^{-1} can be related to ν(Sr-F) and ν(Sr-O) respectively. The bands around 3450 and 1650 cm^{-1} corresponds to presence of surface hydroxyl groups or moisture. The band at 3007 and 1083 cm^{-1} observed due to ν(C-H) and ν(C-O) stretching vibrations could be due to hydrocarbon residue in prepared catalysts. The presence of Sr-O and O-H band confirms the formation of partially hydroxylated strontium fluorides catalyst in the final catalyst.

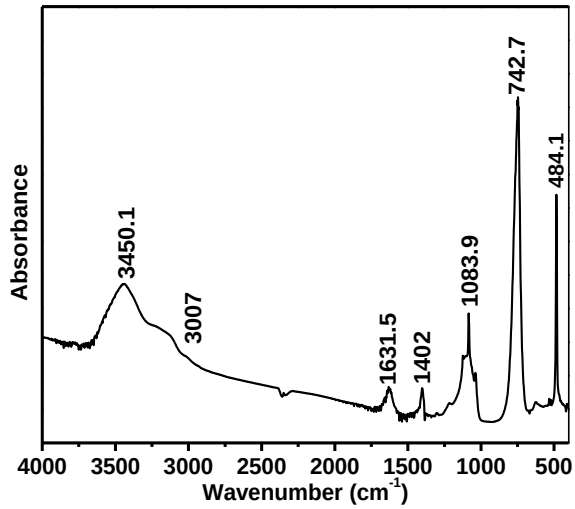

Figure 4.2. FTIR spectrum of Pd-SrF_2-71 catalyst

4.3.4. BET surface area

Nitrogen sorption studies were performed to study the surface area, pore diameter and pore volume (Fig. 4.3). The isotherms showed type IV character typical for mesoporous materials with a H1 type hysteresis loop and porous texture. The BET surface area and total pore volume of the catalyst was found to be 57 m^2g^{-1} and 0.11 $cc.g^{-1}$ respectively.

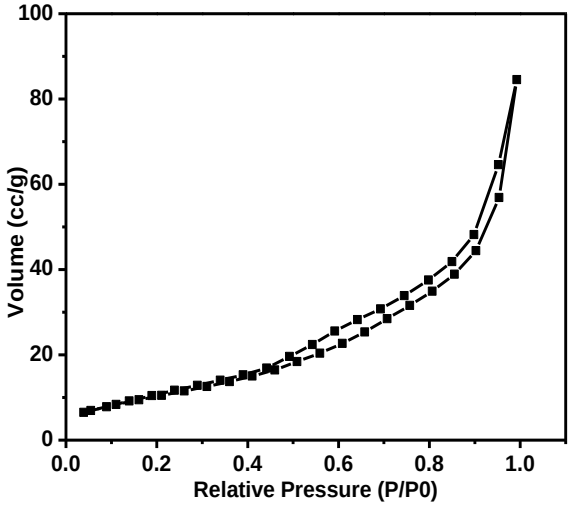

Figure 4.3. BET Surface area plot of Pd-SrF_2-71 catalyst.

Typically the surface area of Pd-SrF_2-71 was observed to be intermediate between metal fluorides from same group in periodic table like Pd-MgF_2-71 (140 m^2g^{-1}) and Pd-BaF_2-71 (8 m^2g^{-1}) prepared under identical conditions. The average pore size was determined using Barrett-Joyner-Halenda (BJH) analysis and found to be 13.1 nm which confirms the mesoporous nature of the catalyst.

4.3.5. Acidity measurements

A. Ammonia- Temperature programmed desorption (NH_3-TPD)

The total acidity as well as the strength of acidic sites on the surface of the catalysts was determined by ammonia-temperature programmed desorption (NH_3-TPD) technique as shown in fig. 4.4.

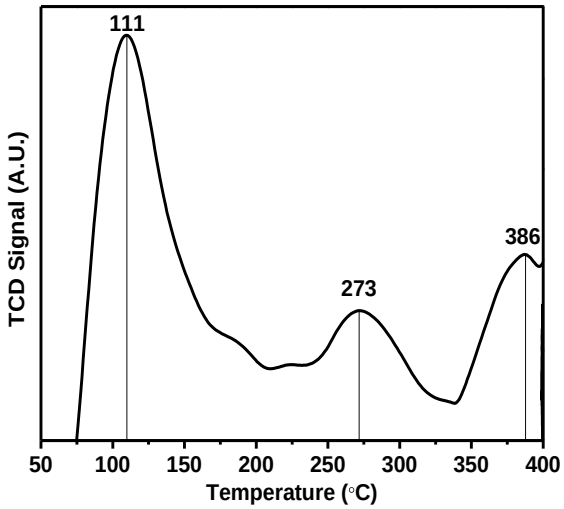

Figure 4.4. NH_3-Temperature program desorption plot of Pd-SrF_2-71 catalyst.

The NH_3 desorption studies indicated the presence of weak, moderate and strong acidic sites with peak maxima corresponds to 111, 276, and 386 °C respectively. Also the total acidity of the catalyst was found to be 0.151 mmol g^{-1}. The total acidity of the catalyst was depends on the degree of fluorination as well as on the nature of the metal alkoxide. Normally a decreasing trend in the acidity of the metal alkoxide was observed down the group in periodic table.

B. DRIFT Spectroscopy

The type of acidity present on the catalyst surface was studied by DRIFT spectroscopy of adsorbed pyridine (pK_a = 5.25). The subtracted FTIR spectrum of absorbed pyridine on Pd-SrF_2-71 surface is shown in fig. 4.5. The FTIR peak at 1445 and 1545 cm^{-1} shows presence of Lewis and Brønsted acidic sites respectively while the peak at 1490 cm^{-1} represents presence of both Lewis and Brønsted acidity on the surface of oxide materials in adsorbed pyridine spectrum [41]. Similarly, the bands in the adsorbed pyridine spectrum of Pd-SrF_2-71 are assignable to coordinately bound pyridine [41, 42]. The pyridinium ion (PyH^+) produced by the reaction of pyridine with Brønsted acid sites showed bands around 1542 and 1640 cm^{-1}. The coordinately bound pyridine on Lewis acid sites shows bands around 1452 and 1610 cm^{-1}. This DRIFT indicated the presence of Lewis and Brønsted acidic sites on the surface of Pd-SrF_2-71 catalyst.

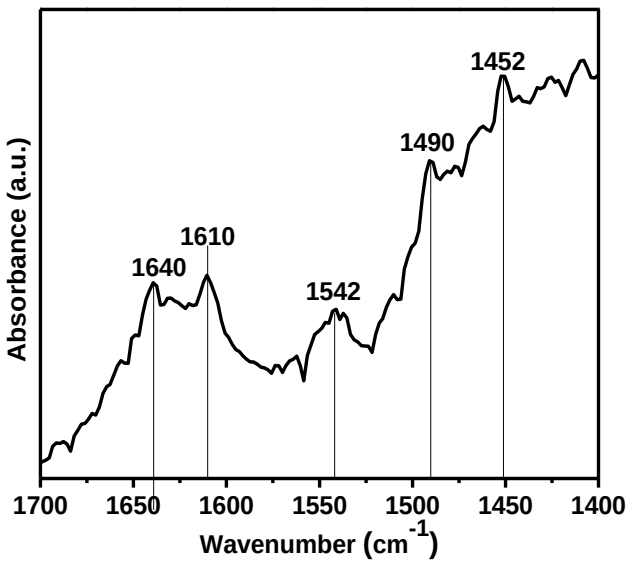

Figure 4.5. FTIR spectrum of adsorbed pyridine on Pd-SrF_2-71 surface at 100 °C.

4.3.6. XPS

XPS was used to derive surface compositional information of the Pd-SrF_2-71 catalyst in fig. 4.6. The montage of survey scan after analysis of Pd-SrF_2-71 catalyst is shown in fig. 4.6 -A. The peaks were annotated to the Sr, F, O and Pd with their core levels. The peaks were standardized with respect to carbon peak at 284.6 eV on surface. Due to non-conductive nature of strontium fluoride some charging of sample was observed. In order to determine the effect of the support on the oxidation state of palladium of the as synthesized samples, the region of Pd was studied further (fig. 4.6-B). Palladium showed presence of two oxidation states namely Pd^0 and Pd^{2+}.

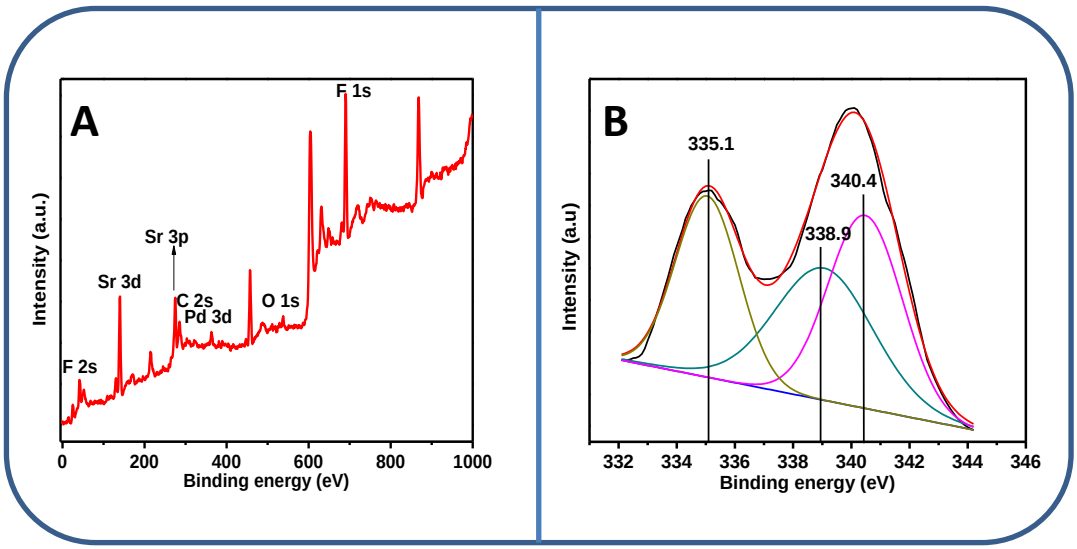

Figure 4.6. XPS of the Pd-SrF_2-71 catalysts (A) Survey scan and (B) scan for binding energy of palladium species.

The two different values of Pd^{2+} may be due to variable coordination of Pd^{2+} species. The peak at 335.1 corresponds to Pd^0 and peaks at 338.9 and 340.4 relates to Pd^{2+} species from palladium acetate and palladium oxide respectively. The ratio of relative abundance (Pd:Pd^{2+}) was observed to be 1:2 approximately. The presence of Pd^0 can be attributed to partial reduction of palladium acetate in presence of dissolved hydrogen which was produced during catalyst synthesis.

4.3.7. SEM and EDAX

The morphology of Pd-SrF_2-71 catalyst was studied by SEM. The representative micrograph of Pd-SrF_2-71 is shown in fig. 4.7. It showed the particles of SrF_2-71 to be of oval shaped of 1.5- 2.0 μm in length and 0.5-1.0 μm in width. The Pd particles were spread throughout evenly on the strontium hydroxyl fluoride

surface. Further the surface composition of catalyst was also determined by EDAX spectroscopy. The results showed the surface palladium composition to be approximately 1.1 wt%.

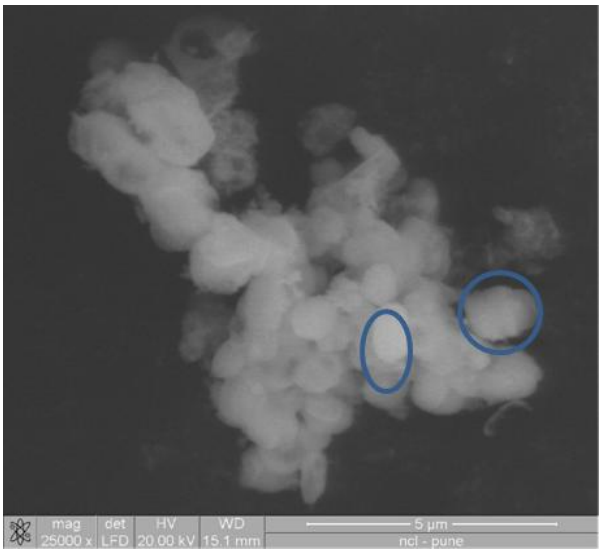

Figure 4.7. SEM image of Pd-SrF_2-71 catalyst.

4. 3.8. HRTEM

The Particle size of palladium was determined by HRTEM analysis. The representative micrograph of Pd-SrF_2-71 is shown in fig. 4.8. The particle size distribution studied by TEM clearly showed the majority of particles with ~7 nm diameter though the particle size distribution spreads up to 20 nm. The palladium particles were found to be in 111 plane as identified from d spacing (d_{111} = 0.223 nm).

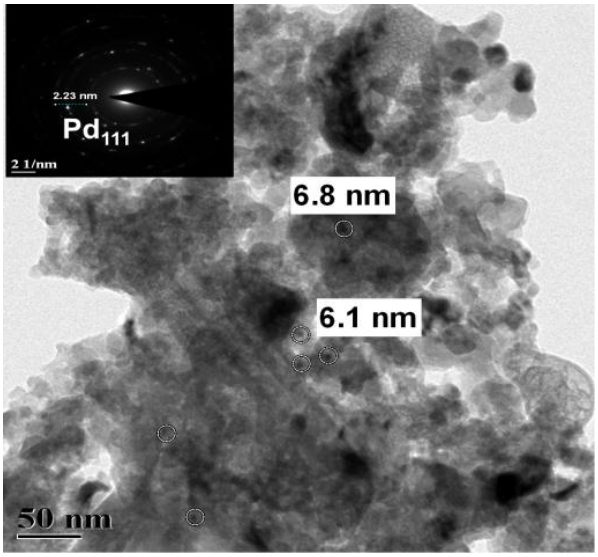

Figure 4.8. Representative HRTEM image of Pd-SrF_2-71 catalyst with SAED pattern.

4.3.9. Catalytic activity for alcoholysis of epoxides

The catalytic activity of Pd-MF_2-71 (where, M = Mg, Sr, Ba) was studied for alcoholysis of epoxide at room temperature initially with cyclohexene oxide as model substrate and ethanol as nucleophile (scheme 4.2). The results obtained with various catalysts are given in table 4.1. In absence of catalyst reaction did not take place even after 2 h time (table 4.1, entry 1). Further a series of palladium supported metal fluoride catalysts were evaluated for catalytic reactions. The Pd-MgF_2-71, Pd-SrF-71_2, Pd-BaF_2-71 catalysts showed 43, 100 and 20% conversion respectively (table 4.1, entry 2-4). It is well known that the Lewis acidity of the catalyst decreases from Pd-AlF_3 to Pd-BaF_2 with increase in basicity [43]. In case of highly acidic catalyst higher conversion has been reported but the higher order of acidity is responsible for decrease in selectivity and generation of byproduct like 1,6-hexandiol. Moreover Pd-BaF_2 showed less conversion with 100% selectivity due to its basic nature. In case of Pd-SrF_2, the acidic and basic sites were found to be balanced to get optimum conversion and selectivity. The catalytic activity of the Pd-AlF_3 was compared which showed 59% conversion under identical reaction conditions (table 4.1, entry 5).

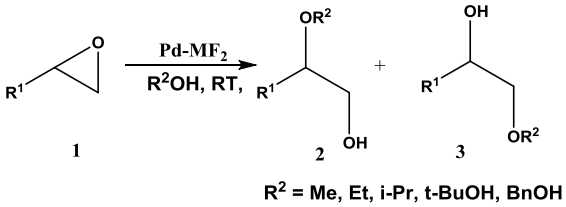

Scheme 4.2. Alcoholysis of epoxides.

Table 4.1. Results of alcoholysis of epoxide[a]

Entry	Catalyst	Conv.[b] (%)	Sel.[b] (%)	Activity (mmol h^{-1} g^{-1}) X 10^4
1	None	0	-	-
2	Pd-MgF_2-71	43	93	3.18
3	Pd-SrF_2-71	100	96	7.00
4	Pd-BaF_2-71	20	96	1.27
5	Pd-AlF_3-71	59	80	2.86

[a]**Reaction conditions**: Cyclohexene oxide: 1 mmol; Ethanol: 2 mL; Catalyst: 0.01 g (10 wt%, 1.0 wt% of Pd loading); Temperature: RT (27 °C). [b] Conv. and Sel. was determined based on GC.

4.3.10. Effects of various reaction parameters

A. Catalyst loading effect

The effect of catalyst loading on alcoholysis of cyclohexene oxide was studied at room temperature in fig. 4.9. The conversion increased with gradual increase in catalyst loading. The 1 wt% catalyst loading gave 9% conversion which was increasing to 70% for 15 wt% loading in 1 h at room temperature. There was marginal decrease in selectivity at high catalyst loading.

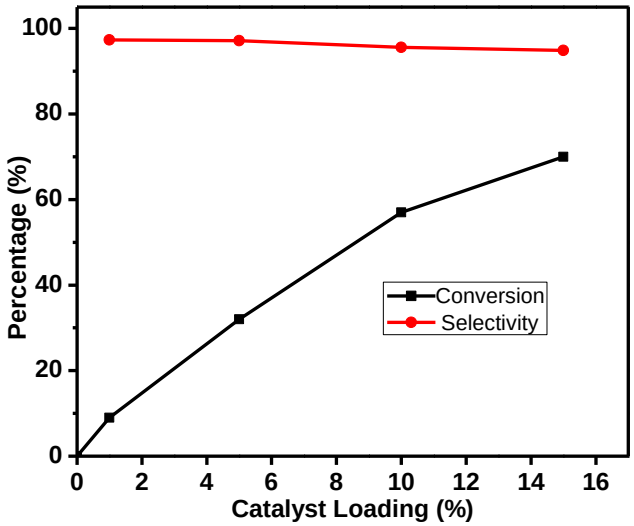

Figure 4.9. Catalyst loading effect using Pd-SrF_2-71 catalyst.

Reaction conditions: Cyclohexene oxide: 5 mmol (0.54 g); Ethanol: 2 mL; Temperature: RT (27 °C). Time: 1 h.

B. Temperature effect

Epoxide ring opening of cyclohexene oxide was studied at various temperatures ranging from room temperature to 70 °C in ethanol with 10 wt% loading of Pd-SrF_2-71 catalyst as shown in fig. 4.10. It was observed that with gradual increase in reaction temperature from room temperature (27 °C) to 70 °C, the time for 100% conversion of cyclohexene oxide decreased from 120 to 30 min without much decrease in selectivity. The increase in rate of reaction revealed to increase in rate of intermolecular collision. Although the rate of reaction was higher at 70 °C, room temperature is always preferred. Therefore room temperature was considered as optimum temperature for carrying out further reactions.

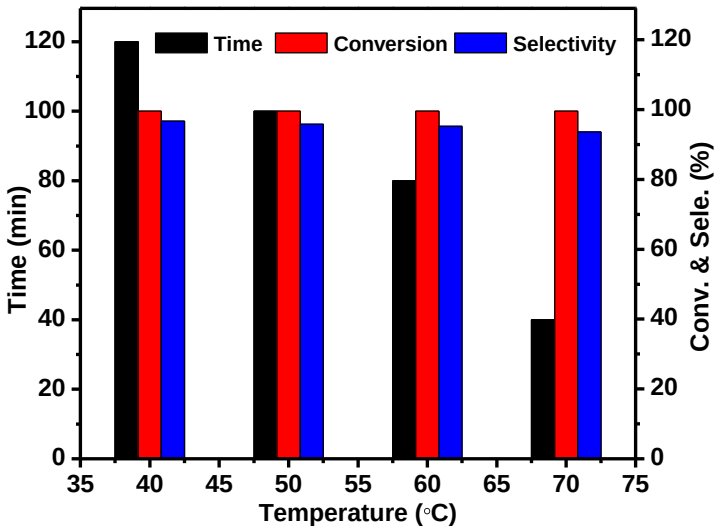

Figure 4.10. Temperature effect study using Pd-SrF_2-71 catalyst.

Reaction conditions: Cyclohexene oxide: 2 mmol (0.196 g); Catalyst (Pd-SrF_2): 0.02 g; Ethanol: 2 mL.

C. Time profile study

The conversion of the cyclohexene oxide increased with increase in reaction time at room temperate in ethanol as shown in fig. 4.11. A virtually linear time-conversion profile has been observed for ethanolysis of cyclohexene oxide. The selectivity of the 2-ethoxycyclohexanol decrease to 96% after complete conversion of cyclohexene oxide after 2 h which was found to be constant upto 2.5 h at room temperature.

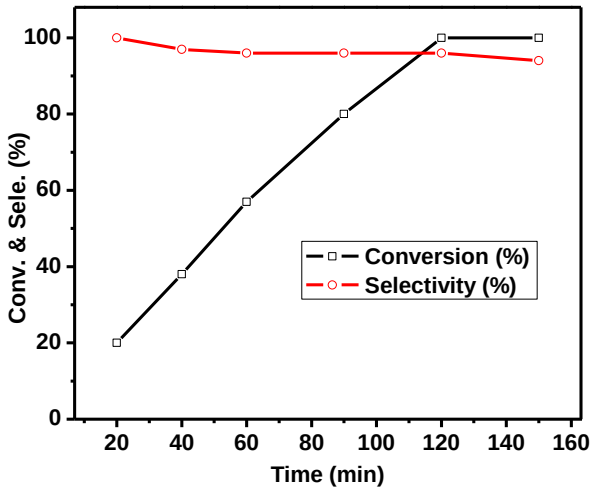

Figure 4.11. Time profile study using Pd-SrF_2-71 catalyst.

Reaction conditions: Cyclohexene oxide: 2 mmol (0.196 g); Catalyst (Pd-SrF_2-71): 0.02 g (10 wt% of cyclohexene oxide); Ethanol: 2 mL; Temperature: RT (27 °C).

4.3.11. Substrate scope study

After optimizing the reaction conditions for ethanol as a nucleophile with cyclohexene oxide as a model reaction, the applicability of the catalyst to other epoxides and alcohols was evaluated. The reaction of cyclohexene oxide with methanol and ethanol gave 98 and 96% yield respectively (table 4.2, entry 1-2). The reaction of 2-propanol gave lower yield (57%) as compared to ethanol as a nucleophilic source (table 4.2, entry 3). This may be due to the steric effect of two methyl groups, which hinders the reaction site resulting in the lowering of cyclohexene oxide conversion into the desired product. Similar behavior was also observed when the reaction was carried out with t-butyl alcohol which showed 25% yield (table 4.2, entry 4). This observation can be explained by the fact that *tertiary* butyl alcohol is even more bulky, having three methyl groups which increases the steric hindrance and which lower the activity in nucleophilic substitution reaction. When benzyl alcohol was used as nucleophile 99% yield was observed (table 4.2, entry 5). Although the steric hindrance in benzyl alcohols is higher than *t*-butyl alcohol, the higher nucleophilicity may be responsible for increment in the rate of the reaction. Further styrene oxide was used as substrate to check the effect of catalyst on regioselectivity (table 4.2, entry 5-10).

The rate of the reaction was found to be depending on nucleophilicity of the alcohol but also on steric hindrance of epoxide. The yields of β-alkoxyalcohols were decreased from methoxyl to t-butoxyl (92-18%) due to increase in bulkier nature of nucleophile (table 4.2, entry 5-9), which increased to 72% in case of benzyl alcohol (table 4.2, entry10). The reaction of epichlorohydrin with methanol and ethanol showed 89 and 78% yields respectively (table 4.2, entry 11-12). When bulkier alcohols like 2-propanol and 2-methyl-2-propanol was used as nucleophile, the yield decreased to 53 and 36% respectively (table 4.2, entry 13-14) which again increased to 65% with benzyl alcohol as nucleophile (table 4.2, entry 15). Remarkably formation of a single regioisomer was observed in all the cases. This formation of stable intermediate in each case led to formation of single regioisomer. In styrene because of formation of stable benzylic carbocation, the reaction follows SN^1 pathway and formed 2 as preferable regio-isomer. In epichlorohydrin, the reaction follows SN^2 pathway due to attack of nucleophile from backside of ring opening, yielding 3 as preferable regioisomer.

Table 4.2. Substrate scope study using Pd-SrF_2-71 catalyst.[a]

Entry	Epoxide	Alcohol	Products ratio (2:3)	Yields[b] (%)
1	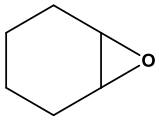	MeOH	*Trans*	98
2		EtOH	*Trans*	96
3		i-PrOH	*Trans*	57
4		t-BuOH	*Trans*	25
5		BnOH	*Trans*	99
6	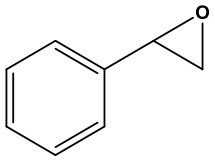	MeOH	100:0	92
7		EtOH	100:0	73
8		i-PrOH	100:0	49
9		t-BuOH	100:0	18
10		BnOH	100:0	72
11	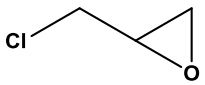	MeOH	0:100	89
12		EtOH	0:100	78
13		i-PrOH	0:100	53
14		t-BuOH	0:100	36
15		BnOH	0:100	65

[a]**Reaction conditions**: Substrate: 0.2 g; Catalyst (Pd-SrF_2-71): 0.02 g (10 wt% w.r.t. substrate); Alcohols: 2 mL; Temperature: RT (27 °C). Time: 2 h. [b] Yields were determined based on GC.

4.3.12. Catalyst recycle study

The recyclability of Pd-SrF_2-71 was studied for optimized ring opening of cyclohexene oxide in ethanol under reaction conditions. After completion of the reaction, the catalyst was separated from reaction mixture by centrifugation followed by filtration using Whatmann filter paper no.1. The catalyst was washed with ethanol (5 mL X 2) and acetone (5 mL) and allowed to dry at 80 °C and used it for subsequent catalytic runs. The same procedure was repeated for three times. However even after three runs, the catalyst exhibited excellent activity as shown in fig. 4.12. It implied that the catalytic system can be used even for three cycles without significant loss of activity.

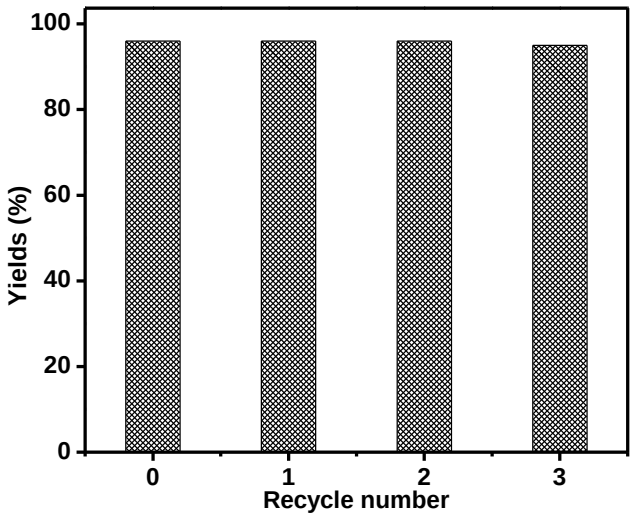

Figure 4.12. Recycle study using Pd-SrF_2-71 catalyst.

Reaction conditions: Cyclohexene oxide: 5 mmol (0.54 g); Pd-SrF_2-71: 0.05 g (10 wt% w.r.t. substrate); Ethanol: 2 mL; Temperature: RT (27 °C). Time: 2 h.

4.3.13. TEM and ICP analysis of recycled catalyst

The TEM image of recycled catalyst after 3rd cycle revealed no agglomeration of Pd on the catalyst surface as shown in fig. 4.13.

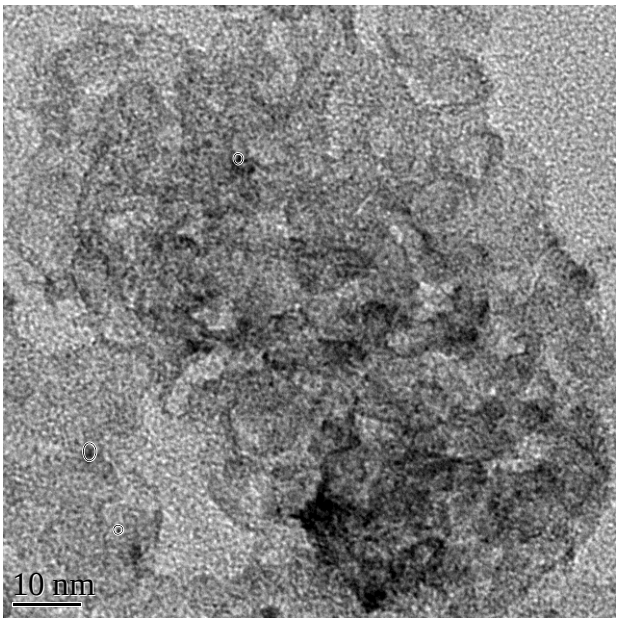

Figure 4.13. TEM image of Pd-SrF_2-71 catalyst after 3rd catalytic recycle.

The size of Pd nanoparticle was found to be in the same range of 6-8 nm when compared with the fresh catalyst (refer fig. 4.8). There was no decrease in the catalytic activity in successive cycles for alcoholysis of epoxides. Filtration test was used to check the Pd leaching in reaction mixture. It was observed that in absence of

catalyst, no further change in cyclohexene oxide conversion was observed even after additional 3 h which confirms no Pd leaching which were also confirmed by ICP-AES analysis of catalyst. The Pd concentration was found to be 0.986 % before reaction and 0.978% after the reaction. Therefore Pd-SrF_2-71 catalyst acts as true heterogeneous catalytic system.

4.3.14. Possible reaction mechanism

Based on the results obtained during catalytic reactions and by comparison with the literature reports, the mechanism for the alcoholysis of epoxide using Pd-SrF_2-71 catalyst has been proposed in scheme 4.3. In case of styrene oxide, nucleophilic alkoxy group attacks in such a way to produce 2-phenyl-2-alkoxy ethanol. While in epichlorohydrin case, the alkoxy group attacks epoxide ring to get 3-chloro-1-alkoxy-2-propanol as only product. Initially the adsorption of epoxide on surface of catalyst takes place which activates epoxide via partial transfer of electrons of oxygen to empty orbital of oxidized palladium to get intermediate **B** (Step 1).

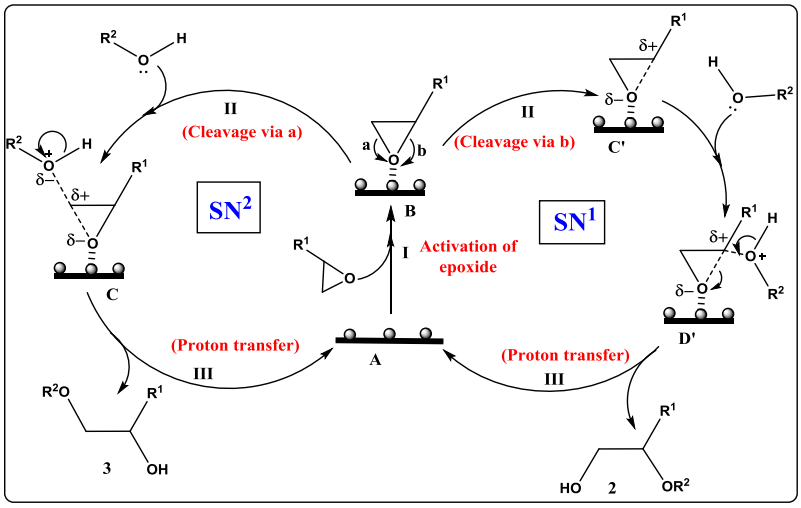

Scheme 4.3. Possible reaction mechanism for regioselective alcoholysis of epoxide using Pd-SrF_2-71 catalyst.

Further attack of nucleophilic oxygen led to open the epoxide ring in two possible ways depending on the nature of alkyl group. In case of electron withdrawing alkyl group, the reaction follows S_N2 pathways to generate intermediate **C** which undergoes simultaneous C-O bond cleavage and backside attack of nucleophilic O-atom of alcohol followed by proton transfer to produce product **3**. In case of electron donating alkyl group, the reaction follows S_N1 pathways to generate

intermediate carbocation **C'** by cleavage of C-O bond. This **C'** carbocation intermediate gets stabilized via resonance and inductive effect which undergoes nucleophilic attack by nucleophilic O- atom of alcohol followed by proton transfer to generate product **2**. The high regioselectivity is due to stabilization of intermediate on species the catalyst surface and results in two different nucleophilic substitution reactions

4.4. Conclusions

In conclusion, Pd-SrF_2-71 proved to be novel and efficient catalyst for room temperature alcoholysis of epoxide. Due to very less acidic nature of catalyst, it may find application for ring opening of epoxides containing acid sensitive functional groups. The catalyst showed very high regioselectivity which depends on the nature of alkyl group of the substrate. One pot method of synthesis, ease of procedure, high order of recyclability, regioselectivity and mild reaction condition showed a new synthetic applications of heterogeneous metal fluoride supported palladium catalyst in synthetic chemistry.

4.5. References

[1] (a) T. N. Birkinshaw, *In Comprehensive Organic Functional Group Transformations*; Oxford, **1995**, *1*, 204; (b) B. Sreedhar, P. Radhika, B. Neelima, N. Hebalkar, *J. Mol. Catal. A: Chem*., **2007**, *272*, 159; (c) B. Das, V.S. Reddy, M. Krishnaiah, Y.K. Rao, *J. Mol. Catal. A: Chem.* **2007**, *270*, 89.

[2] G. Bartoli, M. Bosco, A. Carlone, M. Locatelli, P. Melchiorre, L. Sambri, *Org. Lett*., **2004**, *6*, 3973.

[3] G. Fogassy, C. Pinel, G. Gelbard, *Catal. Commun*., **2009**, *10*, 557.

[4] D. P. Serrano, R. van Grieken, J. A. Melero, A. García, *Appl. Catal. A*,**2007**, *319*, 171.

[5] P. Salehi, M. Dabiri, M. A. Zolfigol, M. A. B. Fard, *Phosphorus, Sulfur Silicon Relat. Elem*., **2004**, *179*, 1113.

[6] A. J. L. Leitao, J. A. R. Salvador, R. M. A. Pinto, M. L. Sàe Melo, *Tetrahedron Lett*., **2008**, *49*, 1694.

[7] J. Wu, H. G. Xia, *Green Chem.*, **2005**, *7*, 708.

[8] (a) T. Kino, H. Hatanaka, M. Hashimato, M. Nishiyama, T. Goto, M. Okuhara, M. Kohsaka, H. Aoki, H. Imanaka, *J. Antibiot*., **1987**, *40*, 1249; b) O. Henze,

W. J. Feast, F. Gardebien, P. Jonkheijm, R. Lazzaroni, P. Leclère, E. W. Meijer, A. P. H. J. Schenning, *J. Am. Chem. Soc.*, **2006**, *128*, 5923; (c) J. E. Arrowsmith, S. F. Campbell, P. E. Cross, J. K. Stubbs, R. A. Burges, D. G. Gardiner, K. J. Blackburnt, *J. Med. Chem.*, **1986**, *29*, 1696.

[9] J. M. Thomas, R. Raja, *Annu. Rev. Mater. Res*., **2005**, 35, 315; (b) P. Botella, A. Corma, S. Iborra, R. Montón, I. Rodríguez, V. Costa, *J. Catal.*, **2007**, *250*, 161.

[10] W. Reeve, I. Christoffel, *J. Am. Chem. Soc.*, **1950**, *72*, 1480.

[11] N. Iranpoor, P. Salehi, *Synthesis*, **1994**, 1152.

[12] J. Barluenga, H. Vázquez-Villa, A. Ballesteros, J. M. González, *Org. Lett*., **2002**, *4*, 2817.

[13] B. H. Kim, F. Piao, E. J. Lee, J. S. Kim, Y. M. Jun, B. M. Lee, *Bull. Korean Chem. Soc.*, **2004**, *25*, 881.

[14] P. Salehi, M. M. Khodaei, M. A. Zolfigol, A. Keyvan, *Synth. Commun.*, **2003**, *33*, 3041.

[15] R. V. Yarapathi, S. M. Reddy, S. Tammishetti, *React. Funct. Polym.*, **2005**, *64*, 157.

[16] H. Firouzabadi, N. Irannpoor, A. A. Jafari, S. Malarem, *J. Mol. Catal. A: Chem.*, **2006**, *250*, 237.

[17] (a) P. R. Likhar, M. P. Kumar, A. K. Bandyopadhyay, *Synlett*, **2001**, 836; (b) N. Iranpoor, B. Zeynizadeh, *Synth. Commun*., **1999**, *29*, 1017; (c)) D. B. G. Williams, M. Lawton, *Org. Biomol. Chem*., **2005**, *3*, 3269.

[18] P. Salehi, B. Seddighi, M. Irandoost, F. K. Behbahani, *Synth. Commun.*, **2000**, *30*, 2967.

[19] M. L. Kantam, K. Aziz, K. Jeyalakshmi, P. R. Likhar, *Catal. Lett.*, **2003**, *80*, 95.

[20] S. Tangestaninejad, M. Moghadam, V. Mirkhani, B. Yadollahi, S. M. R. Mirmohammadi, *Monatsh. Chem.*, **2006**, *137*, 235.

[21] J. S. Yadav, B. V. S. Reddy, K. Harikishan, C. Madan, A. V. Narsaiah, *Synthesis*, **2005**, 2897.

[22] M. Moghadam, S. Tangestaainejad, V. Mirkhani, R. Shaibani, *Tetrahedron*, **2004**, *60*, 6105.

[23] Y. H. Liu, Q. S. Liu, Z. H. Zhang, *J. Mol. Catal. A: Chem.*, **2008**, *296*, 42.

[24] (a) G. H. Posner, D. Z. Rogers, *J. Am. Chem. Soc*., **1977**, *99*, 8208; (b) J. Otera, Y. Niibo, N. Tatsumi, H. Nozaki, *J. Org. Chem.*, **1988**, *53*, 275.

[25] (a) B. M. Choudary, Y. Sudha, *Synth. Commun*., **1996**, *26*, 2989; (b) S. K. Yoo, J. Y. Lee, C. Kim, S. J. Kim, Y. Kim, *Dalton Trans*., **2003**, 1454; (c) D. Barreca, M. P. Copley, A. E. Graham, J. D. Holmes, M. A. Morris, R. Seraglia, T. R. Spalding, E. Tondello, *Appl. Catal. A: Gen.*, **2006**, *304*, 14; (d) M. W. C. Robinson, R. Buckle, I. Mabbett, G. M. Grant, A. E. Graham, *Tetrahedron Lett*., **2007**, *48*, 4723; (e) J. Barluenga, H. Vaezquez-Villa, A. Ballesteros, J. M. Gonza´lez, *Org. Lett*., **2002**, *4*, 2817 (f) C. Torborg, D. D. Hughes, R. Buckle, M. W. C. Robinson, M. C. Bagley, A. E. Graham, *Synth. Commun.*, **2008**, *38*, 205.

[26] S. Wuttke, S. M. Coman, J. Kröhnert, F. C. Jentoft, E. Kemnitz, *Catal. Today*, **2010**, *152*, 2.

[27] S. Wuttke, S. M. Coman, G. Scholz, H. Kirmse, A. Vimont, M. Daturi, S. L. M. Schroeder, E. Kemnitz, *Chem. Eur. J.*, **2008**, *14*, 11488.

[28] S. M. Coman, S. Wuttke, A. Vimont, M. Daturi, E. Kemnitz, *Adv. Synth. Catal.*, **2008**, *350*, 2517.

[29] N. Candu, S. Wuttke, E. Kemnitz, S. M. Coman, V. I. Parvulescu, *Appl. Catal. A*, **2011**, *391*, 169.

[30] P. T. Patil, A. Dimitrov, J. Radnik, E. Kemnitz, *J. Mater. Chem.*, **2008**, *18*, 1632.

[31] A. Negoi, S. Wuttke, E. Kemnitz, D. Macovei, V. I. Parvulescu, C. M. Teodorescu, S. Coman, *Angew. Chem. Int. Ed*., **2010**, *49*, 3134.

[32] S. M. Coman, V. I. Parvulescu, S. Wuttke, E. Kemnitz, *ChemCatChem*, **2010**, *2*, 92.

[33] I. K. Murwani, K. Scheurell, E. Kemnitz, *Catal. Commun.*, **2008**, *10*, 227.

[34] K. Teinz, S. Wuttke, F. Börno, J. Eicher, E. Kemnitz, *J. Catal*., **2011**, *282*, 175.

[35] M. H. G. Prechtl, M. Teltewskoi, A. Dimitrov, E. Kemnitz, T. Braun, *Chem. Eur. J*., **2011**, *17*, 14385.

[36] S. B. Troncea, S. Wuttke, E. Kemnitz, S. M. Coman, V. I. Parvulecu *Appl. Catal. B: Environ.*, **2011**, *107*, 260.

[37] K. Seth, S. R. Roy, B. V. Pipaliya, A. K. Chakraborti, *Chem. Commun*., **2013**, *49*, 5886.

[38] Y. Diao, W. Walawender, C. S. Sorensen, K. J. Klabunde, T. Ricker, *Chem. Mater*., **2002**, *14*, 362.

[39] K. T. Ranjit, K. J. Klabunde, *Chem. Mater*., **2005**, *17*, 65.

[40] S. Wuttke, G. Scholz, S. Rudiger, E. Kemnitz, *J. Mater. Chem*., **2007**, *17*, 4980.

[41] (a) J. Penzien, A. Abraham, J. A. Bokhoven, A. Jentys, T. E. Muller, C. Sievers, J. A. Lercher, *J. Phys. Chem. B*, **2004**, *108*, 4116; (b) F. Bonino, A. Damin, S. Bordiga, C. Lamberti, A. Zecchina, *Langmuir*, **2003,** *19*, 2155; (c) M. I. Zaki, M. A. Hasan, F. A. Al-Sagheer, L. Pasupulety, *Colloids Surf., A*, **2001**, *190*, 261.

[42] K. Tanaka, A. Ozaki, *J. Catal*., **1967**, *8*, 1.

[43] M. Feist, K. Teinz, S. R. Manuel, E. Kemnitz, E. *Thermochim. Acta*, **2011**, *524*, 170.

Chapter 5

SUMMARY AND CONCLUSIONS

Abstract

The thesis describes the sol-gel synthesis of palladium supported metal fluorides and its catalytic applications in various organic transformations which includes industrially important reaction like hydrogenation, oxidation and alcoholysis. This chapter presents a brief summary of the work described in previous chapters and general conclusions arrived from the work.

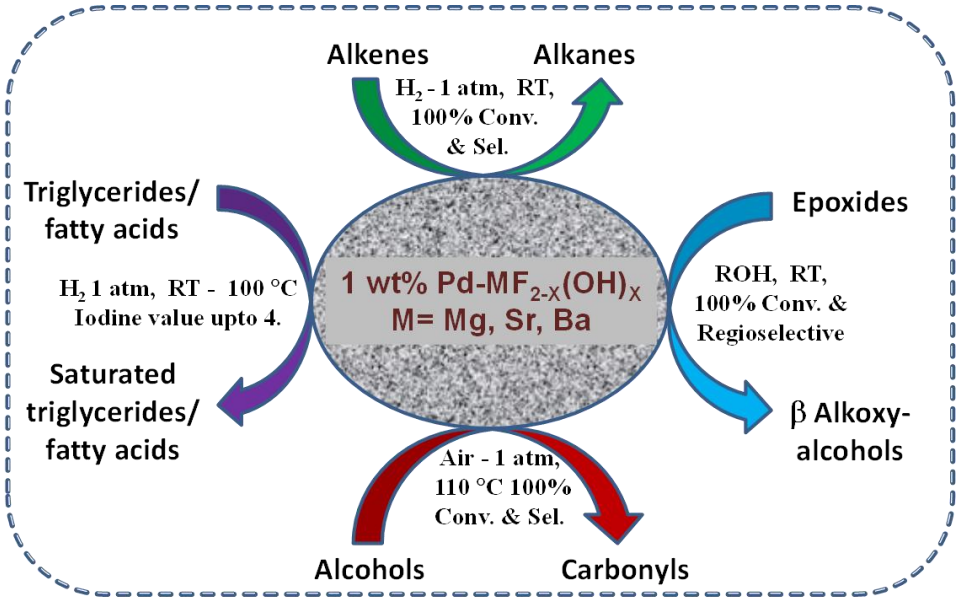

Chapter 1: Introduction

This chapter mainly deals with the general introduction to heterogeneous catalysis with a special emphasis on metal fluoride material in catalysis. A literature survey on metal fluoride in heterogeneous catalysis was discussed. Further general chemistry of palladium and role of metal support interaction in heterogeneous catalysis has been briefed. A general objective and motivation of the Ph. D. work was explained in this chapter.

Chapter 2: Palladium nanoparticles supported on magnesium hydroxyl fluorides: synthesis, characterization and its catalytic applications for selective olefin hydrogenation

This chapter deals with the one pot sol-gel synthesis of palladium supported on metal fluorides using three different concentration of hydrofluoric acid by fluorolytic method. The catalysts were characterized using several physico-chemical techniques. The synthesized catalyst showed high surface area, mesoporous crystalline nature, tunable acidity and strength of acidity. Palladium was observed in Pd^0 and Pd^{2+} oxidation states. The metal-support interactions were observed in catalyst which helped to stabilize finely dispersed Pd nanoparticles on the metal fluoride support. Due to presence of strong metal support interaction the Pd-nanoparticles were arranged in sheet like structure. The catalyst showed very high metal dispersion up to 47%.

The catalyst showed high activity for selective hydrogenation of olefin at room temperature and atmospheric pressure of hydrogen gas in presence of other reducible functional groups. The catalyst was successfully recycled for five cycles without any loss in activity and no Pd leaching was observed in reaction mixture. Further *in-situ* FTIR studies indicated facile activation of hydrogen on the catalyst surface at ambient conditions.

Due to high catalytic activity of Pd supported on magnesium hydroxyl fluoride was used for simple olefinic hydrogenation; it was used for hydrogenation of oils. The catalyst showed high activity for hydrogenation of edible and non-edible oils under ambient reaction conditions. In case of castor oil hydrogenation, iodine number of hydrogenated product could be decreased to 4. The catalyst also showed high activity in presence and absence of solvents. Also the catalyst resulted in high activity for

hydrogenation of edible oils like sunflower and soyabean oils. The catalyst showed high selectivity up to 77% for *cis* products, as well as high recyclability without Pd leaching.

Chapter 3: Palladium supported on barium fluoride: synthesis, characterization and catalytic activity for aerobic oxidation of alcohols

The one-pot synthesis of palladium supported on barium fluoride was carried out from barium metal via barium methoxide using fluorolytic sol-gel method. The synthesized catalyst was characterized using several physico-chemical techniques. The catalyst showed high order of crystallinity, formation of mixed phase of hydroxyl fluorides and low surface area up to 8 $m^2 g^{-1}$. SEM analysis indicated formation of rod shaped barium fluorides of 2-3 μm length and 0.2 – 0.4 μm width. TEM analysis showed presence of nanoparticles of palladium and palladium oxides. The ammonia TPD indicated the presence of very weak acidic sites on the surface of catalyst.

The synthesized catalyst showed high catalytic activity for aerobic oxidation of alcohols to carbonyl compounds at 110 °C under base free conditions. A comparison of catalytic activity with Pd supported on other metal fluoride was also carried out. The catalyst was used for oxidation of several primary and secondary alcohols. The catalyst could be recycled successfully up to 5 cycles without loss in catalytic activity and Pd leaching. The *in-situ* FTIR studies proved that both substrates viz. oxygen and alcohols could be activated on catalyst surface so as to follow Langmuir-Hinshelwood type mechanism.

Chapter 4: Palladium nanoparticles supported on strontium fluoride: synthesis, characterization and catalytic activity for alcoholysis of epoxide

A one pot synthesis of palladium supported on strontium fluoride was carried out using fluorolytic sol-gel method from metallic strontium via strontium methoxide. The synthesized catalyst was characterized using several physico-chemical techniques. The catalyst showed formation of crystalline nature and mixed phases of fluorides and hydroxides with high surface area up to 58 $m^2 g^{-1}$.

The catalyst showed high catalytic activity for alcoholysis of epoxides at room temperature. The method of alcoholysis was generalized using several epoxides and

alcohols. Further the catalyst showed recyclability up to 3 cycles without losing activity and Pd leaching which was confirmed using ICP-AES studies. A general mechanism of alcoholysis was proposed based on type of substrate and stability of intermediate carbocationic species.

In general, palladium supported on alkaline earth metal fluorides synthesized via sol-gel method is new class of palladium based catalysts. The catalyst showed high catalytic activity for reactions like hydrogenation, oxidation and epoxide ring opening. The catalyst showed high recyclability and stabilization of palladium nanoparticle on metal fluoride support due to strong metal-support interactions.

List of Publications

A. Patents

1. The process for hydrogenation of olefinic and acetylenic bonds - **PCT publication, WO2013110995A2.**

2. Organometallic molybdenum acetalide dioxo complex and the process for preparation thereof **– PCT publication, WO2012035555A1**.

B. Papers

1. Simple root for alcohol oxidation to aldehyde with dioxo molybdenum chloride complex with dimethyl sulfoxide, ***Current Catalysis,* 2013, *7*, 237-243.**

2. Palladium nanoparticles supported on magnesium hydroxyl fluorides: an efficient and selective catalyst for olefin hydrogenation – ***ChemCatChem*, 2014, *DOI: 10.1002/cctc.201402469R1*.**

3. Oxygen activation on metal fluoride supported palladium nanoparticle for catalytic aerobic oxidation of alcohols - ***manuscript under preparation.***

4. Alcoholysis of epoxide: An investigation using Pd-MF_2 catalysts -***manuscript under preparation.***

C. Posters

1. Pd nanoparticle supported on sol-gel synthesized magnesium fluorides as an active catalyst for hydrogenation of olefins and triglycerides- **Indus Magic, National Chemical Laboratory, Pune, India – *Dec. 2012***

2. Synthesis of cyclopentadienyl molybdenum acetylide complex and its applications for various catalytic oxidation reactions- **9th Ferrocene Qualliqium, TU Chemnitz, Germany- *Feb 2011***

3. Synthesis of cyclopentadienyl molybdenum acetylide carbonyl complex for catalytic oxidation of alkenes, alcohols, amines and sulfides – **21st National Symposium of Catalysis, Chennai, India - *Dec 2011***

4. Synthesis of cyclopentadienyl dioxo molybdenum butyl complex for catalytic application of selective oxidation aromatic alkanes **– National Chemical Laboratory, Pune, India - *Feb 2011***

5. Synthesis of cyclopentadienyl molybdenum acetylide carbonyl complex for catalytic oxidation of alkenes, alcohols, amines and sulfides - **National Chemical Laboratory, Pune, India - *Feb 2009* – Awarded best poster.**